Surface Modification of Spherical Particles with Bioactive Glycopolymers

Dissertation

Zur Erlangung des akademischen Grades eines Doktors der Naturwissenschaften (Dr. rer. nat.) im Fach Chemie der Fakultät für Biologie, Chemie und Geowissenschaften der Universität Bayreuth

vorgelegt von

André Pfaff

Geboren in Lichtenfels / Deutschland

Bayreuth, 2011

Die vorliegende Arbeit wurde in der Zeit von Juli 2007 bis Januar 2011 in Bayreuth am Lehrstuhl Makromolekulare Chemie II unter der Betreuung von Herrn Prof. Dr. Axel H. E. Müller angefertigt.

Vollständiger Abdruck der von der Fakultät für Biologie, Chemie und Geowissenschaften der Universität Bayreuth zur Erlangung des akademischen Grades eines Doktors der Naturwissenschaften genehmigten Dissertation.

Dissertation eingereicht am: 16.02.2011

Zulassung durch die Promotionskommission: 24.02.2011

Wissenschaftliches Kolloquium: 09.05.2011

Amtierender Dekan: Prof. Dr. Stephan Clemens

Prüfungsausschuss:

Prof. Dr. Axel H. E. Müller (Erstgutachter)

Prof. Dr. Karlheinz Seifert (Zweitgutachter)

Prof. Dr. Birgit Weber (Vorsitz)

Dr. Alexander Wittemann

Meiner Familie

Table of Contents

Chapter 1

Introduction

1.1 Glycopolymers

Since the first studies of carbohydrates performed by Emil Fischer in the late nineteenth century, natural polysaccharides were found to be omnipresent in every living organism. In general, they are of enormous importance due to their appearance as food, biomass and raw materials. Despite of this, they play a major role in many recognition effects, which is the key to a multitude of biological processes, such as embryogenesis, immune defense, microbial and viral infection and cancer metastasis.[1, 2]

1.1.1 Synthetical Strategies towards Glycopolymers of Various Architectures

Glycopolymers, synthetic sugar-containing macromolecules, which display complex functionalities similar to those found in natural glycoconjugates, are attracting ever-increasing interest from the chemistry community due to their role as biomimetic analogues and their potential for commercial applications (Figure 1).

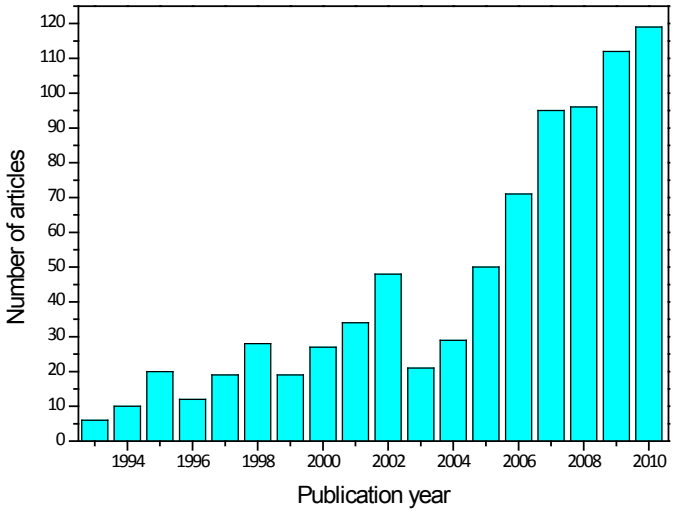

Figure 1. Number of publications involving glycopolymers from 1993 until 2010 (SciFinder, keyword: glycopolymer).

The polymerization of carbohydrate-bearing monomers can be carried out by a plurality of polymerization techniques, including free-radical polymerization (FRP),[3-11] anionic polymerization,[12] cationic polymerization,[13] ring-opening polymerization (ROP)[14, 15] ring-opening metathesis polymerization (ROMP)[16-20] and controlled/"living" radical polymerization (CLRP). The latter include reversible addition-fragmentation chain transfer polymerization (RAFT),[21-29] atom transfer radical polymerization (ATRP)[30-35] and nitroxide mediated polymerization (NMP).[36-40]

Applying these techniques, a plethora of linear glycopolymers bearing various carbohydrate moieties were synthesized and analyzed. Linear glycohomopolymers show an interesting behavior in matters of bioactivity and biorecognition towards proteins, but their use for applications regarding biosensors or drug delivery is often limited. This tempted researchers to synthesize diblock copolymers, in particular amphiphilic diblock copolymers containing a hydrophilic glycopolymer block and a hydrophobic block that can self-assemble into more complex structures. Emphasis was put in the synthesis of block copolymers containing glycopolymers and water-insoluble[41-44] or pH-/temperature-responsive polymers[41, 45-47] which self-assemble into micelles in aqueous solution. As an example, Zhang et al.[47] described the preparation of a poly(acryloylglucosamine)-*block*-poly(N-isopropylacryamide) copolymer which formed micelles above the LCST of PNIPAAm and could be crosslinked by an acid-degradable acetyl-type crosslinking agent. These core-crosslinked micelles were found to be stable against degradation at pH>6, whereas hydrolyzation at pH<4 occurred.

As reported by Ting et al.[28] the self-assembly of a poly(lactide)-*block*-poly(6-*O*-acryloyl-galactopyranose) copolymer in aqueous solution led to the formation of micelles with pendent galactose moieties covering the surface. By introducing a diacrylate the micelles could be crosslinked at the nexus of the copolymer followed by the removal of the poly(lactide) core by aminolysis to form hollow poly(6-*O*-acryloyl-galactopyranose) nanocages.

Adjusting the block length ratio of the hydrophilic and hydrophobic blocks can tune the morphology of the copolymer assemblies from micelles to vesicles. By this, copolymerizing glucosyloxyethyl methacrylate and diethyleneglycol methacrylate[48] as well as butadiene and styrene and subsequent thiol-ene reaction with a thiol-sugar[49] led to

glycopolymer vesicles. In the latter case a remarkable simple and efficient route to glycopolymer vesicles by the use of commercial available compounds in absence of toxic transition metal ions is reported (Figure 2).

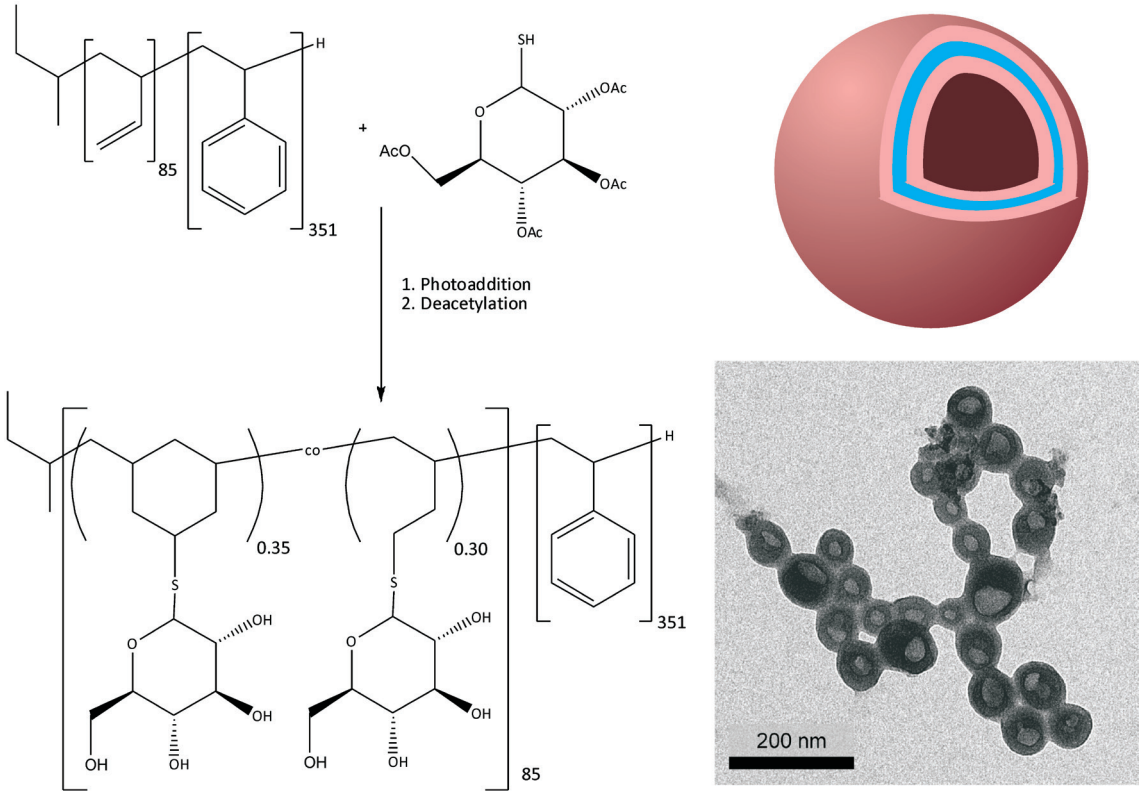

Figure 2. Synthesis of a glycopolymer vesicle by copolymerizing butadiene and styrene and subsequent thiol-ene chemistry.[49]

Beside the self-assembly of glycopolymer-containing amphiphilic copolymers, other synthetic strategies were performed to yield globular glycomacromolecules such as glycostars or dendrimers. Stars with 3, 4, 7 and 25 glycopolymer arms were prepared using the core-first method, either RAFT polymerization or ATRP and multiple initiator group bearing compounds such as modified β-cyclodextrin or silsesquioxane nanoparticles,[26, 30, 50-53] whereas in dendrimer synthesis only mono- or oligosaccharide units were attached to the dendritic surface in the final synthetic step.[54-58]

In contrast to the efforts to achieve perfectly branched glycodendrimers, more facile synthetic strategies were performed to have access to branched and hyperbranched glycopolymers. Self-condensing vinyl copolymerization (SCVCP) of an acrylic or methacrylic initiator-monomer and glucose-containing glycomonomer,[59, 60] ring-opening multibranching polymerization of anhydro carbohydrates[61] and the 'Strathclyde method'[62] have been used

to create branched glycopolymers. SCVCP was also applied to modify the chemical functionalities of solid surfaces. Muthukrishnan et al. reported the synthesis of highly branched polyglycomethacrylates from the surface of silicon wafers, that were functionalized with covalently attached initiators.[63] Furthermore Gao et al. grafted linear and hyperbranched glycopolymers from the surface of multiwalled carbon nanotubes (MWCNTs) (Figure 3).[64] After deprotection of the sugar moieties, water-soluble MWCNTs with high density of hydroxyl groups could be achieved.

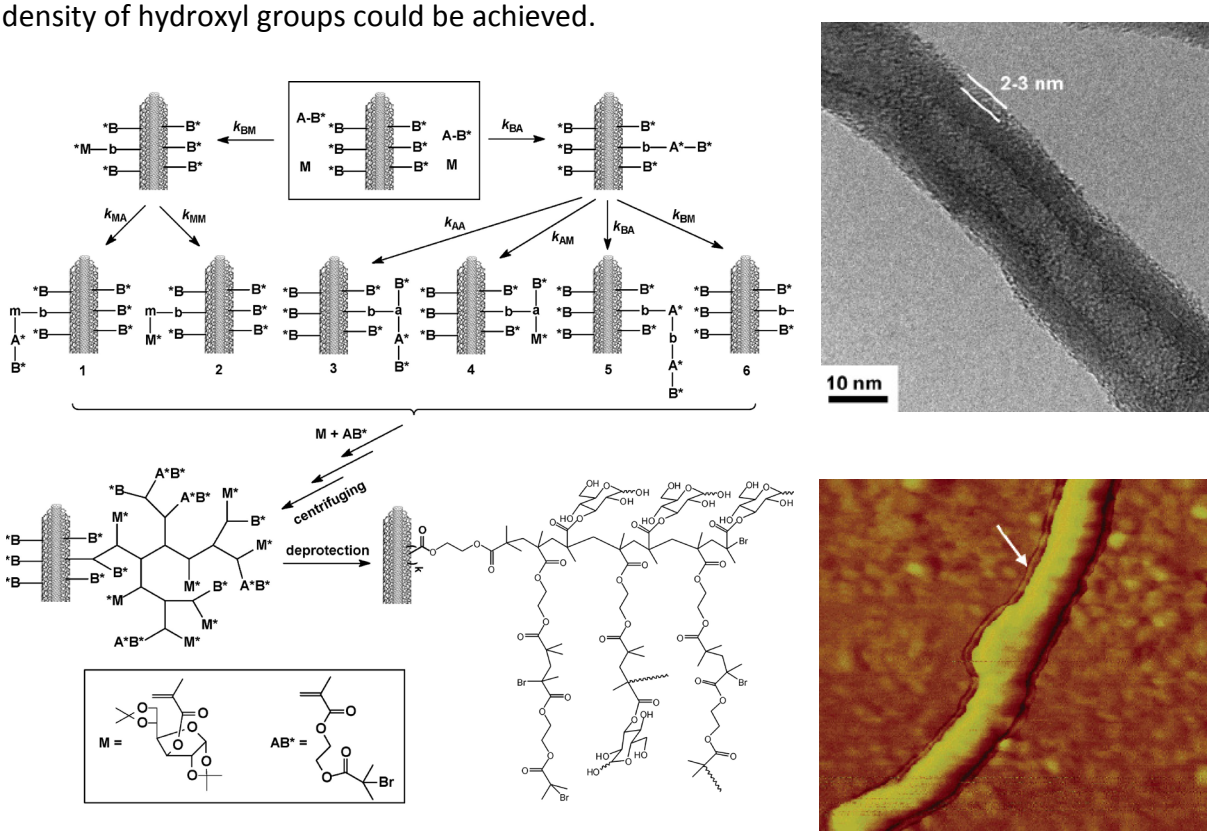

Figure 3. (Left) Synthetic strategy for grafting hyperbranched glycopolymers from the surface of multiwalled carbon nanotubes by SCVCP. (Right) TEM and SFM images of of the prepared glycopolymer tubes. The hyperbranched polymer shell is highlighted.[64]

1.1.2 Chemical Glycobiology

The lock-and-key interactions between carbohydrates and lectins are highly specific, but usually weak with dissociation constants K_d ranging from 10^{-3} to 10^{-6} M. By introducing glycopolymers, these interactions can be strongly increased due to the multivalent effect of clustered saccharides. The importance of multivalency of carbohydrate chains in carbohydrate-lectin interactions has been well cited as the "glyco-cluster effect".[65-68] Molecular recognition capabilities of glycopolymers can be estimated by measuring the

strength of their interactions with appropriate lectins. For this purpose a wide variety of methods, such as hemagglutination inhibition assay (HIA) and surface plasmon resonance (SPR) spectroscopy can be performed. In both cases the basic principle is based on the formation of isolated complexes between lectins and the ligand.[69] Interactions between glycopolymers and lectins are influenced by the density of the sugar molecules as well as the rigidity, molecular weight and architecture of the polymer. Linear carbohydrate-bearing polymers are the most widely tested glycopolymers regarding their ability to bind towards lectins. As an example, Ladmiral et al. clicked different ratios of azido-sugar (galactose/mannose) derivatives to the polymer backbone bearing alkyne functional groups. Quantitative precipitation experiments with these copolymers were carried out and displayed that the average number of Concanavalin A (ConA) bound to the polymers increased with increasing mannose content in the polymer.[31] Boyer and Davis reported that glucosamine-based glycopolymers interact with ConA, while galactosamine-based polymers were not able to form a cluster, confirming the specificity of the interactions between the polymer and lectin.[70] Miyamoto et al. investigated the interaction of wheat germ agglutinin (WGA), which is known to specifically bind to acetylglucosamine, and a acetylglucosamine-carrying polyvinyl ether-poly(isobutyl vinyl ether) block copolymer.[71] They reported a significant increase in binding affinity compared to acetylglucosamine and its oligomers, which can be attributed to multivalent interactions. Furthermore, the used block copolymer exceeded the glyco-homopolymer in binding strength, which can be ascribed to the formation of micellar aggregates of the diblock in aqueous solution and therefore a further increase of the multivalency effect. Thus, micellar aggregates and other complex architectures can display a much higher binding affinity towards binding lectins caused by an increased surface area of spherical and three dimensional structures.

As lectins are ubiquitously present on cell surfaces and take place in recognition and binding events (Figure 4), the incorporation of ligands such as carbohydrates or similar targeting compounds can lead to an increased cellular uptake of desired drugs or imaging tools via receptor-endocytosis.[72-76] Targets for glycopolymeric drugs are among others Alzheimer´s disease, influenza and some cancers.

The multiplicity of influenza viruses and the high number of fatalities that were caused by them led to a continuous search for effective treatments. In general, viral

infection is a multistep process consisting of the entry of the virus in the cell, release of the RNA into the cytoplasm, transport of the RNA into the nucleus and replication of the virus. The influenza virus enters the cell via endocytosis by binding to *N*-acetylneuramic acid residues on the cell via lectin structures known as hemagglutinin fingers. A molecule that could prevent the binding of the virus to the cell in the first place could therefore become a potent prophylactic against influenza. As the interaction of influenza hemagglutinin with monovalent sialosides is weak,[77] the introduction of multivalent ligands could be a promising starting point. Matrosovich et al. reported the first example of an influenza hemagglutinin inhibitor based on a glycopolymer.[78] By the reaction of poly(4-nitrophenylacrylate) with amino-terminated monosialosides, they were able to prepare a series of polymeric sialosides with varying ratio of carbohydrate within the copolymer (Figure 5). Little or no inhibition was detected for monovalent sialosides or glycopolymers carrying only few units of carbohydrates (~5%).

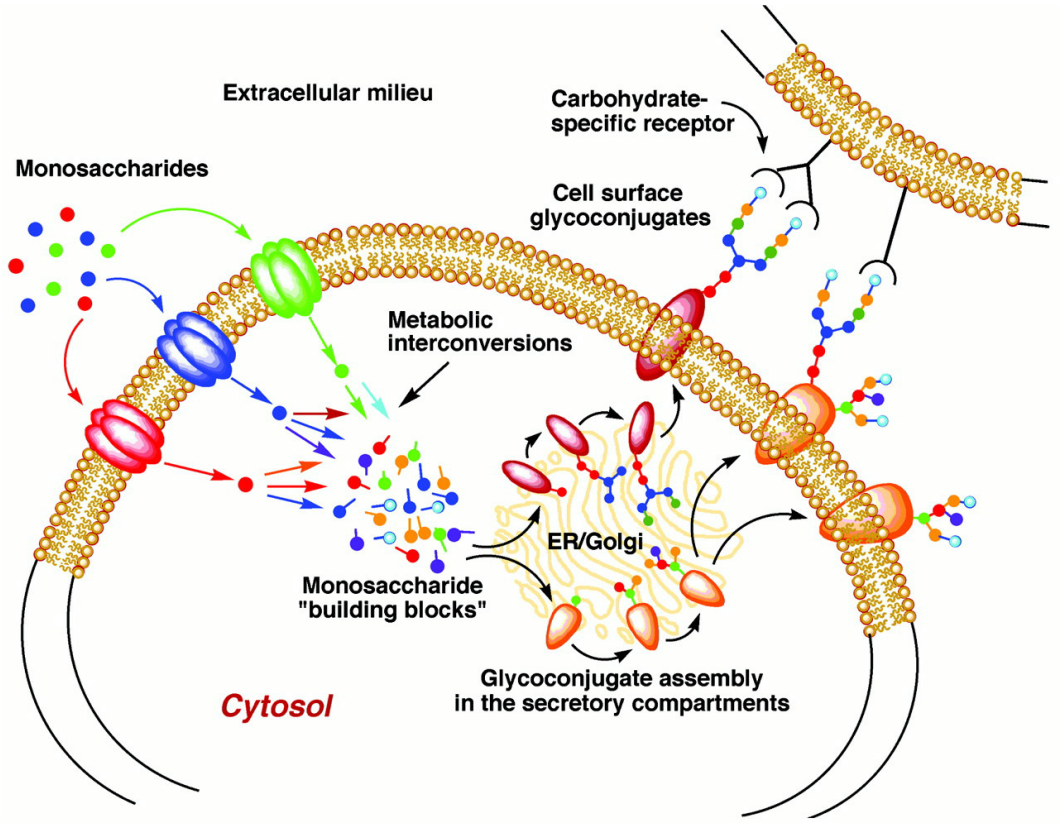

Figure 4. Glycoconjugate biosynthesis and cell surface recognition. Exogenously supplied monosaccharides are taken up by cells and converted to monosaccharide "building blocks" inside the cell. In the secretory compartments the building blocks were assembled into oligosaccharides bound to a protein scaffold. Once expressed in fully mature form on the cell surface, the glycoconjugates can serve as ligands for receptors on other cells or pathogens. Chemical tools can be used to inhibit or control any stage of this process.[79]

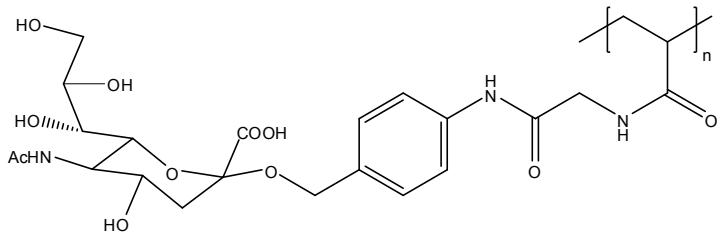

Figure 5. Polymeric multivalent sialosides prepared by Matrosovich et al.[78]

Increasing the sialoside density from 10 to 30% indicated a maximum level of inhibition at intermediate levels of sialylation (20%). In the case of a low density of carbohydrates the binding of one residue does not increase the likelihood of a subsequent group´s binding due to the distance of the sugars within the copolymer. However, a high content of carbohydrates may limit the binding as the steric bulk of the groups overcrowd one another. Furthermore, bulky or charged groups on the comonomer have the tendency to reduce the inhibition effect.[80, 81]

Acquired immune deficiency syndrome (AIDS) is another viral disease that became a major international pandemic. In this case anionic glycopolymers found their way to be considered as HIV treatments. Anionic polysaccharides have been found to hinder the binding of the virus to the cell and therefore the penetration through the cell membrane.[82] Yoshida et al. prepared a sulfated maltoheptose-displaying methacrylic glycopolymer that was able to inhibit the infection of cells with the human immunodeficiency virus (HIV).[83] The inhibitory effect could be further increased by copolymerizing the glycomonomer with methyl methacrylate (MMA) yielding a maximal effect at an incorporation of 80% MMA. At this composition the prepared glycomonomer displayed an inhibition effect that is still 2 orders of magnitude worse than a commonly used anti-retroviral, azidothymidine. But due to the reduced cytotoxicity, it might still be a potential treatment against HIV in the future.

Beside the use of glycopolymers to inhibit the binding of viruses to cells, carbohydrate-displaying polymers find application in glycopolymeric drug-delivery. The main problem in drug treatment in vivo is the occurrence of undesirable side effects due to not sufficient target selectivity or poor pharmacokinetics requiring large doses or regular uptake. This is especially important for anti-tumor drugs, as they are usually toxic and therefore their administration must be accurately controlled in order to not harm healthy cells. To

accommodate these aspects, Ringsdorf introduced a simple model for the targeted drug delivery, called the "magic bullet" method (Figure 6).[84]

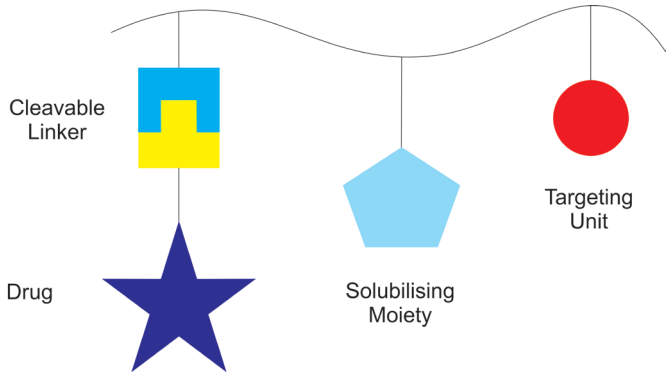

Figure 6. Ringsdorf model for polymeric drug delivery.[84]

For this, a targeting unit, solubilising agent and a cleavable drug are attached to a polymer backbone. As glycopolymers bearing water-soluble carbohydrate moieties, they may act both as solubilising agent and targeting ligand, as they can interact specific with lectins on the surface of cells. Based on this model, Hopewell et al. prepared a polymeric anticancer conjugate, composed of an N-(2-hydroxypropyl)methacrylamide (HPMA) copolymer backbone and pendant doxorubicin (DOX) linked via a peptide spacer (PK2, Figure 7).[85] Furthermore, galactose residues are present to facilitate liver targeting. In general, doxorubicin is a powerful chemotherapy drug but limited in use due to the off-target cardiotoxicity.

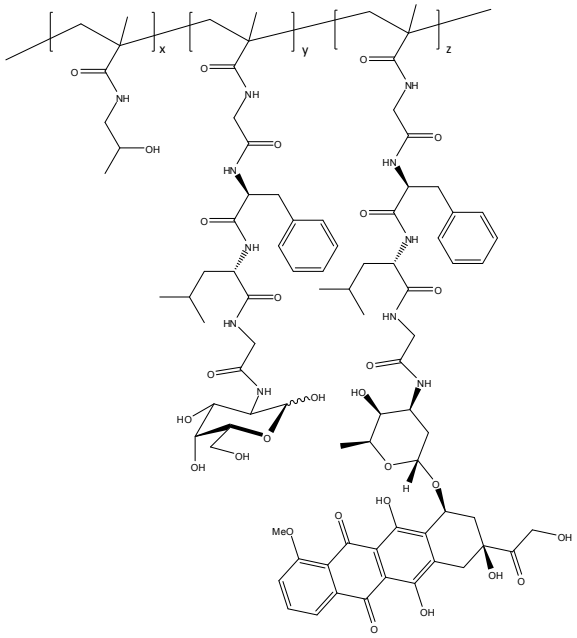

Figure 7. Structure of doxorubicin-conjugated polymer PK2.[85]

A preclinical study in a rat model was used to determine acute and cardiovascular toxicities of the administrated PK2 and free DOX, which were monitored by weight loss and cardiac output respectively. Animals received intravenous doses > 2 mg / kg of free DOX displayed acute toxicity and significant weight loss 8-12 weeks after administration, whereas animals treated with PK2, containing an equal amount of DOX, gained weight. 3 mg / kg of injected free DOX lead to a significant decrease in cardiac output after 12 weeks. None of the animals survived until the 12 week end-point when given 4 mg / kg of free DOX, whereby all animals survived the treatment with PK2. The drug-glycopolymer conjugate was also administrated to patients in a Phase I clinical trial but was found to be unsatisfactory for its planned target.

These are just few of the examples in which glycopolymers have been investigated for therapeutic development and delivery. But still extensive research is required if glycopolymer-based therapeutics are to reach the clinic.

Beside their use as therapeutic compounds, glycopolymers find application in cellular imaging. Up to now, mainly carbohydrate capped quantum dots (QD) have been prepared to create fluorescent materials for cellular imaging. Quantum dots are versatile inorganic probes with unique photophysical properties, including narrow and size-dependent luminescence with broad absorption spectra. By immobilization of carbohydrate-containing thiols on the QD surface, researchers obtained access to mannose-, galactose-, galactosamine- and acetylglucosamine-displaying luminescent particles covered with carbohydrate unimers,[86-88] whereas Sun et al. synthesized glycopolymer-coated QDs utilizing the strong binding of a biotin-terminated lactose-bearing polymer with avidin-coated QDs.[89] In the large majority of carbohydrate functionalized quantum dots, only carbohydrate unimers are attached to the material surface. However, there are examples that sugar-displaying fluorescent particles have potential to be considered as cellular imaging probes. Niikura et al. reported the synthesis of mannose-, glucose-, galactose-, and acetylglucosamine-covered QDs.[87] Binding experiments of the sugar-containing fluorescent particles to HeLa cells revealed a selective binding of acetylglucosamine-diplaying particles, indicating that this moiety is crucial for binding to the cells. The binding of acetylglucosamine-diplaying QDs could be clearly visualized by sliced confocal-laser microscopy images, showing QDs surrounding the nuclei (Figure 8A). Figure 8B-D shows

HeLa cells after staining with an endoplasmic reticulum (ER) marker, nucleus marker and QDs. These images show that the ER marker (green) and the QDs (blue) localized in the same area within the cells. This suggests that the QDs accumulated in the ER due to the successful recognition of the carbohydrate moieties by corresponding lectins in the ER.

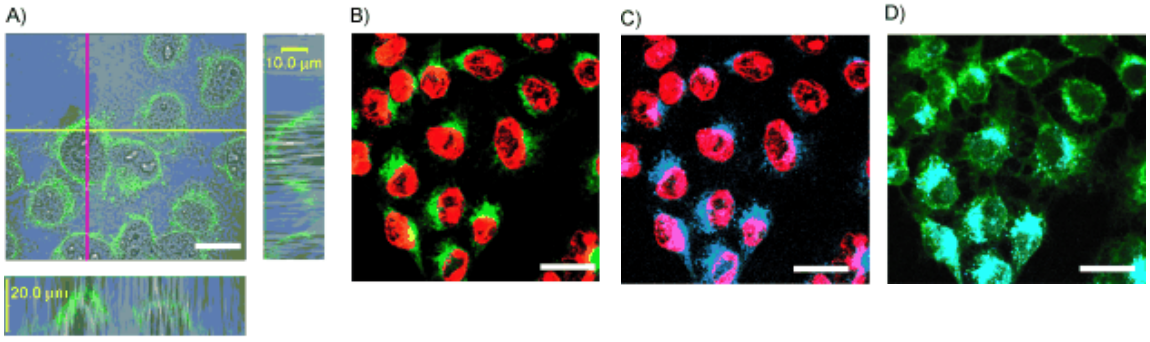

Figure 8. Comparison of subcellular distribution between QDs and the ER marker. A) Three-dimensional subcellular distribution of QDs in HeLa cells. Cross sections along the yellow and red lines are shown. B) Fluorescene image of the ER marker (green) and nuclei (red). C) Fluorescence image of the nuclei (red) and QDs (blue). D) Fluorescence image of the QDs (blue) and ER marker (green). Images were obtained with a confocal-laser microscope. Scale bars = 20µm.[87]

1.2 Surface Modification of Solid Substrates

The surface modification of particles can lead to polymer brushes, ultrathin polymer coatings consisting of polymer chains tethered with one chain end to a solid substrate. One can speak of a polymer brush if the grafting of the chains is sufficiently dense, i.e. when the distance between neighboring grafting points is much smaller than the linear dimensions of the polymer chains. In general, polymer brushes can be prepared by three approaches: “grafting to”, “grafting from” and “grafting through”. The “grafting to” approach involves the attachment of prior synthesized polymer chains to substrates via physisorption[90-94] or chemisorption.[95-99] As grafted chains on the surface increase the steric hindrance and therefore hamper the diffusion of other polymer chains to the reactive sites of the particles, formation of dense polymer brushes via “grafting to” is often limited.

In the “grafting from” approach, the polymerization is initiated from surface-bound initiators. Even if conventional free radical polymerization[100-104] is often used to prepare polymer brushes, most of the polymer brushes prepared by a “grafting from” approach are prepared using surface-initiated controlled radical polymerization methods.[105] These methods are of particular interest as they allow control over brush thickness, composition and architecture of the polymer brushes.

For the “grafting through” approach, double bonds on the surface must be exploited. Growing polymer chains in solution copolymerize with surface bound double bonds during the polymerization. This approach is commonly used for the surface modification of poly(divinylbenzene) microspheres.[106] The different approaches are depicted in Figure 9.

In the following chapters of this thesis glycopolymer chains were attached to solid substrates by various grafting approaches and polymerization techniques. Atom transfer radical polymerization and reversible addition fragmentation chain transfer polymerization were performed to “graft from” spheres and “graft through” surface bound vinyl bonds, while a “grafting to” approach was performed via thiol-ene reactions of thiol-bearing glycopolymers and surface functionalized substrates. The theoretical basics of ATRP, RAFT polymerization and thiol-ene reaction will be described hereafter.

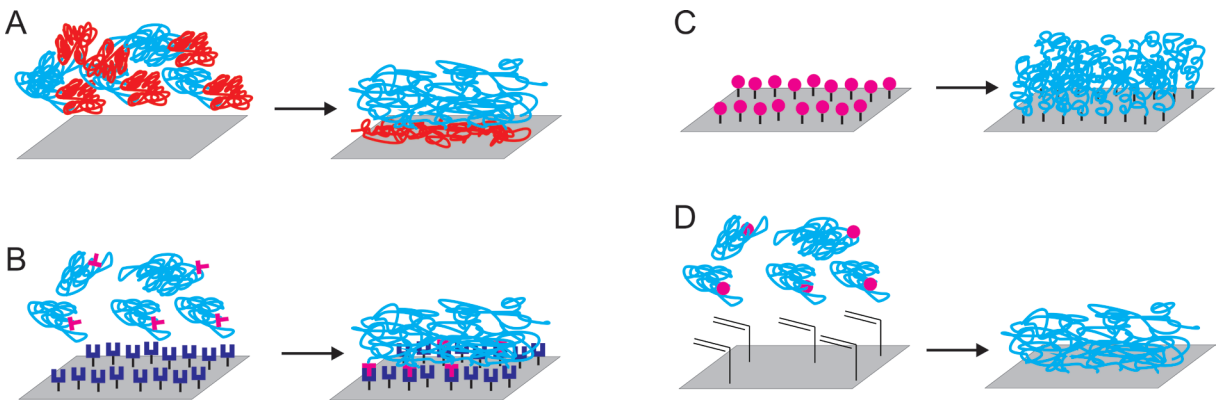

Figure 9. Synthetic approaches for the preparation of polymer brushes. “Grafting to”: polymer brushes grown by (A) physisorption of a diblock copolymer and (B) chemisorption via reaction of end-functionalized polymers and functional groups on the substrate surface. “Grafting from”: (C) polymer brushes grown via surface initiated polymerization. “Grafting through”: (D) during polymerization the reactive chain end copolymerizes with surface-attached double bonds.

1.2.1 Atom Transfer Radical Polymerization (ATRP)

The invention of controlled/”living” radical polymerization methods depicted a powerful alternative to living polymerizations conducted via an ionic, coordination or ring-opening mechanism due to the tolerance regarding functional groups and impurities. ATRP is based on the formation of a rapid dynamic equilibrium between a small amount of growing free radicals and a large amount of the dormant species. The low overall concentration of free radicals ensures a very low rate of irreversible termination compared to the propagation rate. Furthermore, the exchange rate between radicals and dormant species must be faster than the rate of propagation to enable an equal probability of growing for all chains. In ATRP the dormant chains are alkyl halides, whereas free radicals are generated via a catalyzed reaction as shown in Figure 10.

The radicals are generated through a reversible redox process catalyzed by a transition metal complex which undergoes a one-electron oxidation with simultaneous abstraction of a halogen atom (X) from a dormant species (R-X). Polymer chains grow by the addition of the intermediate radicals to monomers similar to conventional radical polymerization. Termination reactions mainly occur through radical coupling and disproportionation.

ATRP is a multicomponent system, consisting of the monomer, initiator with transferable halogen and a catalyst, composed of a transition metal species and ligand.

Many parameters, such as ligand to transition metal ratio, type of ligand, counterion, temperature, solvent or initiator, influence the performance of ATRP.[107]

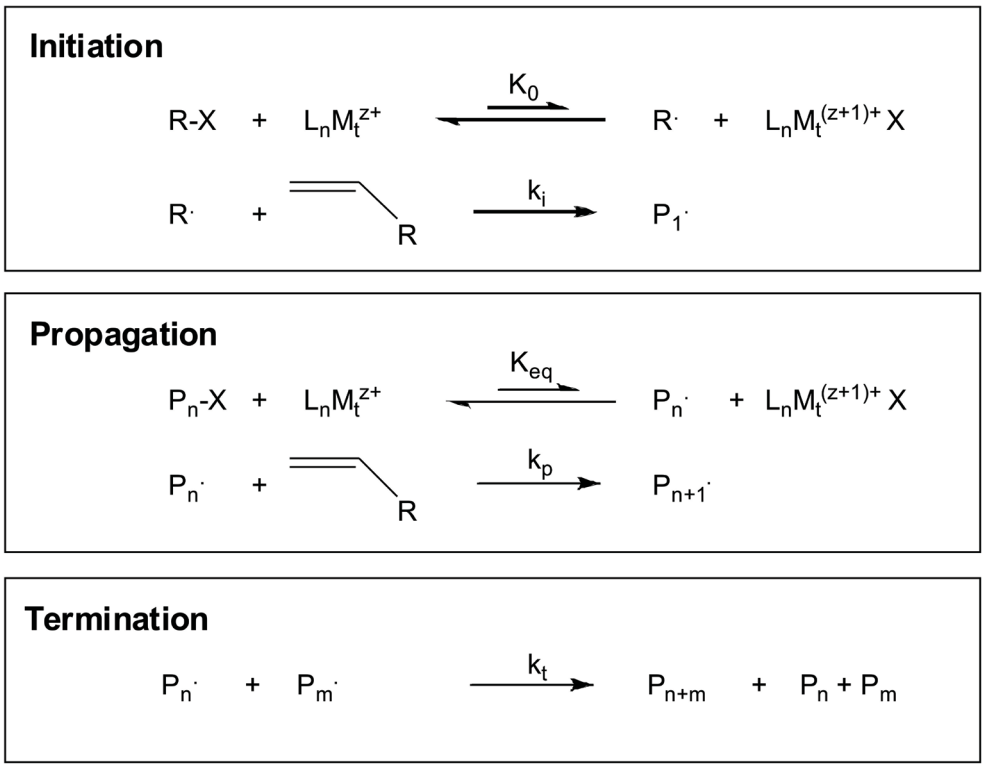

Figure 10. General mechanism for Atom Transfer Radical Polymerization. R-X: alkyl halide; L_n: Ligand; M_t: transition metal.

1.2.2 Reversible Addition Fragmentation Chain Transfer Polymerization (RAFT)

Beside ATRP, reversible addition fragmentation chain transfer polymerization (RAFT) is another prominent type of CRP. RAFT polymerization has proven to be a versatile tool, as they are less oxygen sensitive and are compatible with a wider range of monomers compared to ATRP. A further big advantage is the absence of heavy metals which makes polymers prepared by RAFT polymerization interesting for biomedical applications. RAFT consists of the introduction of a small amount of dithioester with a general structure of Z-C(=S)S-R in a conventional free-radical system. The transfer of the chain transfer agent between growing radical chains, present at very low concentrations, and dormant species, present at higher concentrations, will regulate the growth of the molecular weight and limit termination reactions. The mechanism of RAFT polymerization is depicted in Figure 11.[108]

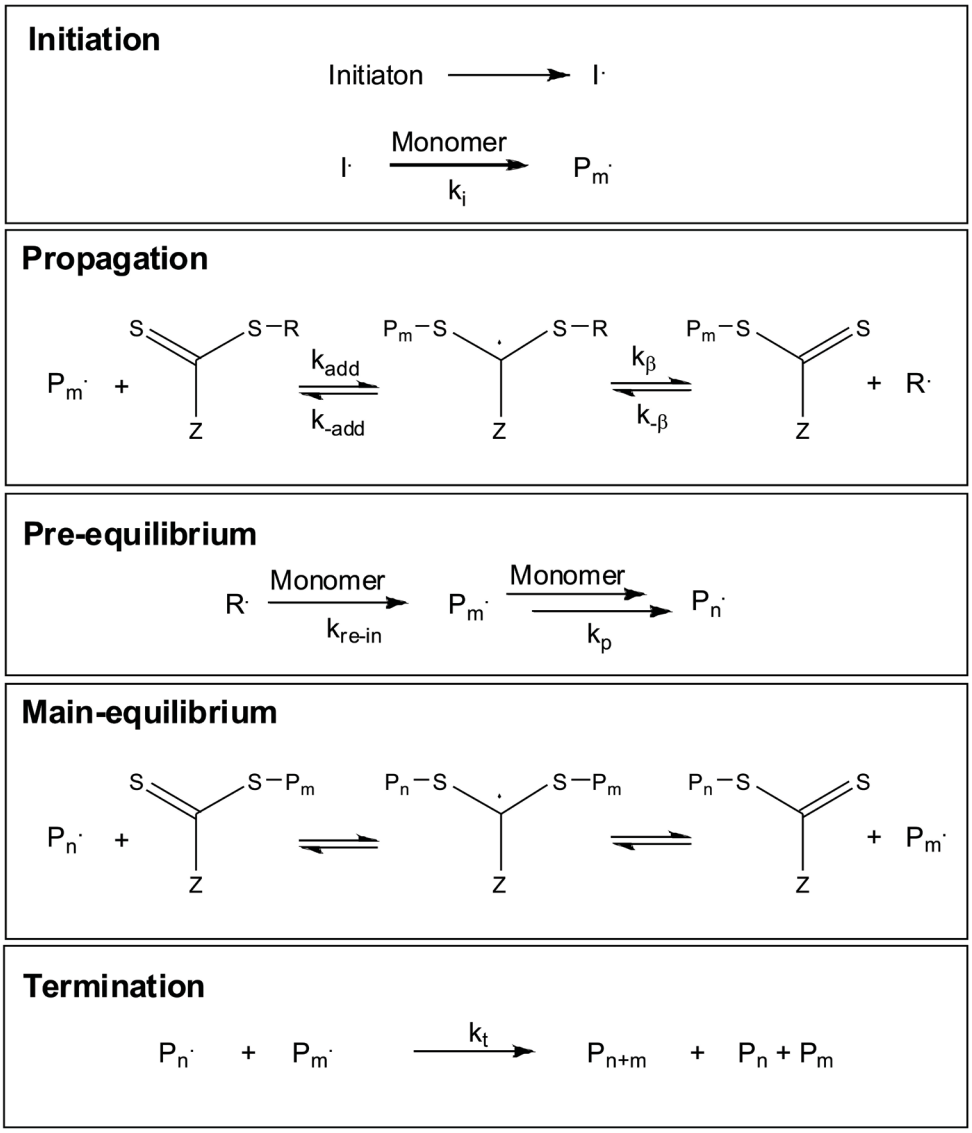

Figure 11. General mechanism for Reversible Addition Fragmentation Chain Transfer Polymerization.

After the decomposition of a radical initiator, the generated radicals react with the monomer. This growing polymer chain adds to the reactive carbon sulfur double bond of the CTA to form a radical intermediate. The fragmentation of the intermediate occurs reversibly either towards the initial growing chain or to free the re-initiating group (R) and a macro RAFT agent. By reacting with monomers, the R group starts a new polymer chain, which will propagate or react back on the macro-CTA. After the complete consumption of initial CTAs, only macro-CTAs are present in the reaction medium (main-equilibrium). In here, a rapid exchange between active and dormant species ensures equal probabilities for all chains to grow leading to narrow molecular weight distributions. Nevertheless, with the polymerization being of a radical nature, termination reactions cannot be fully suppressed.

1.2.3 Thiol-ene reaction

The hydrothiolation of a carbon carbon double bond, the so-called thiol-ene reaction, has been known for over 100 years[109] and still finds application due to its facile and versatile process. In general, almost any thiol can be employed, including highly functional species, and a wide range of enes serve as suitable substrates. The thiol-ene reaction can be performed under radical conditions, involving a photoinitiator or thermal initiator. Under such conditions it proceeds like a typical chain process with initiation, propagation and termination steps (Figure 12, left). Propagation is a two step process consisting of the direct addition of the thiyl radical across the C=C double bond towards an intermediate carbon-centred radical followed by chain transfer to another thiol molecule to give the thiol-ene addition product with anti-Markovnikov orientation. Simultaneously a new thiyl radical is formed.

Beside the radical mediated thiol-ene reactions, hydrothiolations can be performed under mild base or nucleophilic catalysis. For this only enes with an electron deficient C=C bond, e.g. (meth)acrylates, can be used, but given the large number of commercially available activated enes, there is still a remarkable application field for the synthesis of novel materials. The base/nucleophile-mediated addition to an activated ene can also be described as a thiol-Micheal addition. Reaction of a thiol with a base results in deprotonation of the thiol to the corresponding thiol anion that subsequent adds into the activated C=C bond at the electrophilic β-carbon forming an intermediate carbon-centred anion (Figure 12, right). The anion abstracts a proton from another thiol molecule yielding the anti-Markonikov thiol-ene product.[110]

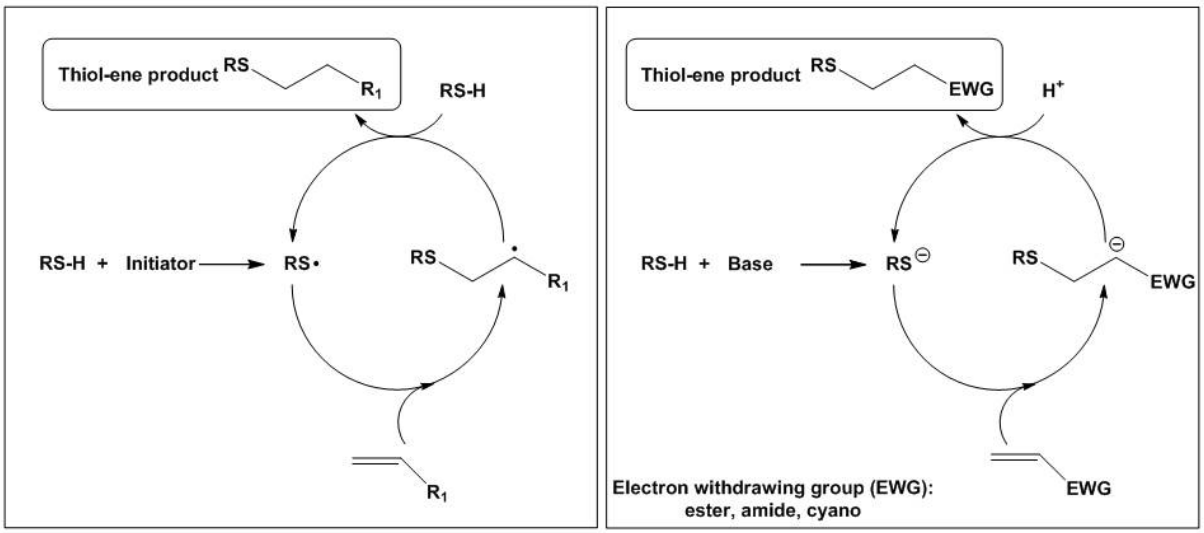

Figure 12. General mechanism for (left) radical and (right) base-mediated thiol-ene reaction.

1.3 Objective of this Thesis

The motivation of this work was to broaden the scope of glycopolymer-covered spherical particles with respect to their interaction towards carbohydrate-binding proteins and potential applications in biomaterial science. One focus of this thesis was the generation of novel nano- and micrometer sized glycopolymer-grafted spheres by applying various grafting techniques, whereby controlled radical polymerization methods, namely reversible addition fragmentation chain transfer (RAFT) and atom transfer radical polymerization (ATRP), were utilized in order to synthesize glycopolymers. However, the synthesis of these particles was not the sole objective of this thesis, and the interactions of these particles with various lectins were also investigated, in order to understand the effect of the specific carbohydrate that was incorporated into the polymer chain, and the architecture of the polymer chain itself. Furthermore, carbohydrate-protein interactions may facilitate the cellular uptake of carbohydrate functionalized particles within the cytoplasm or even nucleus, and such particles may find application as cellular imaging probes.

1.4 References

1. Dwek, R. A. *Chemical Reviews* **1996,** 96, (2), 683-720.
2. Sharon, N.; Lis, H. *Sci Am* **1993,** 268, 82.
3. Furuike, T.; Nishi, N.; Tokura, S.; Nishimura, S.-I. *Macromolecules* **1995,** 28, (21), 7241-7247.
4. Miura, Y.; Ikeda, T.; Kobayashi, K. *Biomacromolecules* **2003,** 4, (2), 410-415.
5. Miura, Y.; Sato, H.; Ikeda, T.; Sugimura, H.; Takai, O.; Kobayashi, K. *Biomacromolecules* **2004,** 5, (5), 1708-1713.
6. Miyachi, A.; Dohi, H.; Neri, P.; Mori, H.; Uzawa, H.; Seto, Y.; Nishida, Y. *Biomacromolecules* **2009,** 10, (7), 1846-1853.
7. Nagahori, N.; Nishimura, S.-I. *Biomacromolecules* **2000,** 2, (1), 22-24.
8. Sato, H.; Miura, Y.; Saito, N.; Kobayashi, K.; Takai, O. *Biomacromolecules* **2007,** 8, (2), 753-756.
9. Serizawa, T.; Yasunaga, S.; Akashi, M. *Biomacromolecules* **2001,** 2, (2), 469-475.
10. Yang, Q.; Wu, J.; Li, J.-J.; Hu, M.-X.; Xu, Z.-K. *Macromolecular Rapid Communications* **2006,** 27, (22), 1942-1948.
11. Yoshizumi, A.; Kanayama, N.; Maehara, Y.; Ide, M.; Kitano, H. *Langmuir* **1998,** 15, (2), 482-488.
12. Loykulnant, S.; Hirao, A. *Macromolecules* **2000,** 33, (13), 4757-4764.
13. Yamada, K.; Yamaoka, K.; Minoda, M.; Miyamoto, T. *J. Polym. Sci. Part A: Polym. Chem.* **1997,** 35, 255.
14. Aoi, K.; Tsutsumiuchi, K.; Aoki, E.; Okada, M. *Macromolecules* **1996,** 29, (12), 4456-4458.
15. Tsutsumiuchi, K.; Aoi, K.; Okada, M. *Macromolecules* **1997,** 30, (14), 4013-4017.
16. Cairo, C. W.; Gestwicki, J. E.; Kanai, M.; Kiessling, L. L. *Journal of the American Chemical Society* **2002,** 124, (8), 1615-1619.
17. Manning, D. D.; Hu, X.; Beck, P.; Kiessling, L. L. *Journal of the American Chemical Society* **1997,** 119, (13), 3161-3162.
18. Mortell, K. H.; Gingras, M.; Kiessling, L. L. *Journal of the American Chemical Society* **1994,** 116, (26), 12053-12054.

19. Mortell, K. H.; Weatherman, R. V.; Kiessling, L. L. *Journal of the American Chemical Society* **1996,** 118, (9), 2297-2298.
20. Murphy, J. J.; Furusho, H.; Michael, R. P.; Nomura, K. *Chemistry - A European Journal* **2007,** 13, (32), 8985-8997.
21. Albertin, L.; Cameron, N. R. *Macromolecules* **2007,** 40, (17), 6082-6093.
22. Albertin, L.; Kohlert, C.; Stenzel, M.; Foster, L. J. R.; Davis, T. P. *Biomacromolecules* **2004,** 5, (2), 255-260.
23. Albertin, L.; Stenzel, M. H.; Barner-Kowollik, C.; Davis, T. P. *Polymer* **2006,** 47, (4), 1011-1019.
24. Albertin, L.; Stenzel, M. H.; Barner-Kowollik, C.; Foster, L. J. R.; Davis, T. P. *Macromolecules* **2004**, (37), 7530.
25. Albertin, L.; Stenzel, M. H.; Barner-Kowollik, C.; Foster, L. J. R.; Davis, T. P. *Polymer* **2005,** 46, (9), 2831-2835.
26. Bernard, J.; Hao, X.; Davis, T. P.; Barner-Kowollik, C.; Stenzel, M. H. *Biomacromolecules* **2005,** 7, (1), 232-238.
27. Lowe, A. B.; Sumerlin, B. S.; McCormick, C. L. *Polymer* **2003,** 44, (22), 6761-6765.
28. Ting, S. R. S.; Gregory, A. M.; Stenzel, M. H. *Biomacromolecules* **2009,** 10, (2), 342-352.
29. Xiao, N.-Y.; Li, A.-L.; Liang, H.; Lu, J. *Macromolecules* **2008,** 41, (7), 2374-2380.
30. Dai, X.-H.; Dong, C.-M. *Journal of Polymer Science Part A: Polymer Chemistry* **2008,** 46, (3), 817-829.
31. Ladmiral, V.; Mantovani, G.; Clarkson, G. J.; Cauet, S.; Irwin, J. L.; Haddleton, D. M. *Journal of the American Chemical Society* **2006,** 128, (14), 4823-4830.
32. Muthukrishnan, S.; Jutz, G.; Andre, X.; Mori, H.; Muller, A. H. E. *Macromolecules* **2004,** 38, (1), 9-18.
33. Muthukrishnan, S.; Nitschke, M.; Gramm, S.; Oezyuerek, Z.; Voit, B.; Werner, C.; Mueller, A. H. E. *Macromol. Biosci.* **2006**, (6), 658.
34. Ohno, K.; Tsujii, Y.; Fukuda, T. *J. Polym. Sci. Part A: Polym. Chem.* **1998,** 36, 2473.
35. Vazquez-Dorbatt, V.; Maynard, H. D. *Biomacromolecules* **2006,** 7, 2297-2302.
36. Götz, H.; Harth, E.; Schiller, S. M.; Frank, C. W.; Knoll, W.; Hawker, C. J. *Journal of Polymer Science Part A: Polymer Chemistry* **2002,** 40, (20), 3379-3391.

37. Narumi, A.; Matsuda, T.; Kaga, H.; Satoh, T.; Kakuchi, T. *Polymer* **2002,** 43, (17), 4835-4840.

38. Narumi, A.; Satoh, T.; Kaga, H.; Kakuchi, T. *Macromolecules* **2001,** 35, (3), 699-705.

39. Ohno, K.; Tsujii, Y.; Miyamoto, T.; Fukuda, T.; Goto, M.; Kobayashi, K.; Akaike, T. *Macromolecules* **1998,** 31, (4), 1064-1069.

40. Sun, X.-L.; Faucher, K. M.; Houston, M.; Grande, D.; Chaikof, E. L. *Journal of the American Chemical Society* **2002,** 124, (25), 7258-7259.

41. Cameron, N. R.; Spain, S. G.; Kingham, J. A.; Weck, S.; Albertin, L.; Barker, C. A.; Battaglia, G.; Smart, T.; Blanazs, A. *Faraday Discussions* **2008,** 139, 359-368.

42. Ramiah, V.; Matahwa, H.; Weber, W.; McLeary, J. B.; Sanderson, R. D. *Macromolecular Symposia* **2007,** 255, (1), 70-80.

43. Suriano, F.; Pratt, R.; Tan, J. P. K.; Wiradharma, N.; Nelson, A.; Yang, Y.-Y.; Dubois, P.; Hedrick, J. L. *Biomaterials* **2010,** 31, (9), 2637-2645.

44. Ting, S. R. S.; Min, E. H.; Escalé, P.; Save, M.; Billon, L.; Stenzel, M. H. *Macromolecules* **2009,** 42, (24), 9422-9434.

45. Chen, X. M.; Dordick, J. S.; Rethwisch, D. G. *Macromolecules* **1995**, (28), 6014.

46. Hetzer, M.; Chen, G.; Barner-Kowollik, C.; Stenzel, M. H. *Macromolecular Bioscience* **2010,** 10, (2), 119-126.

47. Zhang, L.; Bernard, J.; Davis, T. P.; Barner-Kowollik, C.; Stenzel, M. H. *Macromolecular Rapid Communications* **2008,** 29, (2), 123-129.

48. Pasparakis, G.; Alexander, C. *Angewandte Chemie International Edition* **2008,** 47, (26), 4847-4850.

49. You, L.; Schlaad, H. *Journal of the American Chemical Society* **2006,** 128, (41), 13336-13337.

50. Bernard, J.; Favier, A.; Zhang, L.; Nilasaroya, A.; Davis, T. P.; Barner-Kowollik, C.; Stenzel, M. H. *Macromolecules* **2005,** 38, (13), 5475-5484.

51. Qiu, S.; Huang, H.; Dai, X.-H.; Zhou, W.; Dong, C.-M. *Journal of Polymer Science Part A: Polymer Chemistry* **2009,** 47, (8), 2009-2023.

52. Zhang, L.; Stenzel, M. H. *Australian Journal of Chemistry* **2009,** 62, 813-822.

53. Muthukrishnan, S.; Plamper, F.; Mori, H.; Müller, A. H. E. *Macromolecules* **2005,** 38, (26), 10631.

54. Baigude, H.; Katsuraya, K.; Okuyama, K.; Tokunaga, S.; Uryu, T. *Macromolecules* **2003,** 36, (19), 7100-7106.

55. Bhadra, D.; Yadav, A. K.; Bhadra, S.; Jain, N. K. *International Journal of Pharmaceutics* **2005,** 295, (1-2), 221-233.

56. Fernandez-Megia, E.; Correa, J.; Rodriguez-Meizoso, I.; Riguera, R. *Macromolecules* **2006,** 39, (6), 2113-2120.

57. Klajnert, B.; Appelhans, D.; Komber, D.; Morgner, N.; Schwarz, S.; Richter, S.; Brutschy, B.; Ionov, M.; Tonkikh, A. K.; Bryszewska, M.; Voit, B. *Chemistry - A European Journal* **2008,** 14, (23), 7030-7041.

58. Renaudie, L.; Daniellou, R.; Augé, C.; Le Narvor, C. *Carbohydrate Research* **2004,** 339, (3), 693-698.

59. Muthukrishnan, S.; Jutz, G.; André, X.; Mori, H.; Müller, A. H. E. *Macromolecules* **2005,** 38, 9.

60. Muthukrishnan, S.; Mori, H.; Müller, A. H. E. *Macromolecules* **2005,** 38, 3108.

61. Satoh, T.; Kakuchi, T. *Macromolecular Bioscience* **2007,** 7, (8), 999-1009.

62. Besenius, P.; Slavin, S.; Vilela, F.; Sherrington, D. C. *Reactive and Functional Polymers* **2008,** 68, (11), 1524-1533.

63. Muthukrishnan, S.; Erhard, D. P.; Mori, H.; Müller, A. H. E. *Macromolecules* **2006,** 39, (8), 2743-2750.

64. Gao, C.; Muthukrishnan, S.; Li, W.; Yuan, J.; Xu, Y.; Müller, A. H. E. *Macromolecules* **2007,** 40, (6), 1803-1815.

65. Kiessling, L. L.; Pohl, N. L. *Chemistry & Biology* **1996,** 3, (2), 71-77.

66. Lee, Y. C. *FASEB J.* **1992,** 6, (13), 3193-3200.

67. Lundquist, J. J.; Toone, E. J. *Chemical Reviews* **2002,** 102, (2), 555-578.

68. Mammen, M.; Choi, S. K.; Whitesides, G. M. *Angewandte Chemie International Edition* **1998,** 37, (20), 2754-2794.

69. Olsen, L. R.; Dessen, A.; Gupta, D.; Sabesan, S.; Sacchettini, J. C.; Brewer, C. F. *Biochemistry* **1997,** 36, (49), 15073-15080.

70. Boyer, C.; Davis, T. P. *Chemical Communications* **2009**, (40), 6029-6031.

71. Yamada, K.; Minoda, M.; Miyamoto, T. *Macromolecules* **1999,** 32, (11), 3553-3558.

72. David, A.; Kopeccková, P.; Rubinstein, A.; Kopecek, J. i. *Bioconjugate Chemistry* **2001,** 12, (6), 890-899.

73. David, A.; Kopecková, P.; Kopecek, J.; Rubinstein, A. *Pharmaceutical Research* **2002,** 19, (8), 1114-1122.

74. Montet, X.; Funovics, M.; Montet-Abou, K.; Weissleder, R.; Josephson, L. *Journal of Medicinal Chemistry* **2006,** 49, (20), 6087-6093.

75. Shamay, Y.; Paulin, D.; Ashkenasy, G.; David, A. *Journal of Medicinal Chemistry* **2009,** 52, (19), 5906-5915.

76. Sliedregt, L. A. J. M.; Rensen, P. C. N.; Rump, E. T.; van Santbrink, P. J.; Bijsterbosch, M. K.; Valentijn, A. R. P. M.; van der Marel, G. A.; van Boom, J. H.; van Berkel, T. J. C.; Biessen, E. A. L. *Journal of Medicinal Chemistry* **1999,** 42, (4), 609-618.

77. Sauter, N. K.; Bednarski, M. D.; Wurzburg, B. A.; Hanson, J. E.; Whitesides, G. M.; Skehel, J. J.; Wiley, D. C. *Biochemistry* **1989,** 28, (21), 8388-8396.

78. Matrosovich, M. N.; Mochalova, L. V.; Marinina, V. P.; Byramova, N. E.; Bovin, N. V. *FEBS Letters* **1990,** 272, (1-2), 209-212.

79. Bertozzi, C. R.; Kiessling, L. L. *Science* **2001,** 291, (5512), 2357-2364.

80. Lees, W. J.; Spaltenstein, A.; Kingery-Wood, J. E.; Whitesides, G. M. *Journal of Medicinal Chemistry* **1994,** 37, (20), 3419-3433.

81. Spaltenstein, A.; Whitesides, G. M. *Journal of the American Chemical Society* **1991,** 113, (2), 686-687.

82. McReynolds, K. D.; Gervay-Hague, J. *Chemical Reviews* **2007,** 107, (5), 1533-1552.

83. Yoshida, T.; Akasaka, T.; Choi, Y.; Hattori, K.; Yu, B.; Mimura, T.; Kaneko, Y.; Nakashima, H.; Aragaki, E.; Premanathan, M.; Yamamoto, N.; Uryu, T. *Journal of Polymer Science Part A: Polymer Chemistry* **1999,** 37, (6), 789-800.

84. Ringsdorf, H. *Journal of Polymer Science: Polymer Symposia* **1975,** 51, (1), 135-153.

85. Hopewell, J. W.; Duncan, R.; Wilding, D.; Chakrabarti, K. *Human & Experimental Toxicology* **2001,** 20, (9), 461-470. Spain, S. G., Cameron, N. R. *Polym. Chem.* **2011**, 2, 60-68.

86. Kikkeri, R.; Lepenies, B.; Adibekian, A.; Laurino, P.; Seeberger, P. H. *Journal of the American Chemical Society* **2009,** 131, (6), 2110-2112.

87. Niikura, K.; Nishio, T.; Akita, H.; Matsuo, Y.; Kamitani, R.; Kogure, K.; Harashima, H.; Ijiro, K. *ChemBioChem* **2007,** 8, (4), 379-384.

88. Robinson, A.; Fang, J.-M.; Chou, P.-T.; Liao, K.-W.; Chu, R.-M.; Lee, S.-J. *ChemBioChem* **2005,** 6, (10), 1899-1905.

89. Sun, X.-L.; Cui, W.; Haller, C.; Chaikof, E. L. *ChemBioChem* **2004,** 5, (11), 1593-1596.

90. Brandani, P.; Stroeve, P. *Macromolecules* **2004,** 37, (17), 6640-6643.

91. Huang, N.-P.; Michel, R.; Voros, J.; Textor, M.; Hofer, R.; Rossi, A.; Elbert, D. L.; Hubbell, J. A.; Spencer, N. D. *Langmuir* **2000,** 17, (2), 489-498.

92. Kenausis, G. L.; Voros, J.; Elbert, D. L.; Huang, N.; Hofer, R.; Ruiz-Taylor, L.; Textor, M.; Hubbell, J. A.; Spencer, N. D. *The Journal of Physical Chemistry B* **2000,** 104, (14), 3298-3309.

93. Lee, S.; Vörös, J. *Langmuir* **2005,** 21, (25), 11957-11962.

94. Tsukruk, V. V. *Progress in Polymer Science* **1997,** 22, (2), 247-311.

95. Luzinov, I.; Julthongpiput, D.; Malz, H.; Pionteck, J.; Tsukruk, V. V. *Macromolecules* **2000,** 33, (3), 1043-1048.

96. Minko, S.; Patil, S.; Datsyuk, V.; Simon, F.; Eichhorn, K.-J.; Motornov, M.; Usov, D.; Tokarev, I.; Stamm, M. *Langmuir* **2002,** 18, (1), 289-296.

97. Papra, A.; Gadegaard, N.; Larsen, N. B. *Langmuir* **2001,** 17, (5), 1457-1460.

98. Sofia, S. J.; Premnath, V.; Merrill, E. W. *Macromolecules* **1998,** 31, (15), 5059-5070.

99. Tran, Y.; Auroy, P. *Journal of the American Chemical Society* **2001,** 123, (16), 3644-3654.

100. Huang, W.; Skanth; Baker, G. L.; Bruening, M. L. *Langmuir* **2001,** 17, (5), 1731-1736.

101. Ito, Y.; Nishi, S.; Park, Y. S.; Imanishi, Y. *Macromolecules* **1997,** 30, (19), 5856-5859.

102. Lu, Y.; Mei, Y.; Walker, R.; Ballauff, M.; Drechsler, M. *Polymer* **2006,** 47, 4985.

103. Prucker, O.; Ruhe, J. *Macromolecules* **1998,** 31, (3), 592-601.

104. Suzuki, M.; Kishida, A.; Iwata, H.; Ikada, Y. *Macromolecules* **1986,** 19, (7), 1804-1808.

105. Barbey, R.; Lavanant, L.; Paripovic, D.; Schüwer, N.; Sugnaux, C.; Tugulu, S.; Klok, H.-A. *Chemical Reviews* **2009,** 109, (11), 5437-5527.

106. Barner, L. *Advanced Materials* **2009,** 21, (29), 1-7.

107. Matyjaszewski, K.; Xia, J. *Chemical Reviews* **2001,** 101, (9), 2921-2990.

108. Perrier, S.; Takolpuckdee, P. *Journal of Polymer Science Part A: Polymer Chemistry* **2005,** 43, (22), 5347-5393.

109. Posner, T. *Ber. Dtsch. Chem. Ges* **1905,** 38, 646-657.

110. Lowe, A. B. *Polymer Chemistry* **2010,** 1, (1), 17-36.

Chapter 2

Overview of this Thesis

This thesis contains four publications which are presented from chapter 3 to 6.

Glycopolymer-displaying nanospheres were prepared via the combination of emulsion polymerization and conventional or controlled radical polymerization to create a crosslinked core and glycopolymer shell, respectively. These particles show a high affinity to adsorb wheat germ agglutinin (WGA) and can act as carriers for catalytically active gold nanoparticles (Chapter 3).

By applying various grafting approaches glycopolymer chains were densely grafted from poly(divinylbenzene) microspheres to yield galactose-displaying particles. These spheres show a selective binding towards *Ricinus communis* agglutinin (Chapter 4).

Hyperbranched glycopolymer-displaying microspheres were prepared via self-condensing vinyl copolymerization (SCVCP). The incorporation of branch points directly affects the binding affinity of wheat germ agglutinin towards the glycopolymer-grafted particles (Chapter 5).

Magnetic, fluorescent glycopolymer-grafted silica particles were prepared via the combination of sequential RAFT polymerization and thiol-ene chemistry. These carbohydrate functionalized particles enabled the intranuclear imaging of lung cancer cells (Chapter 6).

In this chapter, an overview of the results obtained within this thesis is presented.

2.1 Glycopolymer-Grafted Polystyrene Nanospheres

This project focused upon the preparation of sugar-containing colloidal spherical polymer brushes by two different polymerization approaches. Photopolymerization and ATRP were used to attach glucose- and acetylglucosamine-displaying chains to colloidal polystyrene spheres by a "grafting from" approach. The synthesis of these particles was carried out in three steps: PS core particles were prepared by a conventional emulsion polymerization followed by the incorporation of an initiator and subsequent polymerization of the glycomonomer. A representative example for the synthesis of acetylglucosamine-displaying spheres is depicted in Scheme 1.

Scheme 1. Synthesis of the glucosamine-containing polymer brushes. After deprotection of the sugar moieties, hydrophilic sugar particles were displayed.

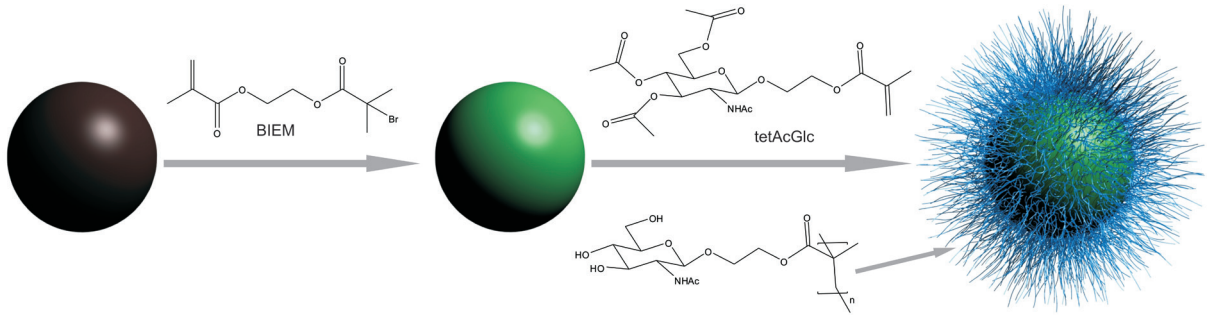

In contrast to conventional radical polymerization, the surface initiated ATRP ensured the growth of well-defined glycopolymer chains from the particle surface (PDI = 1.12). Figure 1 shows FESEM images for pure PS-DVB particles (A) and glycopolymer-grafted brushes (B), respectively. The rough surface and the increase in diameter can be attributed to the grafted glycopolymer chains. Furthermore, the successful attachment of glycopolymer chains was confirmed by IR-spectroscopy. The "grafting from" approach enabled a high grafting density of 0.54 chains per nm^2.

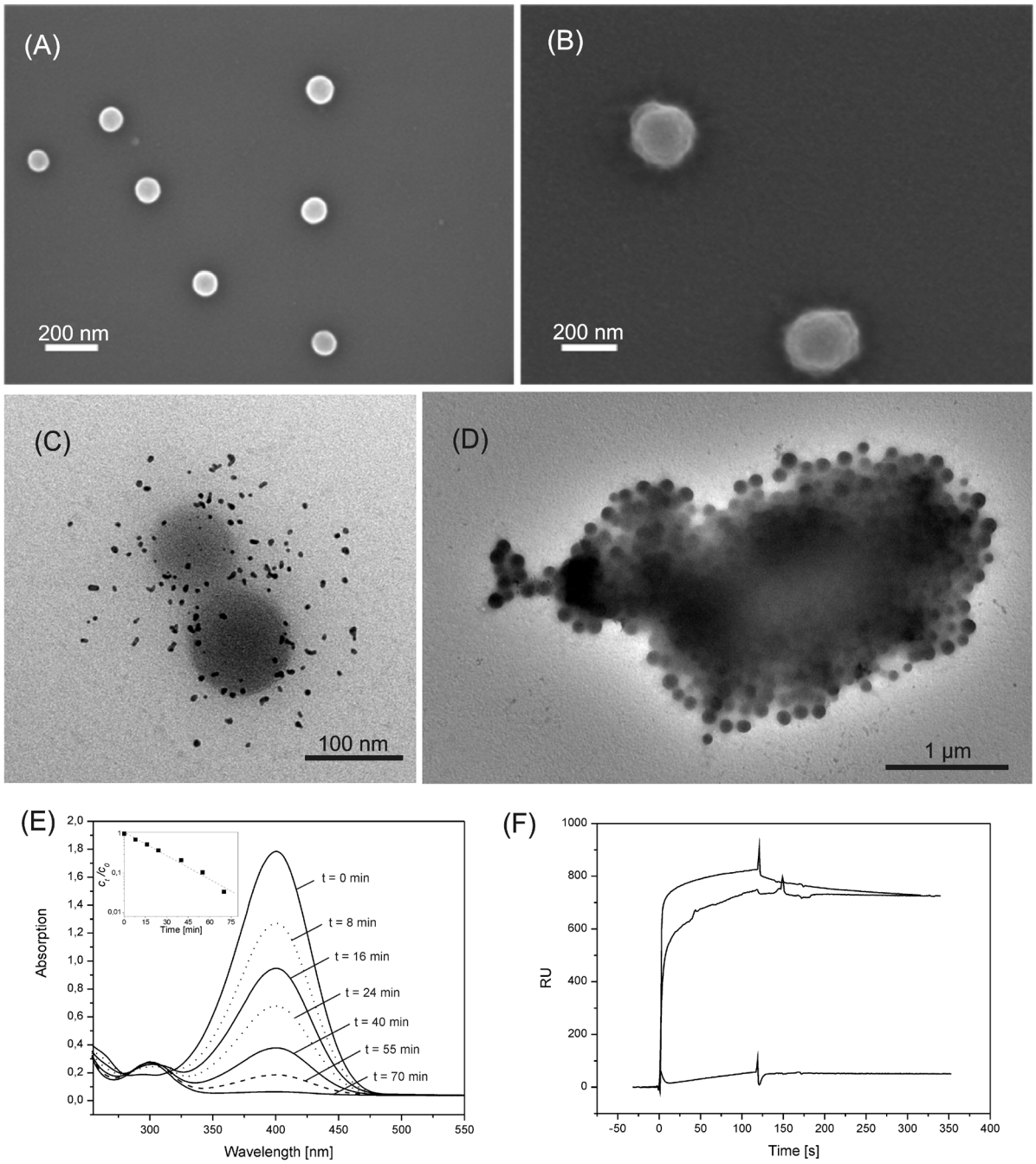

Figure 1. SEM images of (A) pure PS-DVB particles and (B) PS-DVB particles functionalized with protected glycopolymer brushes. TEM images of (C) immobilized gold nanoparticles and (D) WGA on glucosamine-displaying spheres. (E) UV/vis spectrum of catalytic reduction of *p*-nitrophenol in the presence of gold nanocomposite particles and $NaBH_4$. (F) Biacore sensograms of the interaction between linear poly-(*N*-acetylglucosamine) chains (top curve), glycopolymer brushes (middle curve) and *N*-acetylglucosamine sugar unimer (bottom curve) with WGA.

Deprotection of the sugar moieties yielded particles with a high density of hydroxyl groups that could be used to stabilize gold nanoparticles to create carriers for catalytically active gold nanoparticles. The addition of $HAuCl_4$ to an aqueous solution of sugar containing polymer brushes and subsequent reduction of the $AuCl_4^-$ ions by $NaBH_4$ led to the formation

of gold nanoparticles with an average diameter of 6.3 nm within the glycopolymer shell (Figure 1C). The catalytic reduction of *p*-nitrophenol in the presence of gold nanocomposite particles was successfully monitored by UV/vis spectroscopy (Figure 1E). The reaction follows first order rate kinetics with regard to the *p*-nitrophenol concentrations as the concentration of sodium borohydride was adjusted to largely exceed the concentration of *p*-nitrophenol. Thus, a linear relation between $\ln(c_t/c_0)$ versus time *t* has been obtained as shown in the inset of Figure 1E. This demonstrates the capability of the glycopolymer-displaying polymer brushes to act as biocompatible carriers for catalytically active gold nanoparticles.

Investigation of the recognition properties of *N*-acetylglucosamine chains towards lectins via turbidity measurements revealed a selective binding towards the lectin wheat germ agglutinin (WGA) whereas no binding to bovine serum albumin (BSA) or peanut agglutinin (PNA) could be observed. Surface plasmon resonance (SPR) spectroscopy was performed to investigate the association behavior of linear poly(*N*-acetylglucosamine), glycopolymer brush and *N*-acetyl-glucosamine sugar unimer (Figure 1 F). In comparison to linear glycopolymers, spherical brushes show a reduced adsorption to the immobilized lectin, which can be attributed to the fact that the sugar residues next to the core are not available to bind the protein, due to steric hindrance, as well as the reduction of the total mass of sugar-units due to introduction of the polystyrene core. Nevertheless both show adsorptions magnitudes higher than the unimer.

Addition of WGA to the polymer brushes in solution led to the fast formation of large aggregates, whereby UV/vis spectroscopy measurements revealed that 1 mg of glycopolymer brush is able to precipitate 0.5 mg of wheat germ agglutinin. The lectin-polymer brush agglomerates are depicted in Figure 1D.

2.2 Surface Modification of Polymeric Microspheres using Glycopolymers for Biorecognition

Research on core-shell microspheres covered with functional material is a topic of intense current research interest. Among others, cross-linked microspheres based on poly(divinylbenzene) (PDVB) are highly attractive because of their residual double bonds on the surface of the particle which can be easily used to attach single molecules or polymer chains to the surface by various grafting approaches. The aim of this project was the synthesis of two glycopolymer-containing core-shell microspheres by grafting either 6-*O*-methacryloyl mannose (MAMan) (Scheme 1, path a) or 6-*O*-methacryloyl-1,2;3,4-di-*O*-isopropylidene-galactopyranose (MAIGal) (Scheme 1, path b) from the particle surface. In case of MAIGal, three different grafting approaches were utilised, with special emphasis being put on the resulting grafting densities.

Scheme 1. Synthesis of glycopolymer-grafted DVB microspheres.

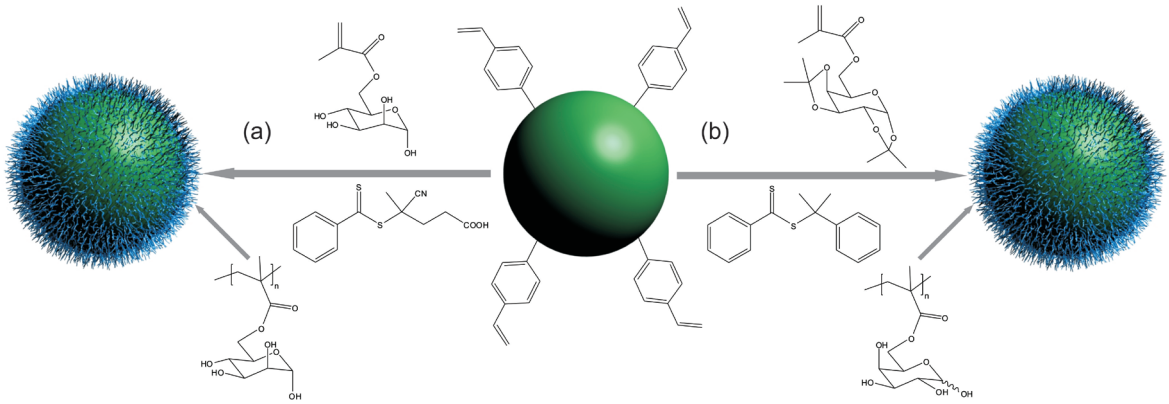

Without the use of protecting group chemistry, RAFT polymerization was the polymerization technique of choice to yield well-defined unprotected PMAMan glycopolymers. Applying the “grafting through” approach, PDVB microspheres covered with a dense shell of mannose-displaying glycopolymer were achieved. Glycopolymer chains were found to be densely grafted through the microspheres (0.43 chains per nm^2 surface area). Scanning electron microscopy (SEM) was used to visualize the particles before (Figure 1, left) and after (Figure 1, right) grafting glycomonomer from the surface. A much rougher surface can be observed in the case of the mannose covered microspheres.

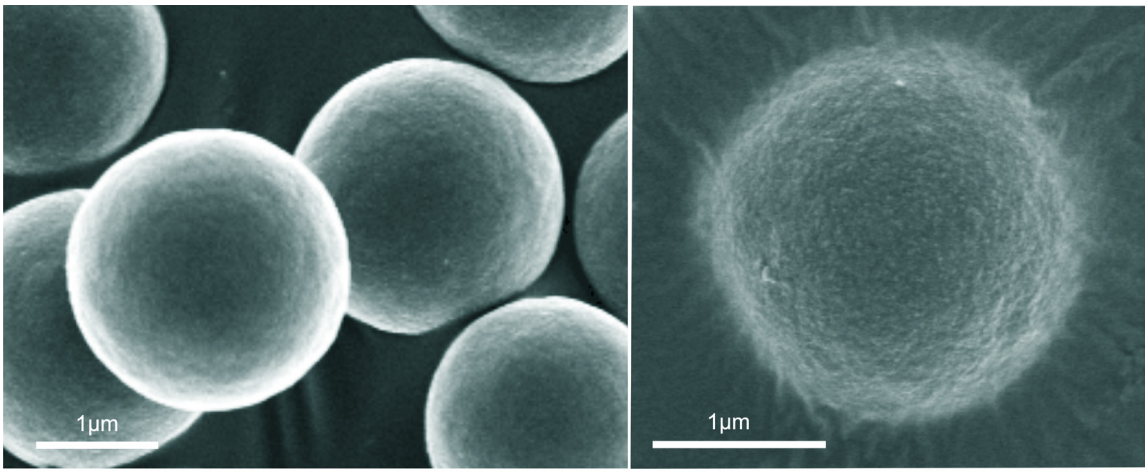

Figure 1. Scanning electron microscopy images of blank (left) and MAMan grafted (right) microspheres.

Lectin interaction studies of mannose-containing polymer revealed no binding towards a series of lectins, suggesting that the esterification of the 6-carbon position of the mannose molecule to form the glycomonomer inhibited its binding to these proteins. Because of the loss of binding ability, we investigated the use of another glycomonomer based on a protected galactose unit for the preparation of sugar-containing microspheres.

For the preparation of the galactose covered spheres we performed three different approaches to affix glycopolymer chains to the particle surface, whereby RAFT polymerization has been used to prepare the glycopolymer chains. Approach 1 was conducted in a similar way to the preparation of the mannose containing microspheres. This "grafting through" technique yielded galactose-displaying particles with a grafting density of 0.22 chains per nm^2. Approach 2, a "grafting from" approach, consisted of prior modification of the particle surface by attaching the chain transfer agent. The calculation of the grafting density led to a surface coverage of 0.35 chains per nm^2, a 1.6 times higher grafting density compared to the first approach. In Approach 3, a strict "grafting onto" technique was used. The use of thiol-ene chemistry showed the lowest grafting density (0.20 chains per nm^2).

After deprotection of the sugar moieties, the galactose-displaying polymer displayed selective binding towards *Ricinus communis* agglutinin (RCA_{120}) whereas no binding to Concanavalin A (Con A) or Bovine serum albumin (BSA) occurred. UV/vis spectroscopy measurements revealed that each grafted glycopolymer chain is capable of binding to 0.7 molecules of RCA_{120}. The particles were found to have a superior binding affinity towards RCA_{120} in comparison to microspheres covered with galactose unimers. Even though

galactose units next to the core are not accessible for binding, the overall amount of bound lectin is four times higher. SEM images of the galactose- and the lectin-galatose-covered microspheres can be seen in Figure 2.

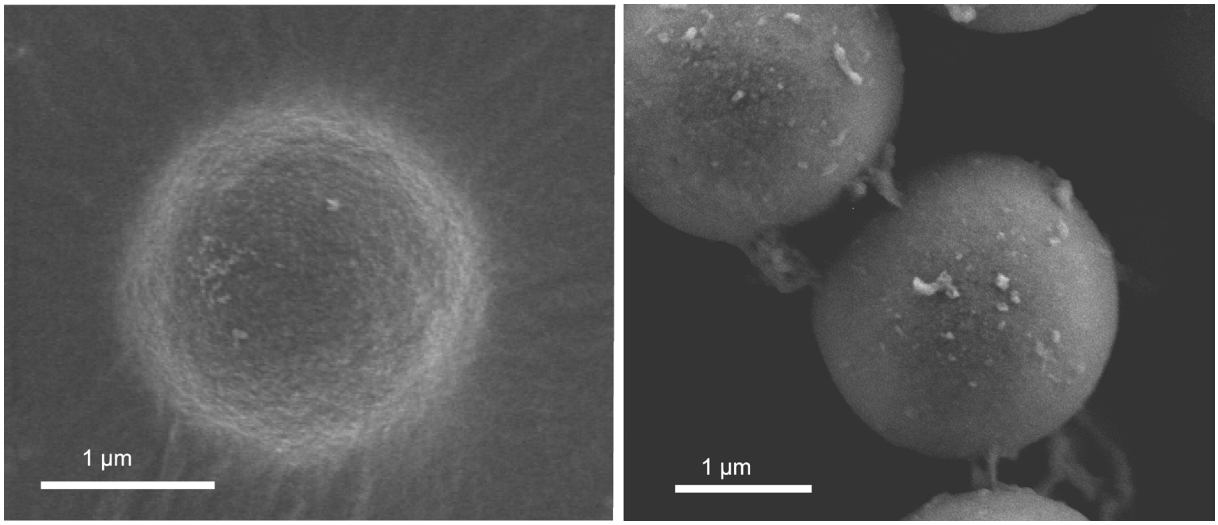

Figure 2. SEM images of galactose-grafted microspheres (left) and protein-microsphere agglomerates (right).

2.3 Hyperbranched Glycopolymer-Grafted Microspheres

The scope of this project was to create core-shell particles covered with three-dimensional glycopolymer structures to investigate the influence of the glycopolymer architecture towards the binding affinity to WGA. The synthesis of highly branched glycopolymers was achieved by atom transfer radical polymerization (ATRP) of the methacrylic AB* initiator-monomer (inimer) 2-(2-bromoisobutyryloxy)ethyl methacrylate (BIEM) and the protected methacrylic acetylglucosamine-displaying glycomonomer 1-methacryloyloxyethyl 2-acetamido-2-deoxy-3,4,6-triacetyl-glucopyranoside (tetAcGlc) via self-condensing vinyl copolymerization (SCVCP) as depicted in Scheme 1.

Scheme 1. General Route towards branched glycopolymers via SCVCP.

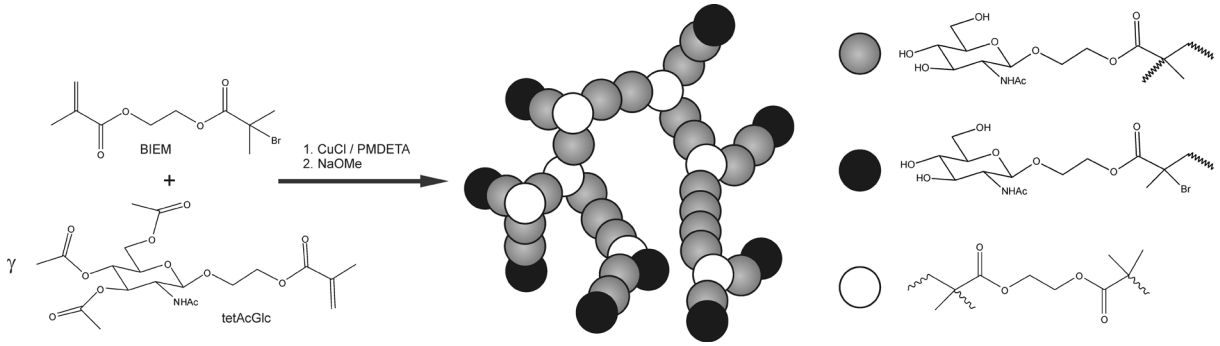

Prior to the surface grafting of hyperbranched glycopolymers to PDVB microspheres, the formation of ungrafted hyperbranched glycopolymers of different glycomonomer-to-inimer ratios (γ) via SCVCP was investigated. First-order kinetic plots of the prepared branched glycopolymers revealed a decreasing apparent rate of polymerization k_{app} with increasing content of BIEM in the feed (Figure 1). Although more initiator groups were introduced with decreasing γ, the lower k_{app} indicates a fast formation of macroinimers but slow condensation of these macroinimers with each other.

The dependence of the Mark-Houwink exponent α on the theoretical fraction of branch points is depicted in Figure 2. The decrease of the Mark-Houwink exponent α from γ = 15 to γ = 1 confirms the increase of branch points with increasing amount of BIEM in the feed.

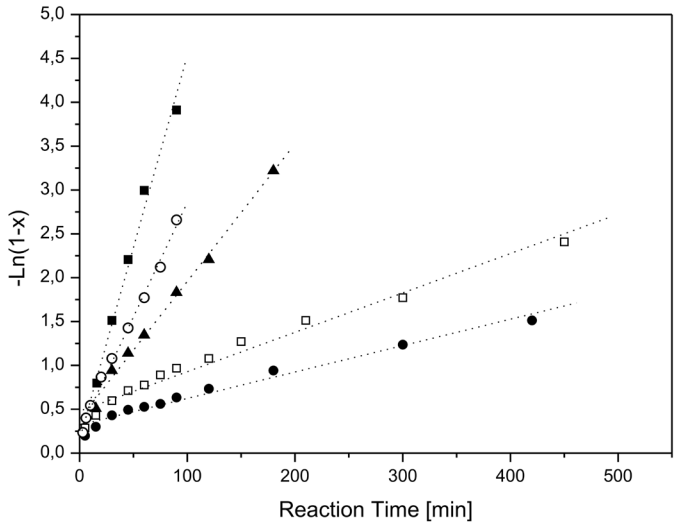

Figure 1. First-order kinetic plots for the SCVCP of BIEM and tetAcGlc at different comonomer ratios γ. Filled squares: γ = 15, filled triangles: γ = 5, open squares: γ = 2 and filled circles: γ = 1. The ATRP of linear PtetAcGlc with a monomer to initiator ratio $[tetAcGlc]_0/[EBIB]_0$ = 100 is given for comparison (open circles).

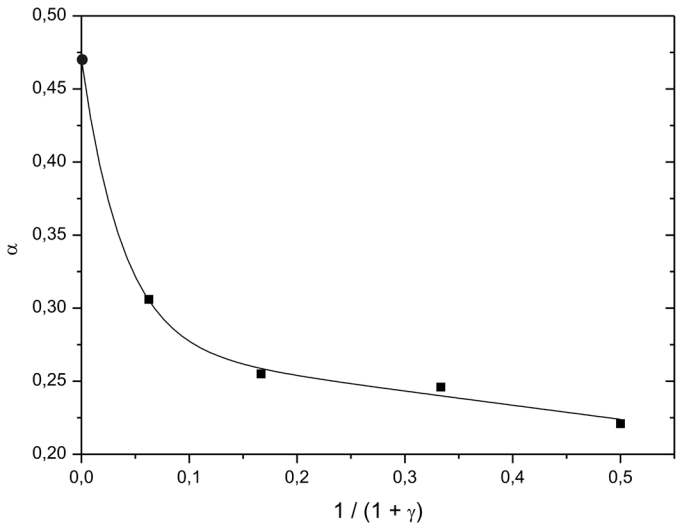

Figure 2. Dependence of the Mark-Houwink exponent α on the comonomer ratio γ. Filled square: mixture of linear PtetAcGlc with different molecular weights.

The successful pathway towards hyperbranched glycopolymers was adapted to create core-shell particles consisting of PDVB microspheres onto which hyperbranched polymers have been grafted (Scheme 2, path b). Furthermore, microspheres covered with linear acetylglucosamine-displaying polymer have been prepared via ATRP (Scheme 2, path a) to compare the different particles in terms of surface coverage and binding affinity towards WGA.

Scheme 2. Synthesis of linear (path a) and hyperbranched (path b) glycopolymer covered microspheres.

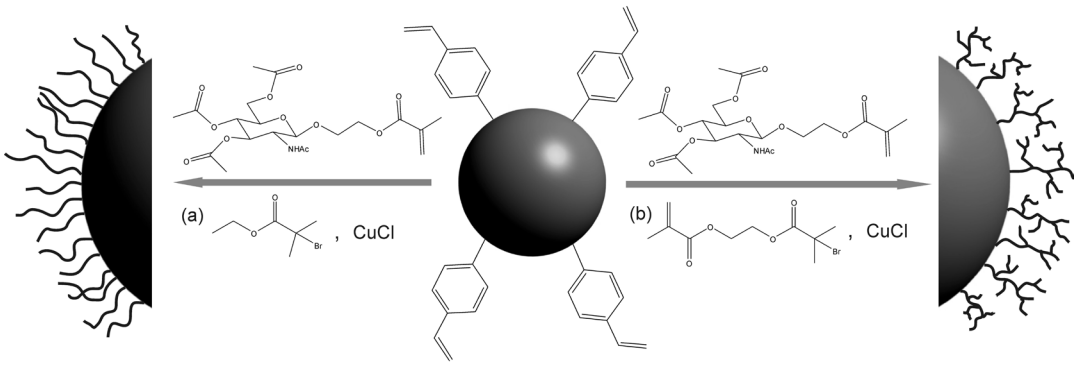

After elemental analysis of the different polymer grafted spheres to determine the oxygen content, one can calculate the amount of grafted copolymer. It was found, that an increase in incorporated inimer, which results in more compact and branched structures, directly leads to an increase in particle coverage (1.6 – 2.4 wt.-%).

Deprotection of the sugar moieties led to acetylglucosamine-displaying spheres that could be easily dispersed in water and therefore enabled the investigation of the binding behavior of these sugar-covered microspheres towards the lectin WGA. UV/vis spectroscopy measurements revealed that with increasing content of BIEM in the copolymer, the amount of adsorbed protein per mg of grafted acetylglucosamine on the sphere increased. The incorporation of approximately 50% of the hydrophobic linker BIEM for γ = 1 led to an increase in adsorption of 26% compared to the branched glycopolymer with γ = 5 and 16% compared to the linear glycopolymer grafted particles.

SEM images of the ungrafted and grafted microspheres are shown in Figure 3. After adsorption of wheat germ agglutinin, more organic matter covered the spheres, and marked agglutination of the spheres is clearly visible.

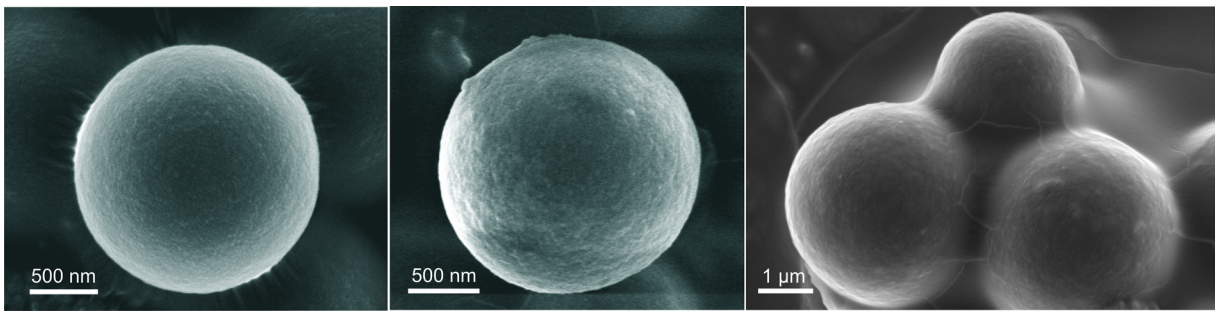

Figure 3. SEM images of (left) ungrafted and glycopolymer grafted (γ = 1) microspheres (middle) before and (right) after addition of wheat germ agglutinin.

2.4 Magnetic, Fluorescent Glycopolymer Hybrid Nanoparticles for Intranuclear Optical Imaging

This project comprised the synthesis of fluorescent, magnetic galactose-displaying core-shell nanospheres by grafting a glycocopolymer consisting of 6-*O*-methacryloyl-galactopyranose (MAGal) and 4-(pyrenyl)butyl methacrylate (PyMA) onto silica-encapsulated iron oxide particles (Scheme 1). The surface modification of functional particles with carbohydrates should not only improve the biocompatibility and solubility, but also have an influence on the cellular uptake of the particles.

Scheme 1. Synthesis of glycopolymer-grafted magnetic, fluorescent nanoparticles.

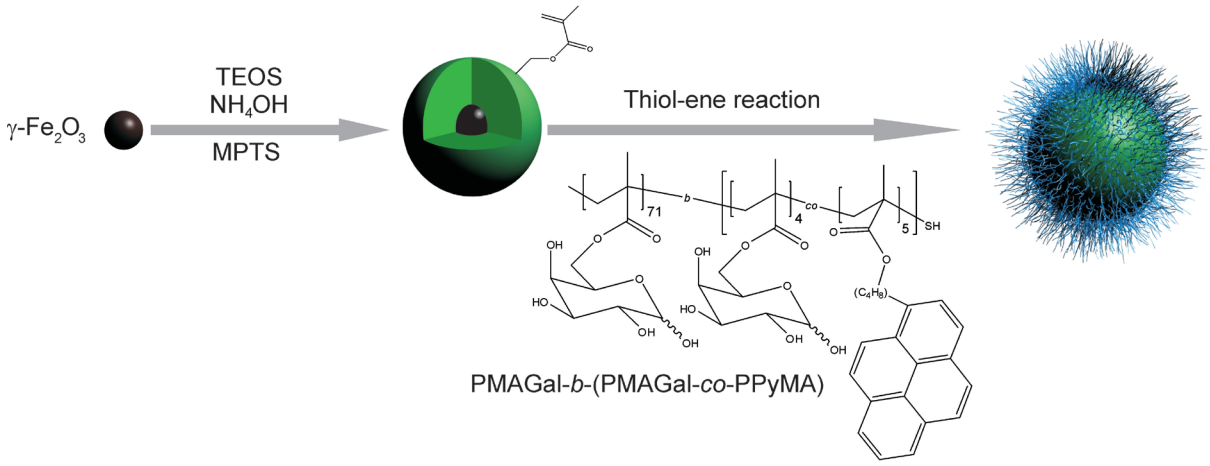

To create a fluorescent glycopolymer that can be attached onto silica spheres, we performed sequential RAFT polymerization of a protected glycomonomer and a fluorescent pyrene-carrying methacrylate, followed by the deprotection of the sugar moieties under acidic conditions. After aminolysis of the RAFT agent, the formed thiol end group is able to react with the double-bond bearing silica particles via Michael addition. The successful attachment of the fluorescent glycocopolymer chains to the surface of the magnetic silica spheres was confirmed by UV/vis spectroscopy measurements and vibrating sample magnetometry (VSM, Figure 1). The resulting magnetization curves indicate that neither the encapsulation of the maghemite particles with silica nor the grafting of glycocopolymer chains had a significant influence on the superparamagnetic properties.

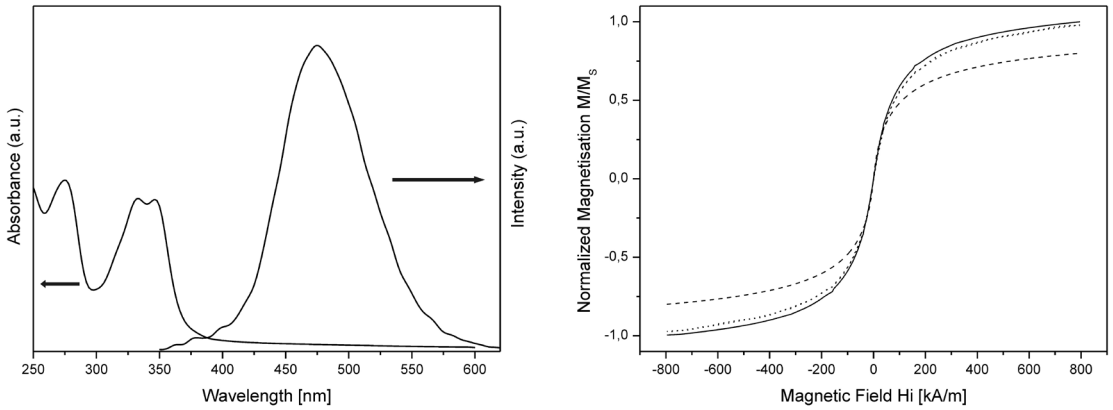

Figure 1. (Left) UV/vis absorption and fluorescence spectra of glycocoplymer-grafted nanospheres. (Right) Magnetic hysteresis curves of γ-Fe_2O_3 nanoparticles (solid line), silica encapsulated γ-Fe_2O_3 particles (dotted line) and glycocoplymer grafted nanospheres (dashed line).

The incorporation of pyrene into the core-shell particles allows their localization within cells by microscopy experiments as pyrene is a fluorescent dye with a high quantum yield and is stable against photobleaching. In fact the particles could be localised in cells (adenocarcinomic human alveolar basal epithelial cells (A549)) using both epifluorescence and confocal microscopy. Moreover, epifluorescence microscopy images (Figure 2, A-D) showed the preferential location of the nanospheres next to and within the cell nucleus, the membrane of which was stained with anti-NUP98-FITC (Figure 2 C and F). Confocal microscopy experiments confirmed the presence of the glycocopolymer grafted magnetic particles within the cell nucleus (Figure 2, E-G); confocal z-stacks proved that the particles were indeed located inside the cells and not stacked to the cell surface.

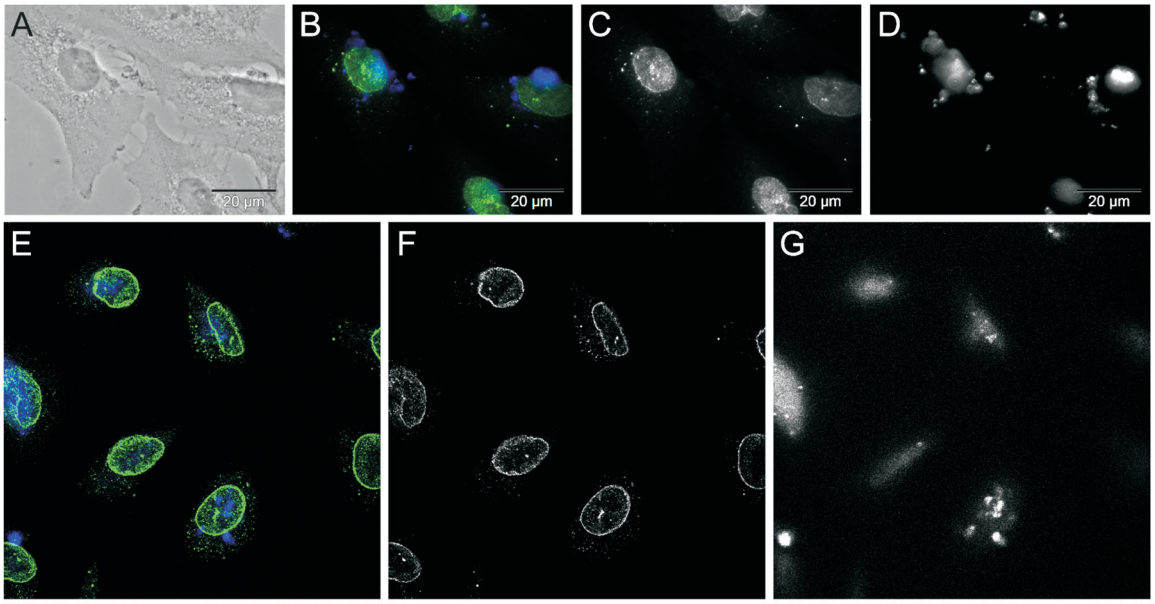

Figure 2. Microscope images of A549 cells exposed to glycopolymer-grafted nanoparticles: (A-D) epifluorescence microscope, (E-G) confocal microscope. (A) transmission image of cells, (B, E) merged fluorescence images, (C, F) fluorescence image that exclusively shows the green light emitting parts (nuclear membrane) and (D, G) blue (pyrene) emitting part (glycocopolymer covered nanospheres).

As both glycoconjugates and carbohydrate-binding proteins are omnipresent in the cytoplasm and the nucleus, the galactose moieties in the outer sphere of the nanoparticle could have caused their nuclear uptake. A member of the galectin family, known for its binding affinity towards β-galactosides, might be the responsible lectin in this context.

2.5 Individual Contributions to Joint Publications

The results presented in this thesis were obtained in collaboration with others, and have been published or are submitted to publication as indicated below. In the following, the contributions of all the coauthors to the different publications are specified. The asterisk denotes the corresponding author.

Chapter 3

This work is published in *Macromol. Biosci.*, 2011, 11, 199-210 under the title:

"Glycopolymer-Grafted Polystyrene Nanospheres"

by André Pfaff, Vaishali S. Shinde, Yan Lu, Alexander Wittemann, Matthias Ballauff and Axel H. E. Müller*

I conducted all experiments and wrote the publication.

Exceptions are stated in the following:

Vaishali S. Shinde performed the experiments regarding the photopolymerization towards glycopolymer-grafted nanospheres and was involved in the discussion.
Yan Lu prepared the ungrafted polystyrene particles and was involved in the discussion.
Alexander Wittemann was involved in the discussion.
Matthias Ballauff and Axel H. E. Müller were involved in the discussion and corrections of this manuscript.

Chapter 4

This work is published in *Eur. Polym. J.*, 2011, 47, 805-815 under the title:

"Surface Modification of Polymeric Microspheres using Glycopolymers for Biorecognition"

by André Pfaff, Leonie Barner, Axel H. E. Müller* and Anthony M. Granville*

I conducted all experiments and wrote the publication.

Exceptions are stated in the following:

Leonie Barner was involved in the discussion.

Axel H. E. Müller and Anthony M. Granville were involved in discussion and corrections of this manuscript.

Chapter 5

This work is published in *Macromolecules*, 2011, 44, 1266-1272 under the title:

"Hyperbranched Glycopolymer-Grafted Microspheres"

by André Pfaff and Axel H. E. Müller*

I conducted all experiments and wrote the publication.

Exceptions are stated in the following:

Axel H. E. Müller was involved in discussion and corrections of this manuscript.

Chapter 6

This work is submitted to *Biomacromolecules* under the title:

"Magnetic, Fluorescent Glycopolymer Hybrid Nanoparticles for Intranuclear Optical Imaging"

by André Pfaff, Anja Schallon, Thomas M. Ruhland, Alexander P. Majewski, Holger Schmalz, Ruth Freitag and Axel H. E. Müller*

I conducted all experiments and wrote the publication.

Exceptions are stated in the following:

Anja Schallon performed epifluorescence microscope measurements and was involved in the discussion.
Thomas M. Ruhland was involved in the discussion.
Alexander P. Majewski prepared the iron oxide particles and was involved in the discussion.
Holger Schmalz was involved in the discussion.
Ruth Freitag and Axel H. E. Müller were involved in the discussion and corrections of this manuscript.

Chapter 3

Glycopolymer-Grafted Polystyrene Nanospheres

André Pfaff,[1] Vaishali S. Shinde,[1,2] Yan Lu,[3,4] Alexander Wittemann,[4]

Matthias Ballauff[3,4] and Axel H. E. Müller[1*]

[1] Makromolekulare Chemie II and [4] Physikalische Chemie I,

Universität Bayreuth, 95440 Bayreuth, *axel.mueller@uni-bayreuth.de*

[2] Department of Chemistry, University of Pune, Pune 411007, Maharashtra, India

[3] Soft Matter and Functional Materials, Helmholtz-Zentrum Berlin für Materialien und Energie GmbH, 14109 Berlin

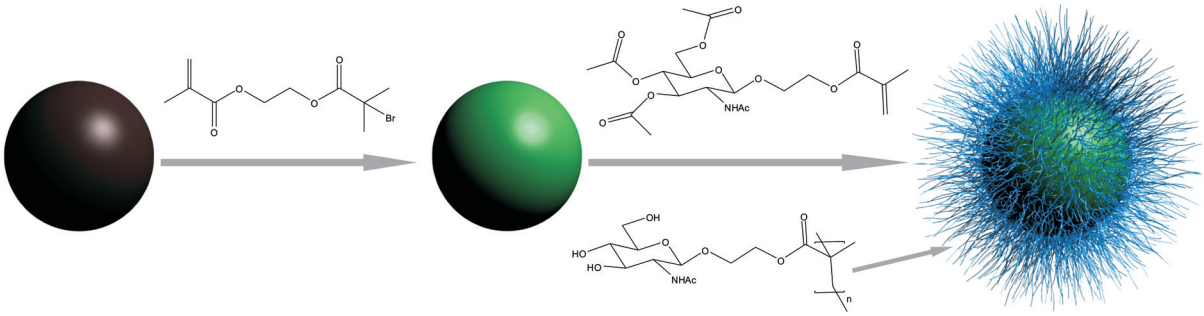

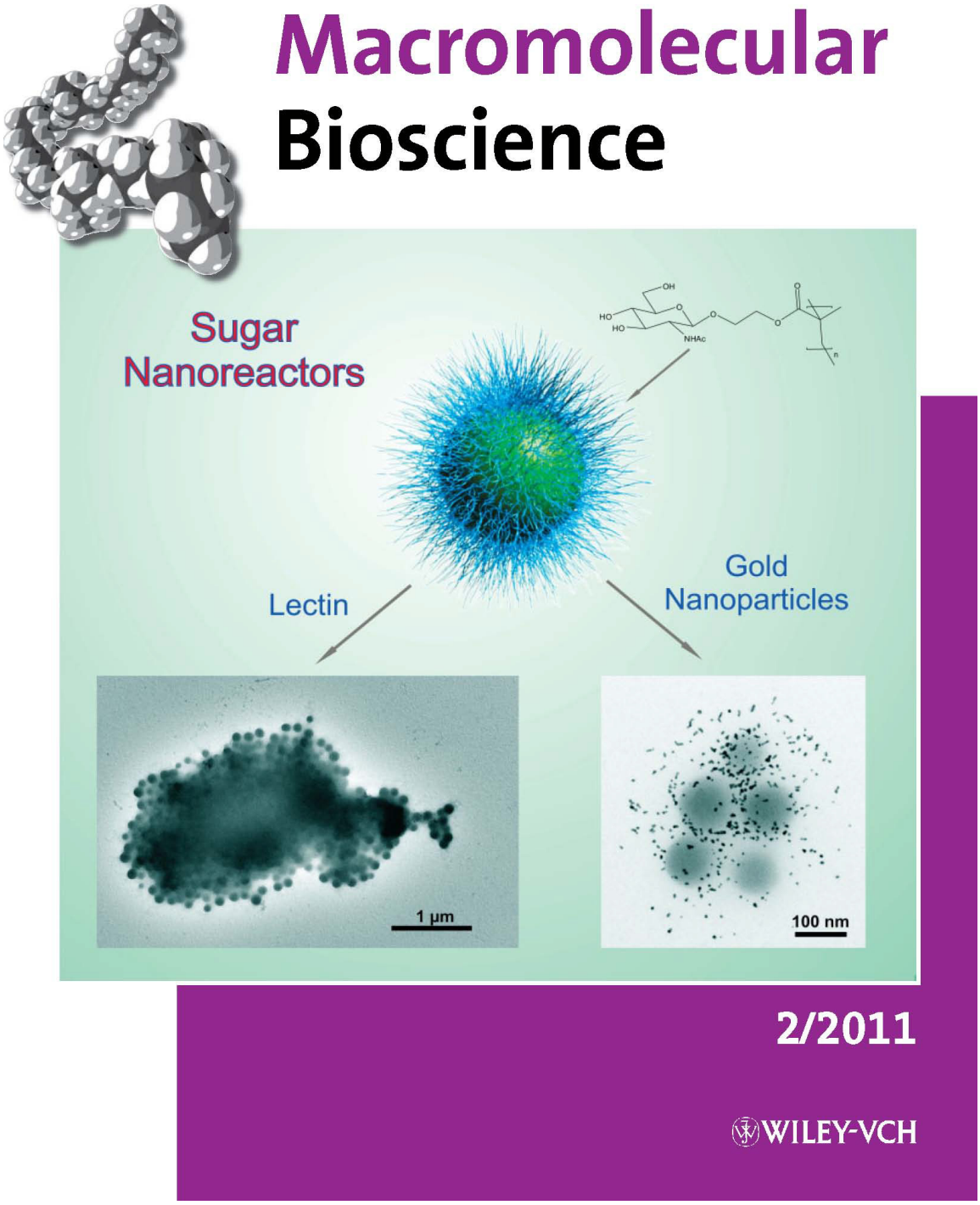
Macromolecular
Bioscience
Sugar
Nanoreactors
Lectin
Gold
Nanoparticles
1 µm
100 nm
2/2011
WILEY-VCH

Abstract

The synthesis and characterization of spherical sugar-containing polymer brushes consisting of PS cores onto which chains of sugar-containing polymers have been grafted via two different techniques are described. Photopolymerization in aqueous dispersion using the functional monomer MAGlc and crosslinked or non-crosslinked PS particles covered with a thin layer of photo-initiator yielded homogeneous glycopolymer brushes attached to spherical PS cores. As an alternative, ATRP was used to graft poly(*N*-acetylglucosamine) arms from crosslinked PS cores. Deprotection of the grafted brushes led to water-soluble particles that act as carriers for catalytically active gold nanoparticles. These glycopolymer chains show a high affinity to adsorb WGA whereas no binding to BSA or PNA could be detected.

Keywords: Atom Transfer Radical Polymerization (ATRP); glycopolymer; gold nanoparticles; lectin recognition; spherical brush

3.1 Introduction

Glycopolymers, synthetic sugar-containing macromolecules, which display complex functionalities similar to those found in natural glycoconjugates are attracting ever-increasing interest from the chemistry community due to their role as biomimetic analogues and their potential for commercial applications.[1-5] They are used as surfactants,[6] texture-enhancing food additives,[7] drug release systems,[8, 9] and biologically active polymers.[10, 11] It is now clear that structural control of glycopolymers has a significant impact on their recognition functions, which has prompted researchers to develop new synthetic routes to a variety of sugar-displaying polymers with controlled architectures and functionalities.[12-14] Various types of synthetic polymers bearing sugar residues have been described, such as linear polymers,[15] comb polymers,[16] dendrimers,[17] and crosslinked hydrogels.[18]

In particular, carbohydrate-modified vinyl polymers have been extensively investigated because of their relatively simple synthesis via radical polymerization. In this case, controlled/"living" radical polymerizations have been reported as a very facile approach for well-defined and controlled synthesis of glycopolymers.[19-23]

In this paper, we describe the synthesis of sugar-containing colloidal spherical polymer brushes by two different polymerization approaches. Photopolymerization of the

functional monomer 3-*O*-methacryloyl-*D*-glucose (MAGlc) was used to attach glycopolymer chains to colloidal polystyrene (PS) spheres by a "grafting from" technique.[24, 25] As shown in Scheme 1, the synthesis of these particles can be carried out in three steps: In the first step, PS core particles are prepared by a conventional emulsion polymerization.[26] In the second step of emulsion polymerization, these core particles are covered by a thin layer of the photo-initiator 2-[*p*-(2-hydroxy-2-methylpropiophenone)]-ethyleneglycol methacrylate (HMEM). In the third step, polymerization of MAGlc is started by UV irradiation of the suspension of these latex particles. By this grafting-from strategy sugar-displaying polymer brushes are generated on the surface of the core particles.

Scheme 1. Synthesis of the sugar-displaying polymer brush via photo-induced free radical polymerization.

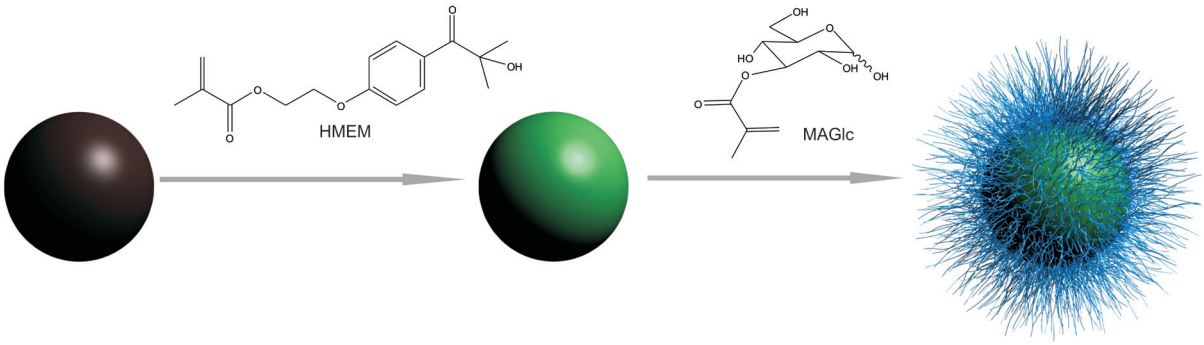

The use of an unprotected functional monomer for the preparation of polymer brushes by means of photopolymerization avoided potentially damaging deprotection steps. Moreover, crosslinked PS core particles covered with a thin layer of photo-initiator were used for the first time for photopolymerization. Until now, all spherical polymer brush systems reported by Ballauff and coworkers are limited to water-soluble monomers in aqueous condition.[27-29] The use of crosslinked PS core particles makes the photopolymerization also possible for water insoluble monomers in organic solvents.

The increase with time of PS-MAGlc particle size under UV-irradiation was studied by means of dynamic light scattering (DLS), whereas cryogenic transmission electron microscopy (cryo-TEM) was the method of choice to study the morphology of the brushes in situ. All data discussed herein, demonstrate the successful preparation of glucose-displaying polymer brushes by photopolymerization.

Furthermore, we investigated the use of a protected glycomonomer, tetraacetylglucosamine (tetAcGlc), and a controlled radical polymerization technique,

namely atom transfer radical polymerization (ATRP), to create spherical polymer brushes with well-defined poly-(*N*-acetylglucosamine) arms. Using the "grafting from" approach, chains were grown from a crosslinked polystyrene core covered with a thin layer of ATRP initiator (Scheme 2). The subsequent deprotection of the sugar units led to water soluble spherical brushes consisting of poly-(*N*-acetyl-*D*-glucosamine) chains.

Scheme 2. Synthesis of the glucosamine-containing polymer brushes via emulsion polymerization and subsequent ATRP. After deprotection of the sugar moieties, hydrophilic sugar particles were obtained.

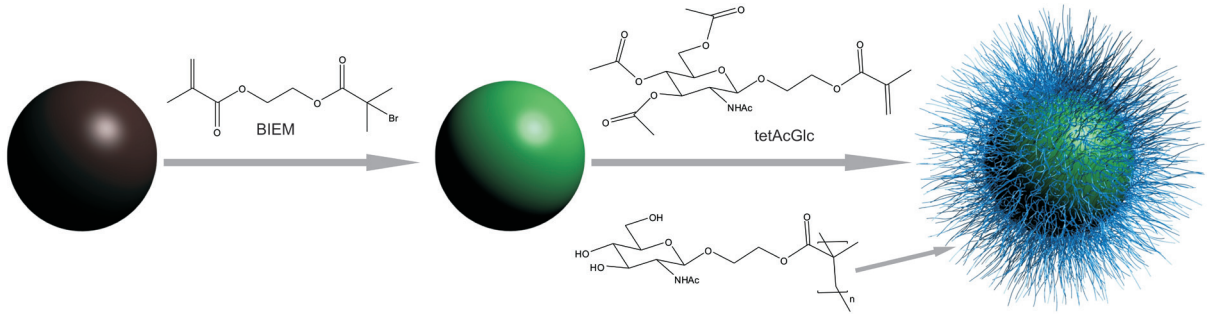

One motivation for the preparation of these sugar-containing polymer brushes was to investigate whether these brushes could act as carriers for catalytically active gold nanoparticles. In general, gold nanoparticles are of special interest because of their potential applications in electronic, optical and biomedical materials.[30-35]

Apart from this, glycopolymers are of great interest because of binding interactions between carbohydrates and lectins. Interactions between saccharides and proteins are usually weak but can be markedly increased by displaying multiple saccharides in close proximity to each other, yielding multivalent binding sites, commonly known as the "glyco-cluster effect".[36] Therefore, we were interested in developing polymerization methodology capable of producing poly-(*N*-acetylglucosamine) chains as glycomimetics, and subsequently in investigating their binding behavior to wheat germ agglutinin (WGA) using turbidity measurements and surface plasmon resonance (SPR) spectroscopy.

3.2 Experimental Section

Materials.

Bovine Serum Albumin (BSA; 66 kDa, 96%, Aldrich), Wheat Germ Agglutinin (WGA; 36 kDa, Aldrich), Peanut Agglutinin (PNA; 110 kDa, Aldrich), 4-(2-hydroxyethyl)piperazine-1-ethansulfonic acid (HEPES, 99%, Aldrich), 2-acetamido-1,3,4,6-tetra-*O*-acetyl-2-deoxy-*D*-glucopyranose (99%, Glycon), 1,2:5,6-di-*O*-isopropylidene-*D*-glucofuranose (Aldrich), methacrylic anhydride (Aldrich), trimethylsilyl trifluoromethanesulfonate (98%, Aldrich), CuCl (99%, Acros), 10-camphorsulfonic acid (98%, Aldrich), hydroxyethyl methacrylate (98%, Acros), sodium dodecyl sulfate (SDS; Fluka) and peroxodisulfate (KPS; Fluka) were used without further purification. Styrene (BASF) was destabilized by Al_2O_3 column and stored in the refrigerator. *N,N,N´,N´´,N´´*-pentamethyldiethylenetriamine (PMDETA; 99%, Aldrich), 1,1,4,7,10,10-hexamethyltriethylenetetramine (HMTETA; 97%, Aldrich), divinylbenzene (DVB, Aldrich) and ethyl 2-bromoisobutyrate (EBiB; 98%, Aldrich) were distilled and degassed. CM-5 Sensor chip and the amine coupling kit containing NHS, EDC and ethanolamine-hydrochloride for interaction studies, were purchased from Biacore AB. Tris(2-(dimethylamino)ethyl)amine (Me_6 TREN) was synthesized according to the method described by Ciampolini et al.[37] The synthesis of 2-[*p*-(2-hydroxy-2-methylpropiophenone)]-ethyleneglycol methacrylate (HMEM) has been described previously.[38] The sugar-based functional monomer MAGlc was synthesized by deprotection of 3-*O*-methacryloyl-1,2:5,6-di-*O*-isopropylidene-*D*-glucofuranoside (MAIGlc) as reported by Teunis.[39] The 2-step synthesis of the protected glycomonomer tetAcGlc was carried out according to literature: after formation of the intermediate 2-Methyl-2-(3,4,6-tri-O-acetyl-1,2-dideoxy-α-D-glucopyrano)-[2,1-d]-2-oxazoline,[40] the final product could be achieved by a ring opening reaction with hydroxyethyl methacrylate.[41] The synthesis of methacrylic inimer 2-(2-bromoisobutyryloxy)ethyl methacrylate (BIEM) was carried out according to the method described earlier.[42, 43]

Characterization.

Dynamic light scattering (DLS) measurements were performed in sealed cylindrical scattering cells (d = 10 mm) at a scattering angle of 90° on an ALV DLS/SLS-SP 5022F equipment

consisting of an ALV-SP 125 laser goniometer with an ALV 5000/E correlator and a He-Ne laser with the wavelength λ = 632.8 nm. The CONTIN algorithm was applied to analyze the obtained correlation functions. Apparent hydrodynamic radii were calculated according to the Stokes-Einstein equation. Prior to the light scattering measurements the sample solutions were filtered using Millipore PTFE filters with a pore size of 5 µm.

Gel permeation chromatography (GPC) measurements were performed on a set of 30 cm SDV-gel columns of 5 µm particle size having a pore size of 10^2, 10^3, 10^4 and 10^5 Å with refractive index and UV (λ = 254 nm) detection. GPC was measured at an elution rate of 1 mL/min with THF as solvent. GPC with a multiangle light scattering detector (MALS-GPC) was used to determine the absolute molecular weights. THF was used as eluent at a flow rate of 1.0 mL/min: column set, 5µm PSS SDV-gel 10^3, 10^5 and 10^6 Å, 30 cm each; detectors, Agilent Technologies 1200 Series refractive index detector and Wyatt HELEOS MALS detector equipped with a 632.8 nm He-Ne laser. The refractive index increments of the different polymers in THF at 25 °C were measured using a PSS DnDc-2010/620 differential refractometer.

NMR-spectroscopy: ^{1}H and ^{13}C NMR spectra were recorded on a Bruker 300 AC spectrometer using $CDCl_3$ or DMSO-d_6 as solvent and internal solvent signal.

Fourier-Transform Infrared Spectroscopy (FT-IR) was carried out on a Spectrum 100 FT-IR spectrometer from Perkin Elmer. For measurements the U-ATR unit was used. The dried samples were directly placed on top of the U-ATR unit for measurements.

Elemental analysis was performed by Mikroanalytisches Labor Pascher, Remagen, Germany.

Field-emission scanning electron microscopy (FESEM) was performed using a LEO Gemini microscope equipped with a field emission cathode.

UV/vis spectroscopy was performed on a Lambda 25 spectrometer of Perkin Elmer.

Transmission electron microscopy (TEM) images were taken with a Zeiss CEM902 EFTEM electron microscope operated at 80 kV or a Zeiss EM922 OMEGA EFTEM electron microscope operated at 200 kV. Both machines are equipped with an in-column energy

filter. Samples were prepared through deposition of a drop of micellar solution (concentration 0.1 g/L) onto the carbon coated TEM grids. Afterwards the remaining solvent was removed with a filter paper.

For *Cryogenic Transmission Electron Microscopy (Cryo-TEM)* studies, a drop of the sample solution (c ~ 0.5 wt.-% in water) was placed on a lacey carbon-coated copper TEM grid (200 mesh, Science Services, München, Germany), where most of the liquid was removed with blotting paper, leaving a thin film stretched over the grid holes. The specimens were shock vitrified by rapid immersion into liquid ethane in a temperature controlled freezing unit (Zeiss Cryobox, Zeiss NTS GmbH, Oberkochen, Germany) and cooled to approximately 90 K. The temperature was monitored and kept constant in the chamber during all the preparation steps. After freezing the specimens, they were inserted into a cryo-transfer holder (CT3500, Gatan, München, Germany) and transferred to a Zeiss EM922 OMEGA EFTEM instrument. Examinations were carried out at temperatures around 90 K. The transmission electron microscope was operated at an acceleration voltage of 200 kV. Zero-loss filtered images (Δ E = 0 eV) were taken under reduced dose conditions (100 – 1000 $e \cdot nm^{-2}$). All images were registered digitally by a bottom mounted CCD camera system (Ultrascan 1000, Gatan), combined and processed with a digital imaging processing system (Gatan Digital Micrograph 3.9 for GMS 1.4).

Surface Plasmon Resonance (SPR) analysis were performed according to literature using a BIAcore 2000 (Biacore AB).[44] After chip activation with 0.1 M NHS and 0.4 M of EDC, the lectin WGA was directly immobilized onto the chip at a concentration of 0.5 $mg \cdot mL^{-1}$ in sodium acetate buffer (10mM, pH = 5). Upon immobilization, the chip was capped by exposure to 1M ethanolamine. After measurements the chip was regenerated by the injection of 5µL of H_3PO_4 (50mM) followed by HEPES-buffer.

Synthesis.

Synthesis of glucose-containing polymer brushes via photo-induced free-radical polymerization. Non-crosslinked PS cores or crosslinked PS cores covered with a thin layer of photo-initiator were prepared by conventional emulsion polymerization. In a typical run, 2.07g SDS was dissolved in 820 g water under stirring. Then, 208 g styrene was added (in the case of preparation of crosslinked PS core, 6.48 g DVB was added as crosslinker). The

polymerization was started by adding the initiator (0.44g KPS dissolved in 20g water in advance) to the solution. The reaction was run at 80°C for one hour and an additional hour at 70°C. 10.64 g HMEM dissolved in 9 g acetone was added under starved conditions at 70°C. The slow addition (0.5 mL/min) ensured that the monomer HMEM does not form new particles. After the last addition, the latex was cooled down to room temperature and purified by serum replacement against the 10-fold volume of pure water. The sugar-containing brush was prepared by photopolymerization. Diluted PS core solution (1~2 wt.-%) was mixed with defined amount of functional monomer MAGlc (30 mole percent (mol-%) with regard to the amount of styrene) under stirring. The reactor (Heraus Noblelight TQ 150 Z3) was degassed by repeated evacuation and subsequent addition of nitrogen at least 5 times. Photopolymerization was done by use of UV/vis radiation (wavelengths 200-600) at room temperature for one hour. Vigorous stirring ensured homogeneous conditions. To remove possible coagulum the latex was filtered over glass wool. The suspension was purified by exhaustive ultrafiltration against deionized water.

ATRP towards linear poly(tetraacetylglucosamine) (PtetAcGlc). All polymerizations were carried out in a round-bottom flask sealed with a septum. A representative example is as follows: a mixture of CuCl (1.08 mg, 0.0109 mmol), ethyl 2-bromoisobutyrate (2.12 mg, 0.0109 mmol) and tetAcGlc (0.5 g, 1.09 mmol) in DMSO (2.0 g) were degassed for several minutes. After addition of HMTETA (2.51 mg, 0.0109 mmol) the color of the solution turned into green, indicating the dissolution of CuCl. At timed intervals, samples of the reaction solution were withdrawn to monitor the reaction kinetics, whereas the conversion was detected by ^{1}H-NMR. The solution was passed through a silica column and the polymer subsequently precipitated from THF into diethylether.

Synthesis of crosslinked N-acetylglucosamine brushes via ATRP. In a typical run, 0.40 g SDS was dissolved in 250 g water under stirring. Then 20.16 g styrene mixed with 1.30 g DVB was added. The polymerization was started by adding the initiator (0.30 g KPS dissolved in 15g water in advance) to the solution. The reaction was run at 80°C for one hour. 2.70 g inimer (BIEM) dissolved in 7.30 g acetone was added under starved conditions at 70°C. The slow addition (0.5 mL/min) ensured that the inimer does not form new particles. After the last addition, the latex was cooled down to room temperature, purified by serum replacement against the 10-fold volume of pure water, dialysed against dioxane and freeze-

dried. Elemental analysis revealed a bromine content of 1.95 wt.-%. For the following ATRP, 55.5 mg of crosslinked PS-inimer cores and 0.758 g of tetAcGlc (1.65 mmol) were added to a round bottom flask containing 3 g DMSO and placed briefly in a sonic bath to create a homogenous dispersion. After addition of 0.57 mg (0.0029 mmol) ethyl 2-bromoisobutyrate as sacrificial initiator and 1.63 mg (0.016 mmol) CuCl the mixture was degassed for 15 minutes, followed by addition of HMTETA (3.79 mg, 0.016 mmol). After 90 minutes, the conversion was determined by ^{1}H-NMR and the resulting brushes were separated from free polymer in the solution by repeated ultracentrifugation. The free polymer was collected, freeze-dried and analyzed by GPC. Elemental analysis of the glycopolymer grafted nanospheres revealed an oxygen content of 33.4 wt.-%.

Deprotection of protected poly-(N-acetylglucosamine) chains. Deprotection of linear PtetAcGlc and protected sugar-containing brushes were performed according to literature.[45] Under these conditions the ester bond does not undergo hydrolysis. The nanospheres were finally cleaned by serum replacement against purified water (membrane: cellulose nitrate with 100 nm pore size supplied by Schleicher & Schuell).

Formation of gold nanoparticles. The preparation of Au nanoparticles in an aqueous solution was carried out by the chemical reduction of metal salt – brush mixture with sodium borohydride. For a typical experiment, 0.011 g $HAuCl_4$, dissolved in 5 ml water, was added to aqueous suspension of brushes (0.1 g brushes diluted with 20 g of water), and the mixture was stirred for 30 minutes under N_2. Thereafter, sodium borohydride (0.022 g dissolved in 5 g water) was quickly added to the solution under vigorous stirring for one hour. Finally, the Au nanocomposite particles were cleaned by serum replacement against purified water (membrane: cellulose nitrate with 100nm pore size supplied by Schleicher & Schuell).

Catalytic reduction of 4-Nitrophenol. 0.5 ml sodium borohydride solution (60 mmol/l) was added to 2.5 ml 4-nitrophenol solution (0.12 mmol/l) contained in a glass vessel. After that a given amount of the Au composite particles was added. Immediately after the addition of the composite-particles, UV spectra of the sample were taken every 30 seconds in the range of 250-550 nm.

Turbidity measurements. The lectin recognition activity of linear poly-(*N*-acetylglucosamine) chains was evaluated by changes in the turbidity of solution with time at

λ = 600 nm and room temperature after the addition of protein solutions (0.5 mg/mL) to the polymer solution (0.5 mg/mL) in HEPES-buffer.

3.3 Results and Discussion

Synthesis of glucose-containing polymer brushes via photo-induced free-radical polymerization. The synthesis of PS core particles by emulsion polymerization, and polyelectrolyte brushes by photopolymerization has been previously reported.[26, 38] Here, we report the surface modification of latex particles by grafting MAGlc chains to form a spherical brush. A two-step emulsion polymerization implements a photo-initiator function on the particle surface. After photolysis of the HMEM groups, the radicals formed initiate the polymerization of the shell, which was confirmed by the increase in particle size via dynamic light scattering (Figure 1). Since the radius of the PS core particles is known, DLS leads directly to the thickness *L* of the brush layer. From Table 1, when 30 mol-% monomer was used for photopolymerization, *L* = 60.9 nm and 91.7 nm have been obtained for the non-crosslinked PS-MAGlc brush particles and crosslinked PS-DVB-MAGlc brush particles, respectively. This indicates the formation of polymer brushes on the core surface. Due to the free radical mechanism the total yield after the photopolymerization is slightly less than 50% due to the generation of one surface-bound and one free radical.

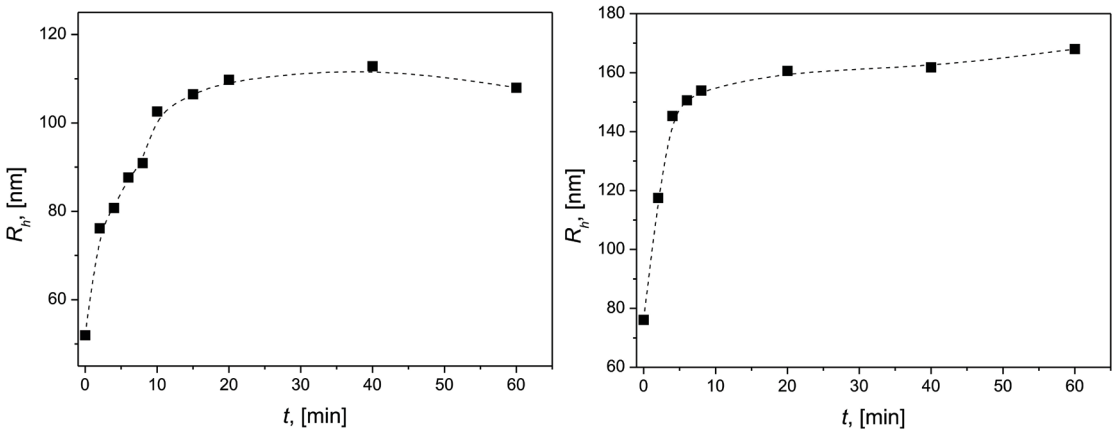

Figure 1. Increase of the particle size of non-crosslinked PS-MAGlc brushes (left) and crosslinked PS-DVB-MAGlc brushes (right) with UV irradiation time, as measured by DLS at 25°C.

Table 1. Characterization of the sugar-containing polymeric brushes.

Label[a)]	PS [g]	MAGlc [g]	Water [g]	R_{core} [b)] [nm]	L [b) c)] [nm]
PS-MAGlc	1.5	1.07	167	52.0	60.9
PS-DVB-MAGlc	2.9	2.14	280	76.1	91.7

[a)] Solid content for PS core dispersion is 8.09 wt.-% and for crosslinked PS core is 2.16 wt.-%. [b)] R_{core} and L are measured by DLS at 25°C and at an angle of 90°. [c)] Thickness of the brush layer.

Figure 2 presents typical Field-emission scanning electron microscopy (FESEM) and cryo-TEM images for the sugar-containing latex particles. From the FESEM image, it can be clearly seen that practically monodisperse PS-MAGlc particles are prepared by photopolymerization. The two dimensional assemblies are caused by capillary forces during drying of the suspensions. Moreover, the dark corona around the spherical PS core particles indicates the formation of polymer brushes on the PS core surface. Individual polymer chains do not provide sufficient contrast to monitor them individually. The cryo-TEM micrograph shows bundles that arise from "frozen" fluctuations of the grafted chains. The polymer density decreases with R^{-2} as does the contrast.[46]

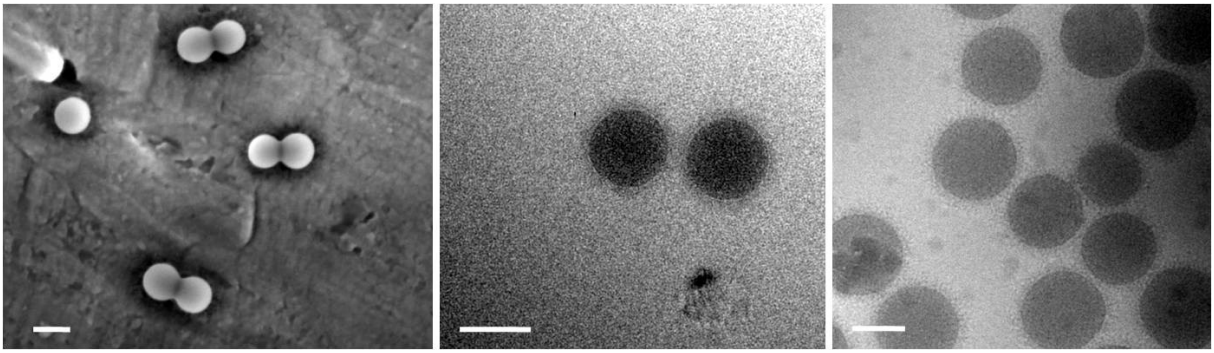

Figure 2. FESEM image (left) and cryo-TEM image (middle) of MAGlc brushes anchored to non-crosslinked and crosslinked (right) PS latex particles. The scale bars represent 100nm.

The FT-IR spectra of the PS core particles and the resulting sugar containing polymer brush particles are shown in Figure 3. The characteristic absorptions bands at 3 400 cm^{-1} (due to stretching vibrations of hydroxyl groups of glucose) and at 1 720 cm^{-1} (carbonyl group absorption from functional monomer) can be observed for the resulting brush particles, which demonstrates the generation of sugar-containing brushes onto the PS core particles.

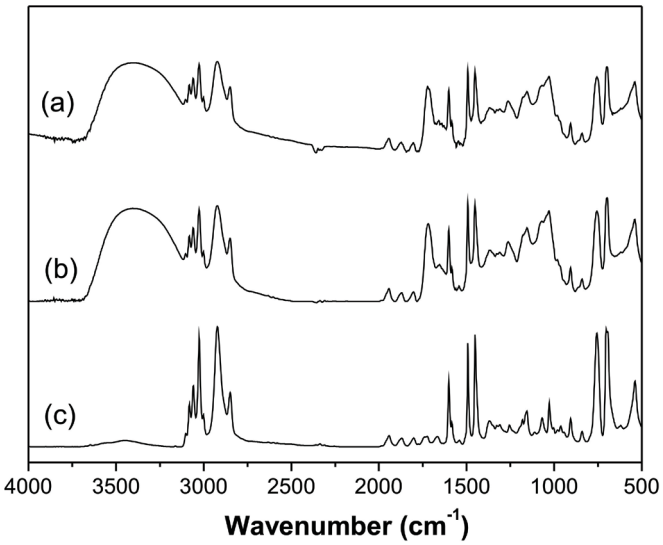

Figure 3. FT-IR spectra of (a) crosslinked PS-DVB-MAGlc, (b) non-crosslinked PS-MAGlc and (c) crosslinked PS-DVB-HMEM particles

The shown data reveal the successful preparation of spherical glycopolymer brushes consisting of crosslinked or non-crosslinked polystyrene cores and glucose-containing shells via photo-induced free-radical polymerization. Nevertheless, the chosen free-radical polymerization technique to build up the shell exhibits two disadvantages: the uncontrolled mechanism and formation of two radicals, which results in broad molecular weight distributions and loss of 50 % of the formed polymer. To overcome these problems, we also investigated the use of ATRP for the preparation of the glycopolymer displaying shell.

Synthesis of *N*-acetylglucosamine-containing polymer brushes via Atom Transfer Radical Polymerization. To find a suitable system for the ATRP of the protected glycopolymer brushes, we first investigated the effect of different ligands on the ATRP towards linear poly-(tetraacetylglucosamine) (PtetAcGlc). The results are summarized in Table 2 and Figure 4. For all polymerizations, ethyl 2-bromoisobutyrate (EBIB) was used as initiator which possesses the same initiating group as the inimer BIEM that was used for the synthesis of the latex particles. The solution polymerization of the protected glycomonomer was conducted using copper-mediated ATRP. When tetAcGlc was polymerized using CuCl/Me_6 TREN at room temperature, the conversion reached 90% (as determined by ^{1}H-NMR spectroscopy) after 45 minutes. The number-average molecular weight of PtetAcGlc as

determined by means of GPC using PtBMA standards is M_n = 66 200 g/mol and the polydispersity index is M_w/M_n = 1.29. Comparing the theoretical molecular weight, $M_{n,th}$ = 41 300 g/mol with that determined by GPC, an initiator efficiency I_{eff} = 0.62 can be calculated. Using the non-branched ligand PMDETA led to a narrower molecular weight distribution (PDI = 1.16) and increased initiator efficiency (I_{eff} = 0.81) after 5 hours and a conversion of 52%. As the activity of N-based ligands in ATRP decreases with the number of coordinating sites,[47] the CuCl/HMTETA catalyst system showed a higher polymerization rate than CuCl/PMDETA which led to a conversion of 93% after 90 minutes. With a number-average molecular weight M_n = 49 400 g/mol, a polydispersity index M_w/M_n = 1.09 and an initiator efficiency I_{eff} = 0.86 HMTETA was found to be the most suitable ligand for the polymerization of the protected glycomonomer. The use of a less polar solvent (Anisole) led to a lower polymerization rate even at elevated temperature. Furthermore, the solution became slightly turbid indicating reduced solubility of the formed polymer.

Table 2. Effects of catalyst and ligand on homopolymerization of tetAcGlc.

Run [a)]	Ligand	solvent	T [°C]	t [min]	conv [b)] [%]	$M_{n,GPC}$ [c)] (M_w/M_n) [g/mol]	I_{eff} [d)]
1	Me_6 TREN	DMSO	25	45	90	66 200 (1.29)	0.62
2	PMDETA	DMSO	25	300	52	29 300 (1.16)	0.81
3	HMTETA	Anisole	60	180	31	15 000 (1.19)	0.98
4	HMTETA	DMSO	25	90	93	49 400 (1.09)	0.86

[a)] Initiator: EBiB. Catalyst: CuCl. $[tetAcGlc]_o:[I]_o:[cat]_o:[ligand]_o$ = 100:1:1:1. $[M]_0$ ~ 0.2 g· mL^{-1}. [b)] Monomer conversion as determined by means of ^{1}H-NMR. [c)] Determined by GPC using THF as eluent with PtBMA standards. [d)] Initiator efficiency comparing the theoretical molecular weight and the determined molecular weight by GPC with PtBMA standards.

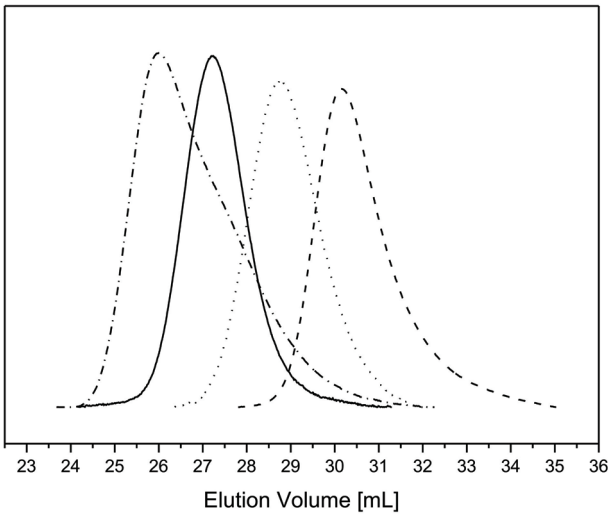

Figure 4. GPC traces of PtetAcGlc obtained by ATRP by the use of Me_6 TREN (run 1, table 2, -.-.), HMTETA in DMSO (run 4, -), PMDETA (run 2, …) and HMTETA in Anisole (run 3, ---).

Kinetic studies on the solution polymerization of tetAcGlc by CuCl/HMTETA (run 4, table 2) in DMSO are summarized in Figure 5-7. Figure 5 shows first-order kinetics even to high monomer conversion which indicates the absence of undesired side reactions. As can be seen in Figure 6, the polymerization exhibits a linear molecular weight increase with conversion. The difference between the theoretical and the experimental molecular weight can be assigned to the PtBMA calibration of the GPC. The polydispersity indices are low (PDI < 1.2) and decrease with conversion of monomer yielding very well-defined chains (PDI < 1.1) at conversions X_p > 90%. Monomodal SEC traces were obtained for the kinetic run (Figure 7). Even at high conversion no high molecular weight shoulder occurred, which would indicate a bi-molecular termination reaction.

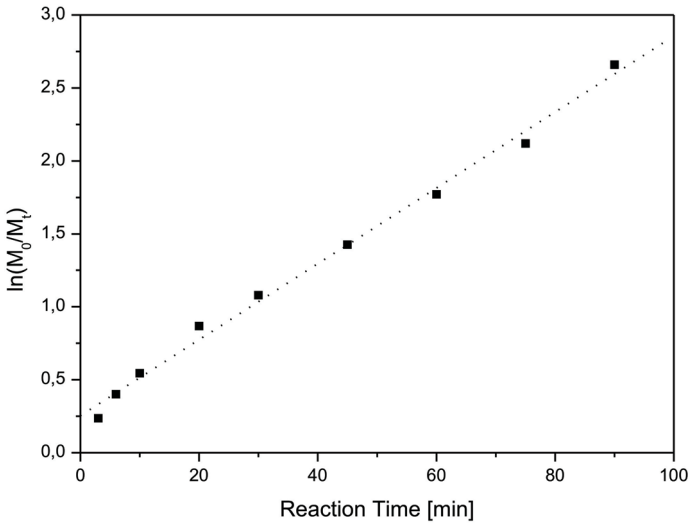

Figure 5. First-order kinetic plot for the polymerization of tetAcGlc (run 4, table 2) in DMSO at RT.

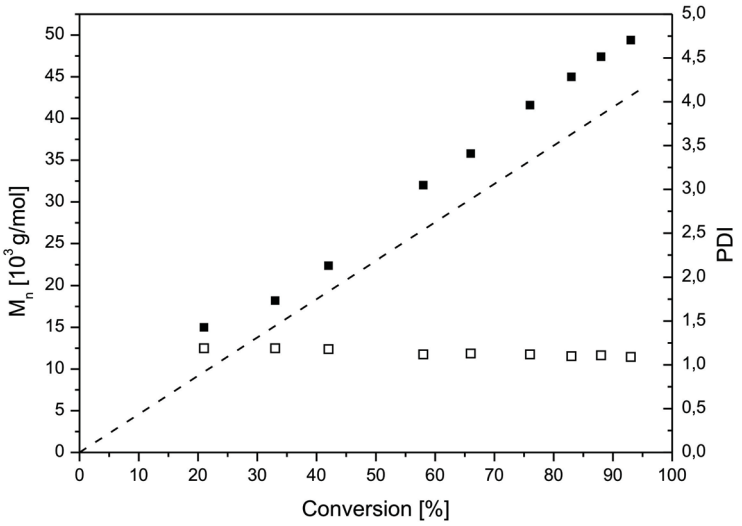

Figure 6. Evolution of molecular weight (filled squares) and polydispersity index (open squares) with conversion. The dashed line shows theoretical molecular weights.

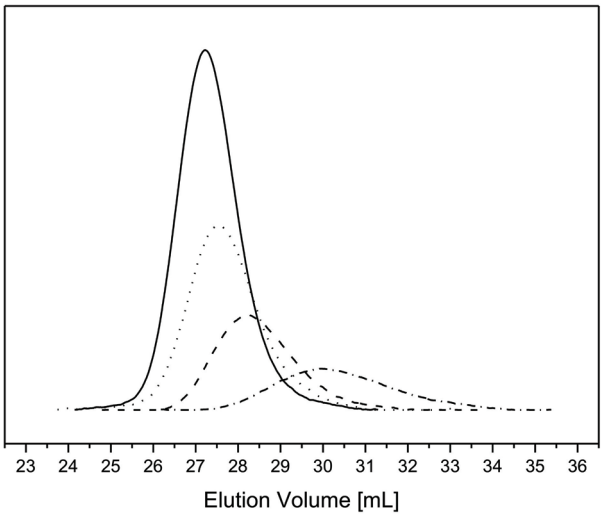

Figure 7. Gel permeation chromatographs of PtetAcGlc evolution over the course of the kinetic run (run 4, table 2). (-) : χ_p = 93%, (…) : χ_p = 83%, (---) : χ_p = 58%, (-.-.) : χ_p = 21%.

To prepare spherical sugar-containing polymer brushes, we chose the same catalytic system (CuCl/HMTETA) as for the successful ATRP of linear PtetAcGlc. In contrast to prior experiments, a certain amount of the initiator EBiB was replaced by surface-bound initiator on the latex particles. The initial ratio of all compounds were set as $[tetAcGlc]_o$:[surface bound initiator+EBiB]$_o$:$[cat]_o$:$[ligand]_o$ = 100:1:1:1. Analogous to the synthesis of linear PtetAcGlc, the polymerization reached 95% after 90 minutes. Given that free polymer in solution and grafted chains have comparable molecular weights and polydispersities,[48-52] the resulting free polymer in solution could be easily characterized by GPC and hence no cleavage of the arms was necessary. After separation of the free polymer from glycopolymer brushes by repeated ultracentrifugation, the number-average molecular weight determined by GPC using PtBMA standards is M_n = 49 800 g/mol and the polydispersity index is M_w/M_n = 1.12. Figure 8 shows FESEM images for pure PS-DVB particles and glycopolymer brushes, respectively. The rough surface and the increase of diameter can be attributed to grafted PtetAcGlc chains.

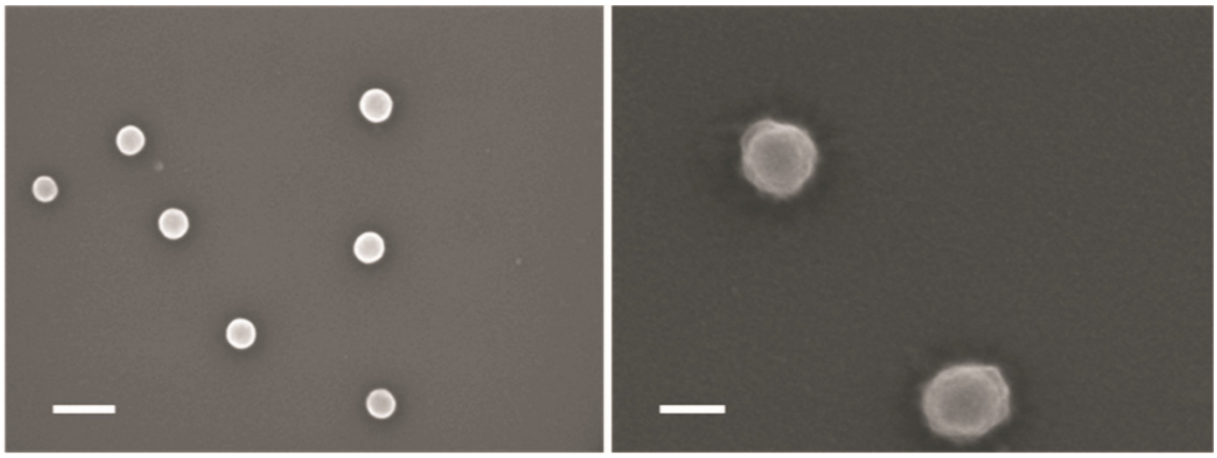

Figure 8. SEM image of pure PS-DVB nanospheres (left) and protected glycopolymer brushes (right) on Si-wafers. The scale bars represent 200 nm.

To calculate the grafting density of the sugar arms on the spheres, the absolute average molecular weight and the corresponding degree of polymerization have to be determined. MALS-SEC measurement of the free polymer led to an absolute M_n = 96 700 g/mol and corresponding degree of polymerization DP = 210. Compared to the theoretical degree of polymerization, DP_{theo} = 95, the determined DP leads to an initiator efficiency of 45%. Elemental analysis of the poly-(tetraacetylglucosamine) covered spheres revealed an oxygen content of 33.4 weight percent (wt.-%). As the oxygen content in the glycomonomer is found to be 38.3 wt.-%, a sugar-PS composition of 87.2 / 12.8 can be calculated. Given the absolute molecular weight of the sugar chains (96 700 g/mol), the amount of grafted sugar, the radius of the PS-particle (50 nm) and hence the surface area ($3.14 \cdot 10^4$ nm^2), 1 g of glycopolymer grafted spheres contain $3.2 \cdot 10^{14}$ spheres and $5.4 \cdot 10^{18}$ glycopolymer chains which leads to a grafting density of 0.54 chains per nm^2 surface area.

Deprotection of the sugar units under basic conditions via NaOMe led to water soluble brushes which were studied by FT-IR spectroscopy, as shown in Figure 9. After grafting PtetAcGlc chains from the particle surface, peaks at 1 750 cm^{-1} and 3 400 cm^{-1} appeared, which can be attributed to carbonyl- and –NH-CO-bonds respectively. After deprotection of the sugar moieties, a higher absorption band at 3 400 cm^{-1}, due to stretching vibrations of the hydroxyl groups of the sugar, can be observed. DLS measurements show an increase of the radius of the nanospheres from 50 nm to 102 nm after grafting of the polymer chains and deprotection of the sugar moieties (Figure 10).

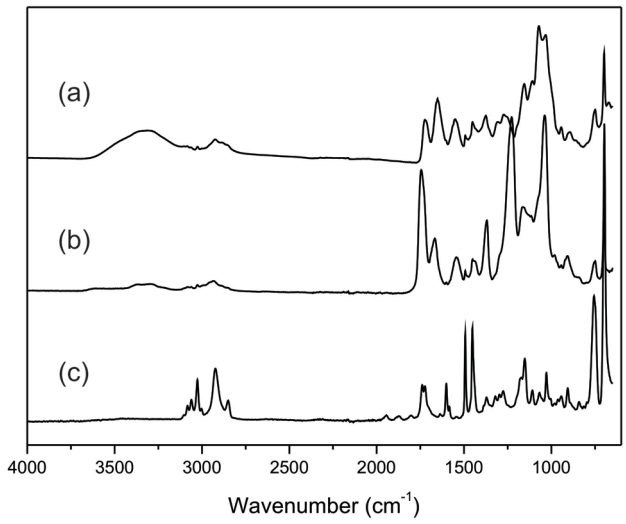

Figure 9. FT-IR spectra of (a) water soluble glucosamine nanospheres, (b) protected glycopolymer brushes and (c) PS-DVB particles.

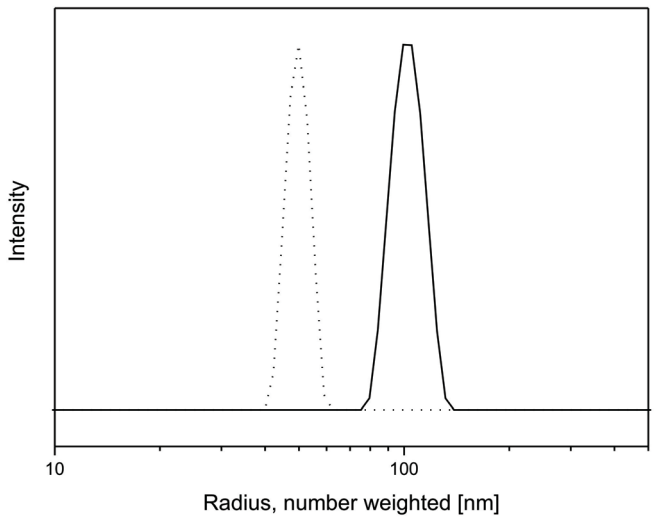

Figure 10. Intensity weighted distribution of hydrodynamic radii of PS-DVB particles in DMSO (…) and deprotected sugar-brushes in water (-).

Spherical brushes as carriers for catalytically active gold nanoparticles. It is known that spherical polycation brushes can act as carriers for catalytically active metal nanoparticles.[53] Here, we investigated the use of non-ionic chains of a bioinspired polymer (poly-*(N*-acetylglucosamine)) for the synthesis of gold nanocomposite particles. The addition

of $HAuCl_4$ to an aqueous solution of sugar containing polymer brushes and subsequent reduction of the $AuCl_4^-$ ions by $NaBH_4$ led to gold nanoparticles with an average diameter of 6.3 nm (Figure 11). This is confirmed by the change of color of the solution from yellowish to violet. The stabilizing of Au nanoparticles is mainly due to the fact that the hydroxyl groups on the surface of the glycopolymer brushes have a high affinity for metal nanoparticles. In addition, the polymer brush will prevent the release and aggregation of the immobilized Au nanoparticles by steric hindrance, and thus exert control of the growth process by diffusion control. For the evaluation of the catalytic activity of the gold nanoparticles, we chose the reduction of *p*-nitrophenol by excess sodium borohydride, which is a frequently used model reaction (Figure 12).[54-56] This reaction can be easily monitored by UV/vis spectroscopy. The characteristic absorption peak of *p*-nitrophenol at 400 nm disappeared, whereas a new peak at 290 nm (due to *p*-aminophenol) appeared. In addition, the reaction follows first order rate kinetics with regard to the *p*-nitrophenol concentrations as the concentration of sodium borohydride was adjusted to largely exceed the concentration of *p*-nitrophenol. Thus, a linear relation between $\ln(c_t/c_0)$ versus time t has been obtained as shown in the inset of Figure 12. The apparent rate constant k_{app} of 0.048 min^{-1} is obtained from the curve of $\ln(c_t/c_0)$ versus time t by linear fit. This demonstrates the capability of the sugar-containing polymer brushes to act as a biocompatible carrier for catalytically active gold nanoparticles.

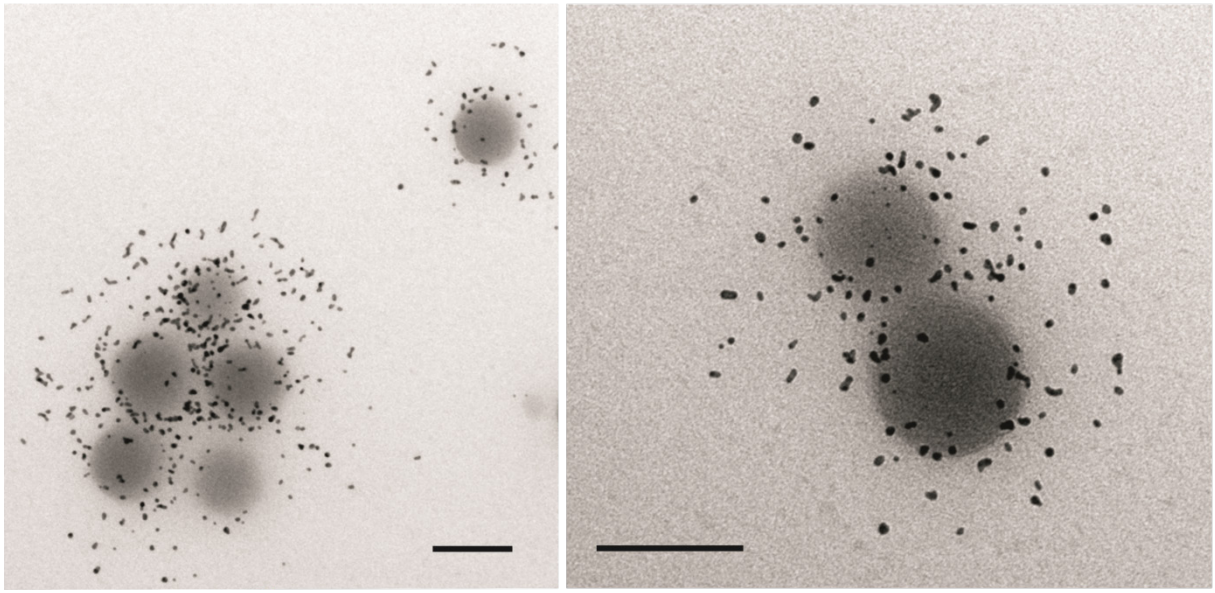

Figure 11. TEM image of gold nanoparticles immobilized on glucosamine brushes. The scale bars represent 100 nm.

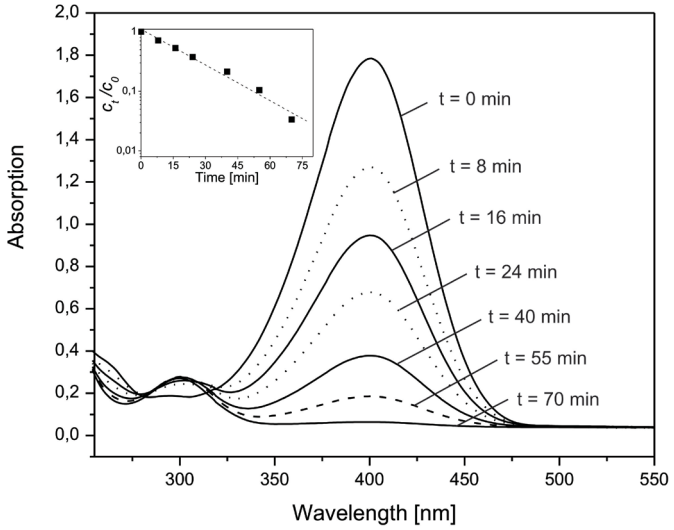

Figure 12. Catalytic reduction of *p*-nitrophenol in the presence of gold nanocomposite particles.

Recognition properties of *N*-acetylglucosamine chains towards lectins. Sugar-binding and cell-agglutinating proteins, so called lectins, are omnipresent in all kind of organisms. In our investigation of the binding activity of the prepared *N*-acetylglucosamine brush towards lectins, wheat germ agglutinin (WGA) played an important role. *N*-acetylglucosamine is the receptor sugar for WGA, whereas preferential binding to dimers and trimers of this sugar occur. Both turbidity measurements and biosensor analysis were used here to investigate the binding behavior of WGA to *N*-acetylglucosamine chains. For turbidity measurements, linear poly-(*N*-acetylglucosamine) chains were mixed with different protein solutions. Emerging protein-saccharide interactions cause the formation of aggregates due to the multiple binding sites of proteins and therefore a decrease in transmission is observed. As a control experiment, peanut agglutinin (PNA) and bovine serum albumin (BSA) were mixed with the polymer solution and displayed no decrease in transmission (Figure 13). In contrast to BSA and PNA, WGA specifically binds to multiple *N*-acetylglucosamine residues[57] and therefore is able to precipitate the polymer. Right after mixing the deprotected polymer (Table 2, run 4) and protein in solution, the transmission dropped to 70% due to the fast formation of aggregates and further decreased to 20% within 25 min.

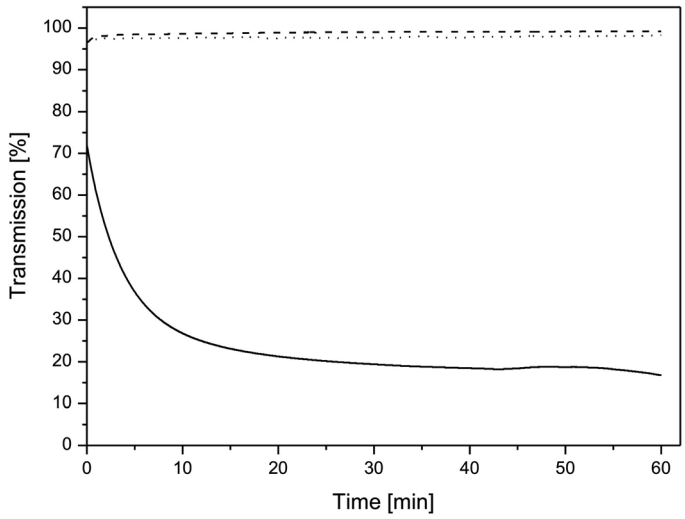

Figure 13. Interactions of poly-(*N*-acetylglucosamine) chains with WGA (solid line), BSA (dashed line) and PNA (dotted line).

Turbidity measurement is a simple method to detect protein-saccharide interaction, but for more detailed investigation biosensor analysis is the method of choice. Surface plasmon resonance (SPR) spectroscopy is often used for the study of lectin-carbohydrate interactions,[58] whereas usually a lectin is immobilized on the sensor chip surface and flushed with a carbohydrate solution. Here, after immobilizing WGA on the surface, an aliquot of the polymer solution (20 µL) was injected and the change in refractive index recorded. The polymer was allowed to associate to the bound protein for 2 min, followed by a dissociation phase of 5 min where the flow channel was flushed with buffer. Finally, the chip was regenerated by injection of H_3PO_4.

To determine the minimum concentration of poly-(*N*-acetylglucosamine) that could be detected in SPR binding experiments, a dilution series was injected over the sensor surface (Figure 14). It can be seen, that even at the lowest concentration (0.1 µM) of injected linear deprotected glycopolymer (Table 2, run 4) a SPR signal could be detected. Furthermore, it is worth mentioning that dissolution only takes place for the two highest concentrations (10 mM and 1 mM), indicating that more dilute solutions of poly-(*N*-acetylglucosamine) were completely bound by the lectin.

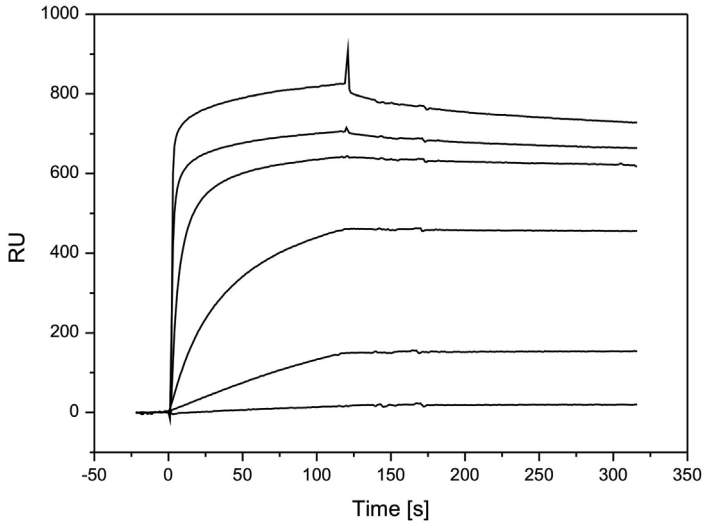

Figure 14. (a) Biacore sensograms of the interaction between linear poly-(*N*-acetylglucosamine) chains with WGA at different concentrations of the injected polymer solutions. Curves from top to bottom: 10 mM (0.33 wt.-%), 1 mM, 100 µM, 10 µM, 1 µM and 0.1 µM.

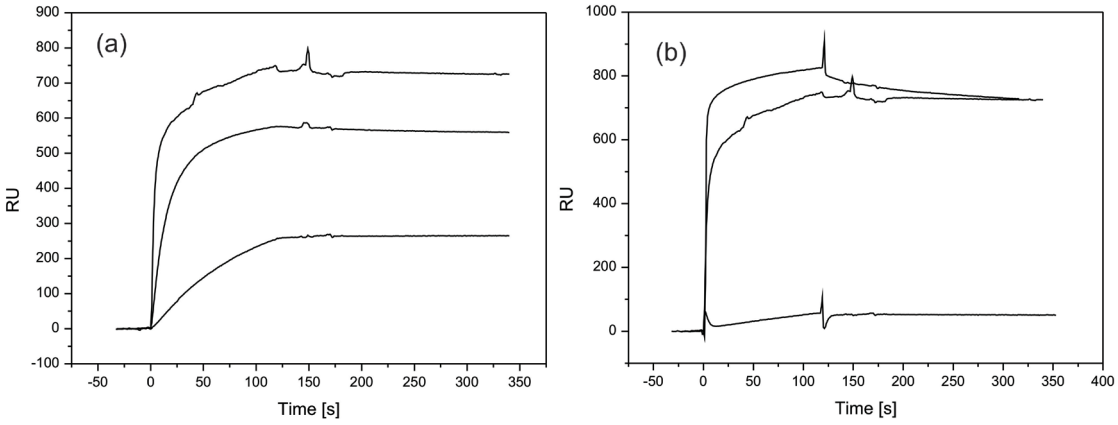

Figure 15. (a) Biacore sensograms of the interaction between glycopolymer brushes with WGA at different concentrations of the injected brush solutions. Curves from top to bottom: 0.33 wt.-%, 0.033 wt.-% and 0.0033 wt.-%. (b) Biacore sensograms of the interaction between linear poly-(*N*-acetylglucosamine) chains (top curve), glycopolymer brushes (middle curve) and *N*-acetylglucosamine sugar unimer (bottom curve) with WGA at c = 0.33 wt.-%.

Figure 15 (a) shows the sensograms of the deprotected glycopolymer brushes with WGA at three different concentrations. Figure 15 (b) compares the association behavior of linear poly-(*N*-acetylglucosamine), glycopolymer brush and *N*-acetylglucosamine sugar unimer. In comparison to linear glycopolymers, spherical brushes show a reduced adsorption

to the immobilized lectin, which can be attributed to unavailability of sugar residues next to the core, due to steric hindrance, and the reduction of the total mass of sugar-units due to introduction of the polystyrene core. Nevertheless both show adsorptions magnitudes higher than the unimer, which can be attributed to the afore mentioned “glyco-cluster” effect.

To visualize the binding affinity of WGA to the spherical brushes, transmission electron microscopy was performed. Therefore a solution of 0.1 wt.-% of brush in water was prepared and vigorously stirred. Immediately after addition of the protein solution (0.5 wt.-% compared to spherical brushes) a drop of the brush-protein solution was placed on a TEM-grid. Figure 16 (a, b) shows typical TEM images of the formed aggregates. Even with the short reaction time and the small amount of lectin, mainly large aggregates can be found, indicating again the strong affinity of WGA to bind to the sugar moieties. In Figure 16 (c) some of only few loose brush-protein complexes can be seen. The contrast of the protein was increased by staining with methyl iodide.

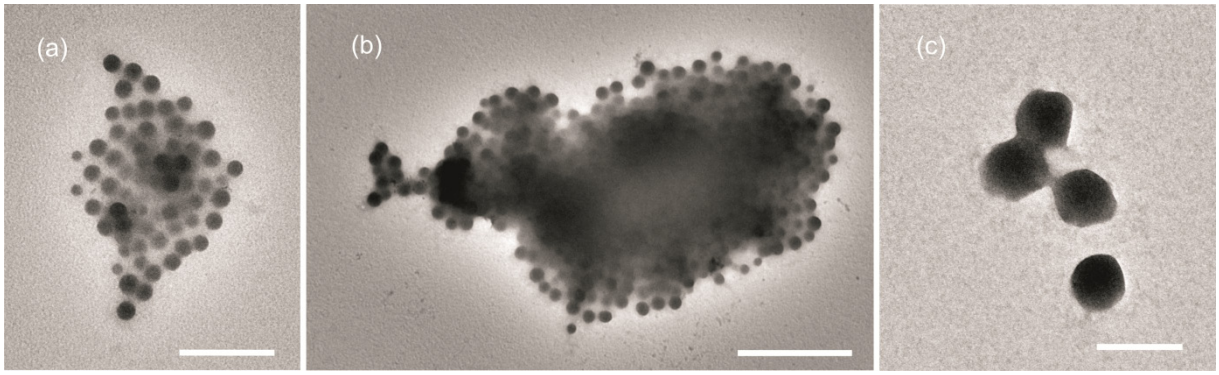

Figure 16. TEM-images of immobilized WGA on the glycopolymer brush surface. (a) unstained and (b) stained WGA-protein aggregate and (c) loose complexes. Scale bars represent 500 (a), 1000 (b) and 200 nm (c).

To determine the amount of protein that can be precipitated by glucosamine-containing nanospheres, UV/vis spectroscopy was performed. Therefore WGA (5.36 mg) in HEPES-buffer (4 mL) was mixed with nanospheres (0.55 mg) and stirred for 5 h. Subsequent separation of the spheres by ultracentrifugation gave a transparent solution which was analyzed by UV/vis spectroscopy. Comparison of UV/vis spectra recorded before and after treatment with sugar-coated spheres showed a decrease of peak height at λ = 276 nm of 5.2 percent which can be attributed to the adsorbed protein on glycopolymer nanospheres. The amount of protein left in solution could therefore be calculated to be 5.08 mg (Δm = 0.28

mg) which means, that 1mg of glycopolymer brush is able to precipitate 0.5 mg of wheat germ agglutinin.

3.4 Conclusions

We present the successful preparation of glycopolymer-displaying spherical brushes by both conventional and controlled radical polymerization. Immobilization of gold nanoparticles led to metal-brush composite particles that were able to catalyze the reduction of nitrophenol to aminophenol. Investigation of the binding behaviour of these brushes towards proteins revealed selective binding to wheat germ agglutinin (WGA). A much higher binding affinity of WGA to glycopolymer chains in comparison to the sugar unimer *N*-acetylglucosamine was observed. Due to the strong and selective binding, potential application for these brushes could be the separation of WGA from other proteins by precipitation of the lectin and subsequent release by breaking up the sugar-lectin complex by H_3PO_4, as indicated by our biosensor analysis.

Acknowledgements

This work was supported by the European Science Foundation within the EUROCORES SONS 2 program (project BioSONS). VSS is thankful to the *Department of Science and Technology (New Delhi, INDIA)* for financial support in the form of a BOYSCAST fellowship. We thank *Marietta Böhm*, *André Gröschel* and *Frank Polzer* for GPC and TEM measurements, respectively. We appreciate *Judicael Parisot* for fruitful discussions and his contribution to this work.

3.5 References

1. Ladmiral, V.; Melia, E.; Haddleton, D. V. *Eur. Polym. J.* **2004,** 40, 431.
2. Wang, Q.; Dordick, J. S.; Linhardt, R. L. *Chem. Mater.* **2002,** 14, 3232.
3. Ting, S. R. S.; Chen, G.; Stenzel, M. H. *Polym. Chem.* **2010**, 1, 1392.
4. Spain, S. G.; Cameron, N. R. *Polym. Chem.* **2011**, 2, 60.
5. Miura, Y. *J. Polym. Sci., Part A: Polym. Chem.* **2007,** 45, (22), 5031.
6. Klein, J.; Kunz, M.; Kowalczyk, J. *Makromol. Chem.* **1990,** 191, 517.

7. Dickinson, E.; Bergenstahl, B. *Food Colloids: Proteins, Lipids and polysaccharides, The Royal Society of Chemistry: Cambridge* **1997**, (192), 417.
8. Kopecek, J.; Kopeckova, P.; Brondsted, H.; Rathi, R.; Rihova, B.; Yeh, P. Y. *Controlled Release* **1992**, (19), 121.
9. Murata, I. J.; Ohya, Y.; Ouchi, T. *Carbohydr. Polym.* **1996**, (29), 69.
10. Muthukrishnan, S.; Nitschke, M.; Gramm, S.; Oezyuerek, Z.; Voit, B.; Werner, C.; Mueller, A. H. E. *Macromol. Biosci.* **2006**, (6), 658.
11. Wang, Y.; Kiick, K. L. *J. Am. Chem. Soc.* **2005**, (127), 16392.
12. Albertin, L.; Stenzel, M. H.; Barner-Kowollik, C.; Foster, L. J. R.; Davis, T. P. *Macromolecules* **2005**, (38), 9075.
13. Aoi, K.; Tsutsumichi, K.; Okada, M. *Macromolecules* **1994,** 27, 875.
14. Fraser, C.; Grubbs, R. H. *Macromolecules* **1995,** 28, 7248.
15. Kasuya, M. C.; Hatanaka, K. *Macromolecules* **1999**, (32), 2132.
16. Choi, S. K.; Manmmen, M.; Whitesides, G. M. *J. Am. Chem. Soc.* **1997**, (119), 4103.
17. Aoi, K.; Itoh, K.; Okada, M. *Macromolecules* **1995**, (28), 5391.
18. Chen, X. M.; Dordick, J. S.; Rethwisch, D. G. *Macromolecules* **1995**, (28), 6014.
19. Albertin, L.; Stenzel, M. H.; Barner-Kowollik, C.; Foster, L. J. R.; Davis, T. P. *Macromolecules* **2004**, (37), 7530.
20. Muthukrishnan, S.; Mori, H.; Müller, A. H. E. *Macromolecules* **2005,** 38, 3108.
21. Muthukrishnan, S.; Plamper, F.; Mori, H.; Müller, A. H. E. *Macromolecules* **2005,** 38, (26), 10631.
22. Narain, R.; Armes, S. P. *Macromolecules* **2003**, (36), 4675.
23. Ohno, K.; Izu, Y.; Yamatomo, S.; Miyamoto, T.; Fukuda, T. *Macromol. Chem. Phys.* **1999**, (200), 1619.
24. Ballauf, M. *Macromol. Chem. Phys.* **2003**, (204), 220.
25. Ruhe, J. *Macromol. Symp.* **1997**, (126), 215.
26. Guo, X.; Weiss, A.; Ballauf, M. *Macromolecules* **1999,** 32, 6043.
27. Lu, Y.; Wittemann, A.; Ballauff, M. *Macromol. Rapid Commun.* **2009,** 30, (9-10), 806.
28. Ballauff, M. *Prog. Polym. Sci.* **2007,** 32, (10), 1135.
29. Wittemann, A.; Ballauff, M. *Phys. Chem. Chem. Phys.* **2006,** 8, (45), 5269.
30. Al-Rawashdeh, N. A. F.; Sandrock, M. L.; Seugling, C. J.; Foss, C. A. J. *J. Phys. Chem. B* **1998,** 102, 361.

31. Demaille, C.; Brust, M.; Tsionsky, M.; Bard, A. J. *Anal. Chem.* **1997,** 69, 2323.
32. Evans, S. D.; Johnson, S. R.; Cheng, Y. L.; Shen, T. *J. Mater. Chem.* **2000,** 10, 183.
33. Maier, S. A.; Brongersma, M. L.; Kik, P. G.; Meltzer, S.; Requicha, A. A. G.; Atwater, H. A. *Adv. Mater.* **2001,** 13, 1501.
34. Storhoff, J. J.; Elghanian, R.; Mucic, R. C.; Mirkin, C. A.; Letsinger, R. L. *J. Am. Chem. Soc.* **1998,** 120, 1959.
35. Vossmeyer, T.; Guse, B.; Besnard, I.; Bauer, R. E.; Mullen, K.; Yasuda, A. *Adv. Mater.* **2002,** 14, 238.
36. Lee, Y. C.; Lee, R. T. *Acc. Chem. Res.* **2002,** 28, (8), 321.
37. Ciampolini, M.; Nardi, N. *Inorg. Chem.* **2002,** 5, (1), 41.
38. Guo, X.; Ballauf, M. *Langmuir* **2000**, (16), 8719.
39. EP 0237131 (1987), Shell Int Research, Teunis, G.
40. Akinori, T.; Terumi, N.; Hisashi, I.; Yoshihito, I.; Tadamichi, H. *Macromol. Rapid Commun.* **2000,** 21, (11), 764.
41. Nishimura, S.-I.; Furuike, T.; Matsuoka, K.; Maruyama, K.; Nagata, K.; Kurita, K.; Nishi, N.; Tokura, S. *Macromolecules* **2002,** 27, (18), 4876.
42. Matyjaszewski, K.; Gaynor, G. S.; Kulfan, A.; Podwika, M. *Macromolecules* **1997,** 30, 5192.
43. Mori, H.; Boeker, A.; Krausch, G.; Mueller, A. H. E. *Macromolecules* **2001**, (34), 6871.
44. Misawa, Y.; Masaka, R.; Maeda, K.; Yano, M.; Murata, T.; Kawagishi, H.; Usui, T. *Carbohydr. Res.* **2008,** 343, 434.
45. Vazquez-Dorbatt, V.; Maynard, H. D. *Biomacromolecules* **2006,** 7, 2297.
46. Wittemann, A.; Drechsler, M.; Talmon, Y.; Ballauff, M. *J. Am. Chem. Soc.* **2005,** 127, (27), 9688.
47. Matyjaszewski, K.; Xia, J. *Chem. Rev.* **2001,** 101, 2921.
48. Barsbay, M.; Gueven, O.; Stenzel, M. H.; Davis, T. P.; Barner-Kowollik, C.; Barner, L. *Macromolecules* **2007,** 40, (20), 7140.
49. Bartholome, C.; Beyou, E.; Bourgeat-Lami, E.; Chaumont, P.; Zydowicz, N. *Macromolecules* **2003,** 36, (21), 7946.
50. Perrier, S. b.; Takolpuckdee, P.; Mars, C. A. *Macromolecules* **2005,** 38, (16), 6770.
51. von Werne, T.; Patten, T. E. *J. Am. Chem. Soc.* **2001,** 123, (31), 7497.

52. Wang, W.; Cao, H.; Zhu, G.; Wang, P. *J. Polym. Sci., Part A: Polym. Chem.* **2010,** 48, (8), 1782.

53. Mei, Y.; Sharma, G.; Lu, Y.; Ballauf, M. *Langmuir* **2005,** 21, 12229.

54. Pradhan, N.; Pal, A.; Pal, T. *Colloids Surf.* **2002,** 196, 247.

55. Wunder, S.; Polzer, F.; Lu, Y.; Mei, Y.; Ballauff, M. *J. Phys. Chem. C* **2010,** 114, (19), 8814.

56. Yuan, J.; Schacher, F.; Drechsler, M.; Hanisch, A.; Lu, Y.; Ballauff, M.; Müller, A. H. E. *Chem. Mater.* **2010,** 22, (8), 2626.

57. Yu, Y. P.; Wu, A. T.; Zou, W.; Chen, C. S.; Wu, S. H. *Tetrahedron Lett.* **2009,** 50, 6130.

58. Duverger, E.; Frison, N.; Roche, A.-C.; Monsigny, M. *Biochimie* **2003,** 85, (1-2), 167.

Chapter 4

Surface Modification of Polymeric Microspheres using Glycopolymers for Biorecognition

André Pfaff,[1] Leonie Barner,[2] Axel H. E. Müller[1] and Anthony M. Granville[3]

[1]Macromolecular Chemistry II, Universität Bayreuth, 95440 Bayreuth, Germany,

[2]Fraunhofer Institute for Chemical Technology, 76327 Pfinztal, Germany,

[2]Centre for Advanced Macromolecular Design, School of Chemical Sciences and Engineering, The University of New South Wales, Sydney, NSW 2052, Australia.

a.granville@unsw.edu.au, axel.mueller@uni-bayreuth.de

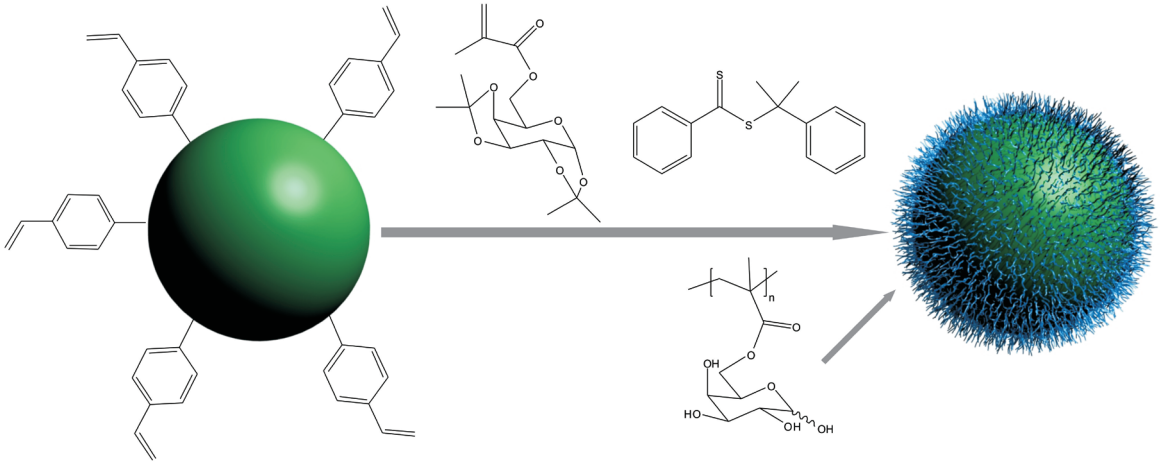

Abstract

We report the synthesis and characterization of sugar-containing microspheres consisting of poly(divinylbenzene) (PDVB) cores onto which chains of galactose- or mannose-bearing polymers have been grafted. PDVB particles prepared by distillation polymerization with a diameter of 2.4 µm containing residual surface vinyl groups were used as starting material. "Grafting from", "grafting through" and "grafting to" techniques were performed and special interest was laid towards the resulting grafting densities. The surface modification via "grafting from" was conducted by reversible addition fragmentation chain transfer (RAFT) polymerization directly from the surface, whereas thiol-ene chemistry was used to affix glycopolymer chains onto the particle surface. The resulting sugar-covered microspheres were analyzed towards their protein recognition activity with a series of lectins.

Keywords: reversible addition fragmentation chain transfer (RAFT) polymerization; glycopolymer; microspheres; thiol-ene reaction

4.1 Introduction

Carbohydrates are involved in a multitude of biological functions in living systems. Glycopolymers, synthetic polymers carrying carbohydrate moieties, have been widely investigated for medical and pharmaceutical applications, like drug delivery,[1, 2] cell culture substrates,[3, 4] macromolecular drugs[5, 6] and surface modifiers.[7, 8] The plurality of potential applications has prompted researchers to develop various synthetic strategies for the preparation of sugar-containing polymers with controlled functionalities and architectures.[9-11] There are several studies on the preparation of well-defined glycopolymers by living polymerization, such as anionic,[12] cationic,[13] ring-opening metathesis[10, 14] and radical polymerization. The latter include Nitroxide-Mediated Radical Polymerization (NMP),[15] Reversible Addition Fragmentation Transfer Polymerization (RAFT),[16] and Atom Transfer Radical Polymerization (ATRP).[17]

In the last decades, much attention has been devoted to the generation of sugar-coated particles using the macromonomer technique,[18] conjugation of sugars on reactive particles,[19, 20] emulsion polymerization[21, 22] and grafting of glycopolymer chains onto particles.[23-25] But up to now, grafting glycopolymers from microspheres cannot be found in

the literature, whereas the research on core-shell microspheres covered with functional material is increasing continuously. Crosslinked microspheres based on poly(divinylbenzene) (PDVB) are highly attractive because of their residual double bonds on the surface of the particle[26] which can be easily used to attach single molecules or polymer chains to the surface by various grafting approaches.[27-33] Recently thiol-ene chemistry was used to affix gluco- and galactothiose unimers to microspheres and saccharide-lectin interactions of the resulting particles were investigated.[29, 31] As interactions between saccharides and proteins can be strongly increased by the "glyco-cluster effect" due to the multivalent effect of clustered saccharides,[34] we were interested in creating a dense shell of glycopolymer around the microspheres to maximize this effect.

As mentioned before, one can use two different techniques, namely "grafting from" and "grafting to", to create core-shell microspheres. Controlled radical polymerization methods like ATRP and RAFT were used to graft polystyrene from PDVB microspheres,[28, 35] whereas RAFT-hetero Diels-Alder cycloaddition (RAFT-HDA),[36] thiol-ene reaction[30] and copper-catalyzed Huisgen 1,3-dipolar cycloaddition of azides and alkynes (CuAAC)[30] were performed to graft polymer chains onto the surface of the particles.

In this paper, we report the synthesis of two glycopolymer-containing core-shell microspheres by grafting either 6-*O*-methacryloyl mannose (MAMan) (Scheme 1, path a) or 6-*O*-methacryloyl-1,2;3,4-di-*O*-isopropylidene-galactopyranose (MAIGal) (Scheme 1, path b) from the particle surface. In the case of the MAIGal, three different grafting approaches were utilised, with special emphasis being put on the resulting grafting densities. "Grafting from" was conducted via prior attachment of the RAFT agent cumyl dithiobenzoate (CDB) to the spheres and subsequent polymerization of the glycomonomer MAIGal, whereas "grafting through" included the simultaneous addition of chain transfer agent and monomer to the p(DVB) spheres. Grafting PMAIGal chains onto the spheres was conducted by aminolysis of poly(MAIGal)-dithiobenzoate RAFT agent and subsequent thiol-ene reaction with residual double bonds on the particle surface.

After deprotection of the sugar moieties, we furthermore investigated the binding behavior of the water soluble mannose- and galactose-containing glycopolymers with a series of lectins by turbidity measurements.

Scheme 1. Synthesis of glycopolymer-grafted DVB microspheres.

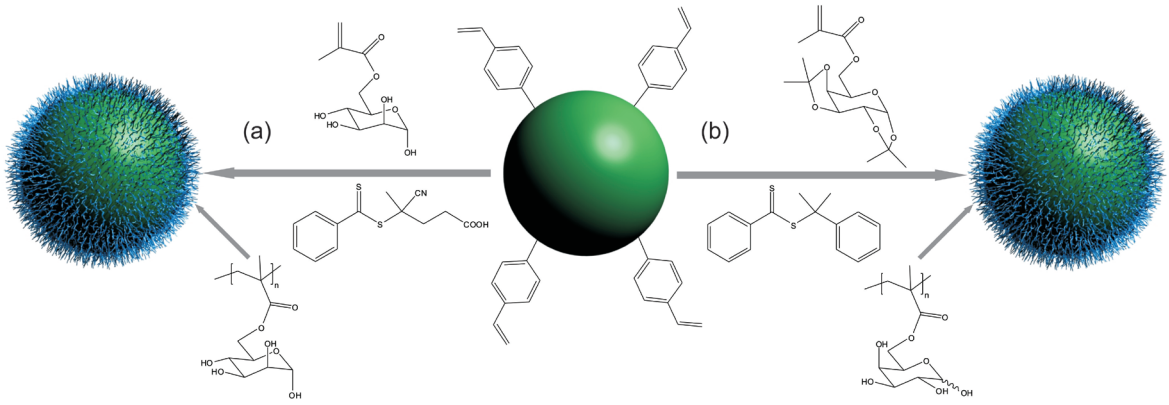

4.2 Experimental Section

Materials

4-(2-hydroxyethyl)piperazine-1-ethansulfonic acid (HEPES, 99.5%, Aldrich), hexylamine (99.5%, Aldrich), Bovine serum albumin (Aldrich), *Ricinus communis* agglutinin (RCA_{120}, Aldrich), Concanavalin A (Con A, Aldrich)), Lens culinaris agglutinin (lentil, Adrich) and Pealectin-I (PSA, Adrich) were all used without further purification. 2,2'-Azobis(2-methylpropionitrile) (AIBN, Aldrich, 98%) was recrystallized twice from methanol prior to use. Glycomonomers 6-*O*-methacryloyl-1,2:3,4-Di-*O*-isopropylidene-galactopyranose (MAIGal)[37] and 6-*O*-methacryloyl mannose,[38] as well as Cumyl dithiobenzoate (CDB)[39] and 4-(Cyanopentanoic acid)-4-dithiobenzoate (CPADB)[40] RAFT agents were synthesized according to literature. PDVB microspheres with a diameter of 2.4 µm were prepared by distillation polymerization of divinylbenzene (Aldrich, 80% divinylbenzene isomers and 20% ethyl styrene isomers) according to literature.[41]

Characterization

Gel permeation chromatography (GPC) measurements for the characterization of PMAIGal were performed on a set of 30 cm SDV-gel columns of 5 µm particle size having a pore size of 10^2, 10^3, 10^4 and 10^5 Å with refractive index and UV (λ = 254 nm) detection. GPC was measured at an elution rate of 1 mL/min with THF as solvent. SEC with multiangle light scattering detector (MALS-GPC) was used to determine the absolute molecular weights. THF was used as eluent at a flow rate of 1.0mL/min: column set, 5µm PSS SDV-gel 10^3, 10^5 and 10^6 Å, 30 cm each; detectors, Agilent Technologies 1200 Series refractive index detector and

Wyatt HELEOS MALS detector equipped with a 632.8 nm He-Ne laser. The refractive index increments of the different PMAIGal polymers in solution at 25 °C were measured to be dn/dc = 0.72 - 0.74 mg/mL using a PSS DnDc-2010/620 differential refractometer. GPC measurements for the characterization of PMAMan were performed in N,N-dimethylacetamide (DMAc) (0.05 wt% LiBr, 0.05% BHT) at 40° C (1mL/min flow rate) using a Shimadzu modular system comprising a DGU-12A solvent degasser, a LC-10AT pump, a CTO-10A column oven and a RID-10A refractive index detector. The system was equipped with a 5.0 mm bead-size guard column (50 x 7.8 mm) followed by four 300 x 7.8 mm linear Phenomenex columns (10^5, 10^4, 10^3 and 500 Å). The calibration curve was generated with narrow polydispersity polystyrene standards ranging from 500 to 10^6 g/mol.

NMR-spectroscopy: ^{1}H and ^{13}C NMR spectra were recorded on a Bruker 300 AC spectrometer using $CDCl_3$ or DMSO-d6 as solvent and internal solvent signal.

Fourier-Transform Infrared Spectroscopy (FT-IR) was carried out on a Spectrum 100 FT-IR spectrometer from Perkin Elmer. For measurements the U-ATR unit was used. The dried samples were directly placed on top of the U-ATR unit for measurements.

Elemental analysis was performed by Mikroanalytisches Labor Pascher, Remagen, Germany.

Field-emission scanning electron microscopy (FESEM) was performed using a LEO Gemini microscope equipped with a field emission cathode.

Turbidity measurements. UV/vis spectroscopy was performed on a Lambda 25 spectrometer of Perkin Elmer. The lectin recognition activity of glycopolymer chains was evaluated by changes in the turbidity of solution with time at λ = 600 nm and room temperature after the addition of polymer solutions (1 mg/mL) to the protein solution (1 mg/mL) in HEPES-buffer.

MALDI-TOF mass spectrometric analysis was performed on a Bruker Reflex III equipped with a 337 nm N_2 laser in the linear mode and 20 kV acceleration voltage. Samples were prepared from THF solution by mixing matrix (trans-3-(3-indoyl)-acrylic acid; 20 g/L) and the sample (1 mg) in a ratio of 20:5. The number-average molecular weight, M_n, of the sample was determined in the linear mode.

Synthesis

RAFT homopolymerization of MAMan glycomonomer. In a round bottom flask 1.0 g (4.028 mmol) MAMan, 5.59 mg (0.020 mmol) CPADB and 0.66 mg (0.004 mmol) AIBN were dissolved in 10 mL DMAc, sealed with a septum and degassed by bubbling with nitrogen for several minutes. After placing the reaction vessel in a 70 °C oil bath, samples of the solution were removed to monitor the reaction kinetics. An aliquot of the solution was analyzed by GPC to determine the molecular weight, whereas the monomer conversion was calculated via ^{1}H-NMR spectroscopy. Polymer purification was performed by precipitating the polymer in methanol, followed by freeze-drying from water.

Grafting of MAMan from microspheres via simultaneous addition of glycomonomer and CTA. In a round bottom flask 100 mg microspheres, 1.0 g (4.028 mmol) MAMan, 5.59 mg (0.020 mmol) CPADB and 0.66 mg (0.004 mmol) AIBN were dissolved in 10 mL DMAc, sealed with a septum, degassed by bubbling with nitrogen for several minutes and the vessel placed in a 70 °C oil bath for 4h. The resulting grafted microspheres were isolated by filtration through a 0.45 µm membrane, washed extensively with water and dried in a vacuum oven. Polymers in solution were also collected, precipitated in methanol and subsequently freeze-dried from water.

RAFT homopolymerization of MAIGal glycomonomer. In a round bottom flask 1.0 g (3.05 mmol) MAIGal, 4.21 mg (0.015 mmol) CDB and 0.83 mg (0.005 mmol) AIBN were dissolved in 10 mL DMF, sealed with a septum and degassed with nitrogen for several minutes. After placing the reaction vessel in a 60 °C oil bath, samples of the solution were withdrawn to monitor the reaction kinetics. An aliquot of each solution was analyzed by GPC to determine the molecular weight, whereas the monomer conversion was calculated via ^{1}H-NMR spectroscopy. Polymer purification was performed by precipitating the polymer in methanol, followed by freeze-drying from dioxane.

Grafting of MAIGal from microspheres via simultaneous addition of glycomonomer and CTA (Approach 1). 100 mg of PDVB-microspheres were placed in a round bottom flask and well dispersed in 10 mL DMF by briefly applying ultrasound and subsequent stirring for 2h. After the addition of 1.0 g (3.0 mmol) MAIGal, 4.0 mg (0.15 mmol) CDB and 0.82 mg (0.005 mmol) AIBN, the vessel was sealed with a septum, degassed with nitrogen for several

minutes and put in a 60°C oil bath. After 15h and 95% conversion, determined by ^{1}H-NMR, the resulting grafted microspheres were isolated by filtration through a 0.45 µm membrane, washed extensively with THF and dried in a vacuum oven. Polymers in solution were also collected, the solution concentrated, precipitated in methanol and subsequently freeze-dried from dioxane.

Grafting of MAIGal from microspheres via prior surface modification with CTA (Approach 2). 300 mg of PDVB-microspheres were dispersed in 30 mL toluene, followed by the addition of 30 mg (0.11 mmol) of CDB and 6 mg (0.37 mmol) of AIBN. The vessel was sealed, degassed with nitrogen for several minutes and placed in a 60 °C oil bath for 48 h. The resulting slightly pink microspheres were isolated by filtration through a 0.45 µm membrane, washed extensively with THF and dried in a vacuum oven. 50 mg of modified microspheres were well dispersed in 5 mL DMF by briefly applying ultrasound and subsequent stirring for 2h. After the addition of 0.5 g (1.5 mmol) MAIGal, 2.0 mg (0.075 mmol) CDB and 0.41 mg (0.003 mmol) AIBN, the vessel was sealed with a septum, degassed with nitrogen for several minutes and put in a 60 °C oil bath. After 9h and 66% conversion, determined by ^{1}H-NMR spectroscopy, the resulting grafted microspheres were isolated by filtration through a 0.45 µm membrane, washed extensively with THF and dried in a vacuum oven. Polymers in solution were also collected, the solution concentrated, precipitated in methanol and subsequently freeze-dried from dioxane.

Grafting of PMAIGal onto microspheres via aminolysis and subsequent thiol-ene reaction (Approach 3). 300 mg (0.0032 mmol) PMAIGal (M_n = 94 700 g/mol; PDI = 1.07), 30 mg PDVB-microspheres and 10 mL DMF were added to a round bottom flask. After the addition of 3.2 mg (0.032 mmol) hexylamine and 1.64 mg (0.01 mmol) AIBN the solution was degassed with nitrogen and stirred for 15 h at 60°C. The resulting grafted microspheres were isolated by filtration through a 0.45 µm membrane, washed extensively with THF and dried in a vacuum oven.

Deprotection of sugar moieties towards water soluble PMAGal chains was performed according to literature.[42]

4.3 Results and Discussion

Synthesis of mannose-containing microspheres. The chemo-enzymatic synthesis of 6-*O*-methacryloyl mannose and the formation of homopolymers and diblocks thereof has been described earlier.[38, 43, 44] Without the use of protecting group chemistry, RAFT polymerization seems to be the polymerization technique of choice to yield well-defined unprotected glycopolymers. In our case the previously used water/ethanol mixtures as the reaction medium were inappropriate to create a homogenous dispersion of the microsphere, which was overcome by changing the solvent to DMF. Kinetic studies on the solution polymerization of linear MAMan by the use of CPADB as chain transfer agent and AIBN as initiator at 70 °C are summarized in Figure 1-3. Figure 1 shows first-order kinetics even to rather high monomer conversion which indicates the absence of undesired side reactions and a short induction period of about 10 minutes. Furthermore, a linear increase of molecular weight with conversion is observed (Figure 2). The difference between the theoretical and the experimental molecular weight can be assigned to the PS-calibration of the GPC. As can be seen in Figure 3, monomodal SEC traces were obtained for the kinetic run, showing no high molecular weight shoulder, i-e. no bi-molecular termination reactions occurred, even at high conversion.

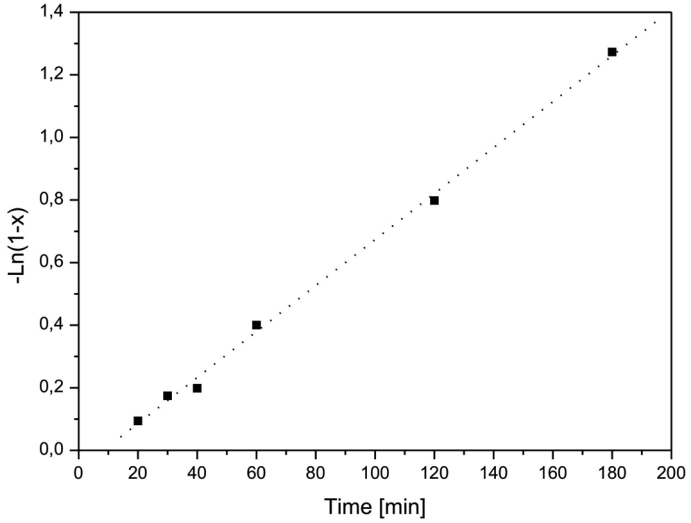

Figure 1. First-order kinetic plot for the polymerization of MAMan in DMF at 70°C.

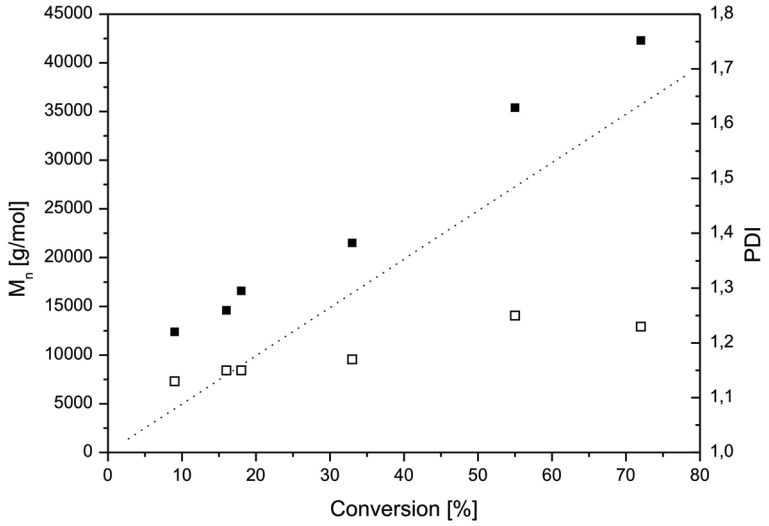

Figure 2. Evolution of molecular weight (filled squares) and polydispersity index (open squares) with conversion. Dashed line shows theoretical molecular weights.

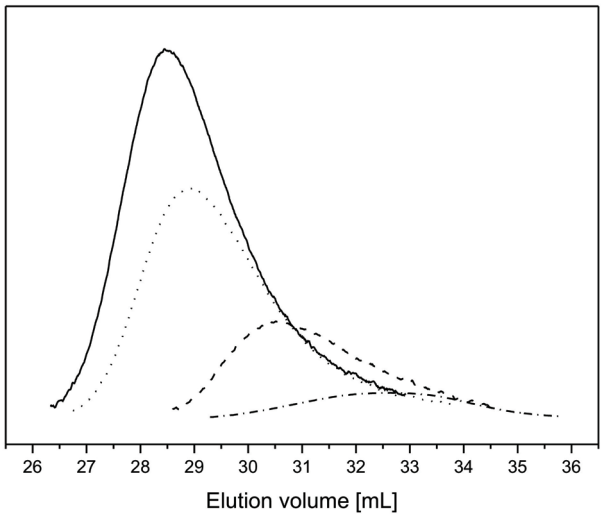

Figure 3. Gel permeation chromatographs of PMAMan as a function of monomer conversion χ_p. (-) : χ_p = 72%, (…) : χ_p = 55%, (- - -) : χ_p = 18%, (-.-.) : χ_p = 9%.

To prepare spherical mannose-containing micropheres we chose the same system (CPADB/AIBN/70°C) as for the successful RAFT polymerization of linear PMAMan. Microsphere core poly(divinylbenzene) particles were prepared by distillation polymerization, having diameters of 2.4 µm and a thin layer consisting of lightly crosslinked

PDVB.[28] The free vinyl groups within this layer enable the surface modification via grafting techniques. “Grafting through” these spheres was conducted by adding glycomonomer, RAFT agent and initiator to the dispersed particles in DMF and heating to 70 °C to start the dissociation of the initiator. During polymerization, growing polymer chains are affixed to the particle surface by copolymerizing with the latent styryl-groups on the spheres, followed by mannose glycomonomer adding to the chain end and extending the brush chain from the surface. After separating the free polymer from the spheres, the successful grafting is optically evident by the color change of the microspheres from white to pink, indicative of the RAFT agent used, as well as the successful suspension of the hydrophilic sugar grafted spheres in comparison to the initial PDVB particles, which accumulate on the water surface. For the calculation of the grafting density the absolute molecular weight of the polymer chains was determined. Given that free polymer in solution and grafted chains have comparable molecular weights and polydispersities,[45-49] characterization of the formed PMAMan in solution was performed by MALDI-ToF MS. Figure 4 shows the corresponding trace with a number average molecular weight M_n = 42 300 g/mol. Elemental analysis of the mannose covered spheres revealed an oxygen content of 2.77 wt%. As the oxygen content in the glycomonomer is found to be 45.1 wt%, a sugar-PDVB composition of 6.1 / 93.9 and a corresponding weight increase of 6.5 percent can be calculated. Given the absolute molecular weight of the sugar chains, the amount of grafted sugar, the radius of the PDVB-particle and hence the surface area (17.510 ^{6} nm^2), 1g of glycopolymer grafted spheres contain $1.16 \cdot 10^{11}$ spheres and $8.69 \cdot 10^{17}$ PMAMan chains which leads to a grafting density of 0.43 chains per nm^2 surface area. Scanning electron microscopy (SEM) was used to visualize the particles before (Figure 5, left) and after (Figure 5, right) grafting glycomonomer from the surface. A much rougher surface can be observed in the case of the mannose covered microspheres.

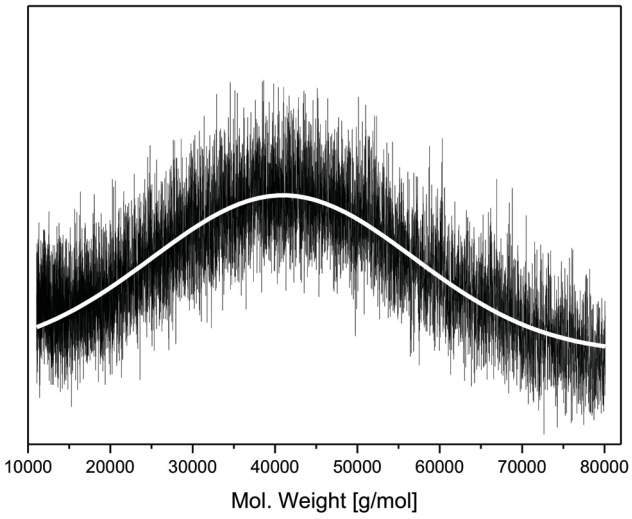

Figure 4. MALDI-TOF MS trace of unbound PMAMan chains in solution showing a number average molecular weight M_n = 42 300 g/mol.

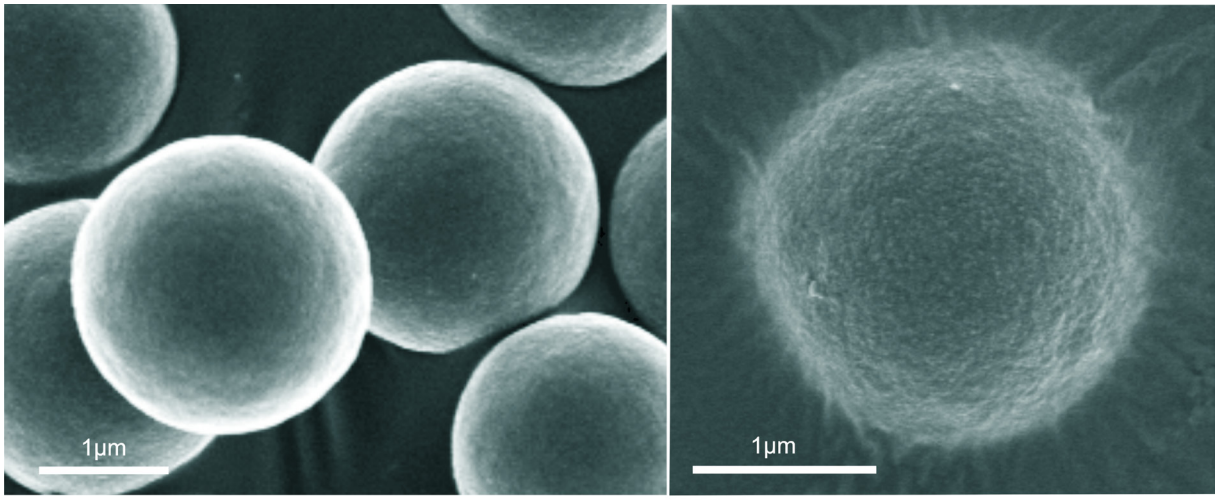

Figure 5. Scanning electron microscopy images of blank (left) and MAMan grafted (right) microspheres. The surface of glycopolymer grafted microspheres is distinctly coarser compared to the blank microspheres.

Finally, lectin interaction studies of mannose-containing polymer were performed. Turbidity measurements with linear PMAMan chains and different lectins were conducted to display any occurring interactions. Due to the multiple binding sites of the lectins, a positive recognition of the sugar molecules leads to the formation of aggregates and therefore to an increase in turbidity. It is known, that mannose-containing glycopolymer chains, which were esterified in the 1-carbon position, show a positive recognition towards Con A.[50-52]

Here, we tested three different proteins (Concanavalin A, Lens culinaris agglutinin and Pealectin-I) that bind specifically to mannose moieties. Unfortunately none of these proteins showed a positive recognition towards PMAMan chains (data not shown). It has been reported that free hydroxy groups in the 3-, 4- and 6-carbon position of mannose are necessary for adequate binding towards Con A.[53, 54] However, no such requirement is provided regarding the other two mannose-binding lectins. Since the turbidity experiments show no binding between PMAMan and either pea or lentil lectins, it is evident that the esterification of the 6-carbon position of the mannose molecule to form the glycomonomer has inhibited its binding with these lectins as well.

Synthesis of galactose-containing microspheres. As the used mannose glycopolymer showed no binding towards the selected proteins, we investigated the use of another glycomonomer based on a protected galactose unit for the preparation of sugar-containing microspheres (Scheme 1). Kinetic studies for the solution polymerization of linear PMAIGal with CDB as RAFT agent and AIBN as initiator are depicted in Figure 6-8. They show the characteristic behavior of a controlled radical polymerization such as linear molecular weight increase with conversion, absence of undesired side reactions and monomodal SEC traces even at high conversion. The rather long inhibition time can be attributed to impurities in the system.[55]

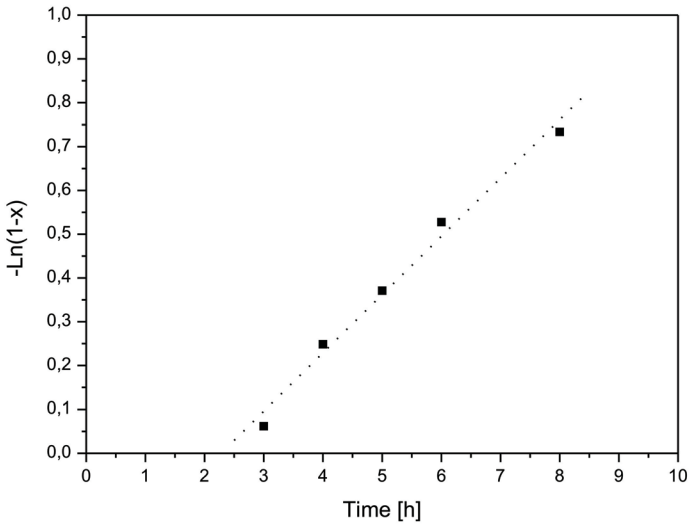

Figure 6. First-order kinetic plot for the polymerization of MAIGal in DMF at 70 °C.

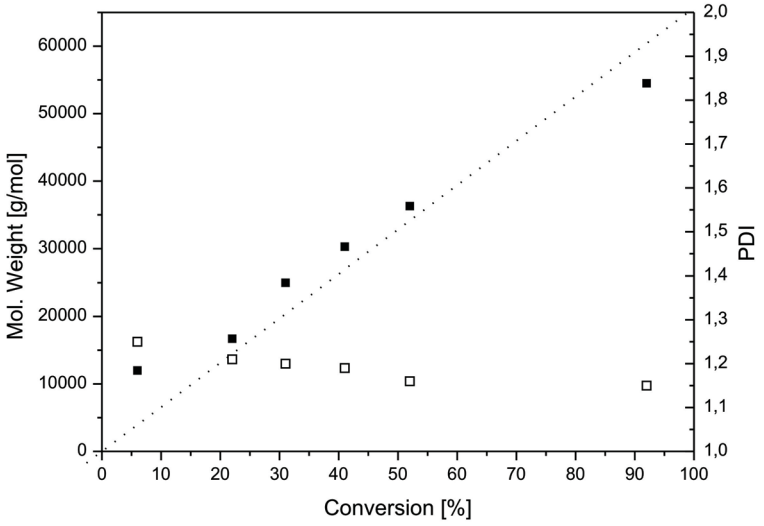

Figure 7. Evolution of molecular weight (filled squares) and polydispersity index (open squares) with conversion for the polymerization of MAIGal. Dashed line shows theoretical molecular weights.

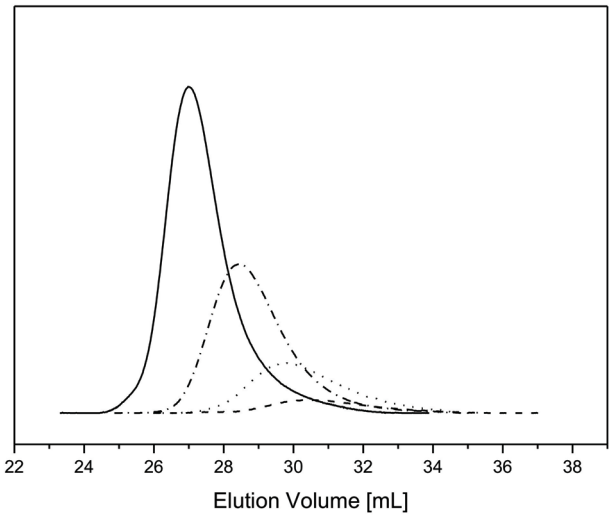

Figure 8. Gel permeation chromatographs of PMAIGal evolution over the course of the kinetic run. (-) : χ_p = 92%, (-.-.) : χ_p = 52%, (...) : χ_p = 22%, (---) : χ_p = 6%.

For the preparation of the galactose covered spheres we performed three different approaches to affix glycopolymer chains to the particle surface. Approach 1 was conducted in a similar way to the preparation of the mannose containing microspheres. To the dispersed PDVB-particles in DMF, glycomonomer, chain transfer agent and initiator were added, the mixture was degassed and put in an oil bath to start the polymerization. After

15h the reaction was stopped and the free polymer in solution was separated from the galactose-covered spheres by filtration and analyzed by SEC (Figure 9).

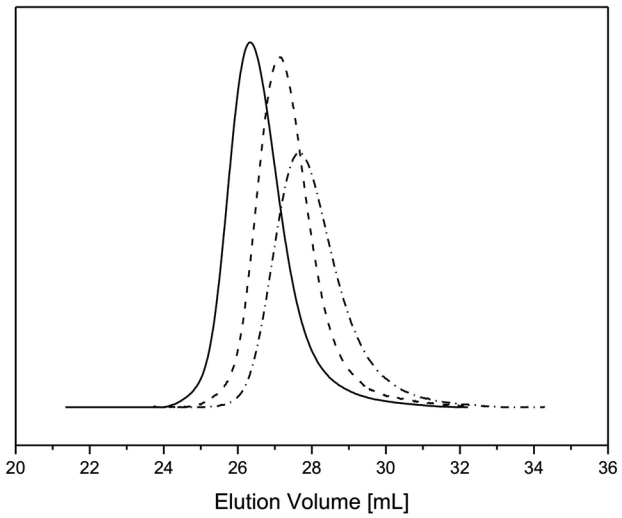

Figure 9. SEC-traces of the soluble part of PMAIGal prepared by Approach 1 (-), Approach 2 (-.-.) and Approach 3 (---).

Table 1. Molecular weights and polydispersity indices of the soluble part of PMAIGal prepared by the different approaches.

Approach	10^3 M_n [g/mol] [a]	PDI [a]	10^3 $M_{n,\,abs}$ [g/mol] [b]
1	65.1	1.14	110.7
2	42.8	1.17	68.5
3	56.1	1.14	94.7

[a] Determined by GPC using THF as eluent with PtBMA standards. [b] Determined by GPC using MALS detector.

Elemental analysis of the purified glycopolymer-covered microspheres led to a sugar-PDVB composition of 8.1 / 91.9 and a corresponding weight increase of 8.8 percent. The absolute number average molecular weight, M_n = 110 700 g/mol, of the formed polymer chains in solution was determined by MALS-SEC with THF as the eluent. The absolute molecular weights of the different approaches are summarized in Table 1.Given the

molecular weight of the chains and the amount of grafted sugar, a grafting density of 0.22 chains per nm^2 was calculated.

Approach 2, a "grafting from" approach, towards galactose–grafted spheres consisted of prior modification of the particle surface by attaching the chain transfer agent (Scheme 2). Therefore microspheres were dispersed in toluene and kept at 60 °C for 2 days after the addition of CDB and AIBN. After purification of the particles via filtration, the successful modification is indicated by a color change from white to pink. Subsequent grafting from these spheres yielded sugar coated particles, and the use of sacrificial chain transfer agent enabled the facile characterization of the formed polymer chains. The absolute number-average molecular weight, M_n = 68 500 g/mol, of these chains was again determined by MALS-SEC. Given a sugar-PDVB composition of 7.9 / 92.1 and a corresponding weight increase of 8.6 percent, determined by elemental analysis, calculation of the grafting density led to a surface coverage of 0.35 chains per nm^2. That means, the prior modification of the particles led to a 1.6 times higher grafting density compared to the first approach. As in Approach 1, grafted chains on the surface increase the steric hindrance and therefore hamper the diffusion of other polymer chains to the reactive sites of the particles, a minor grafting density in comparison to Approach 2 can be expected since the glycomonomer can diffuse more easily to the growing chains.

Scheme 2. Synthesis of galactose containing microspheres by attaching the chain transfer agent to the surface, subsequent grafting MAIGal chains and deprotection of the sugar moieties.

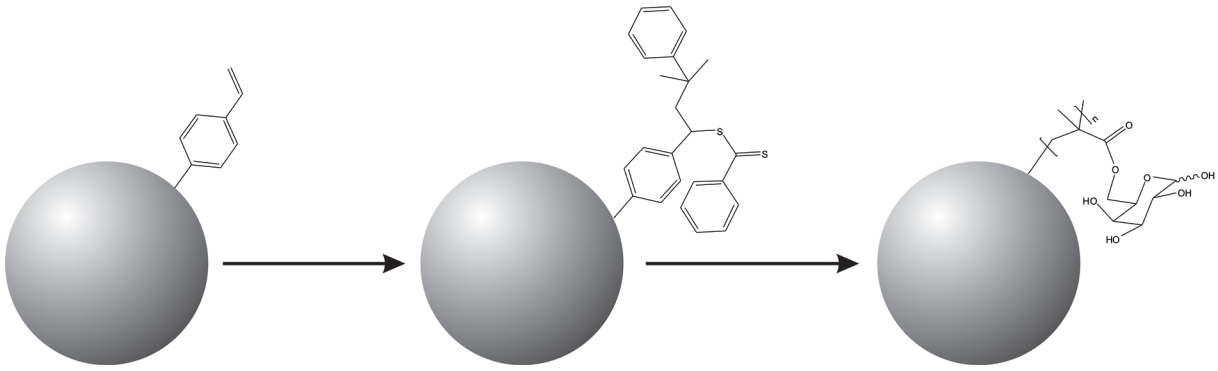

In Approach 3 a strict "grafting to" technique was conducted. As mentioned earlier, there are several ways to graft polymers onto surfaces like RAFT-HDA or CuAAC. In both cases a modification of the particle surface is required for the subsequent click reaction. A

facile method to graft onto PDVB microspheres without prior surface functionalization is to use thiol-ene chemistry. In the presence of primary or secondary amines, RAFT agents undergo aminolysis to form a thiol end group, which is indicated by the disappearance of the characteristic color of the CTA.[56] The resulting functional group is able to undergo a thiol-ene reaction with vinyl groups within the slightly crosslinked poly(divinylbenzene) layer. Here, MAIGal chains were conjugated to spheres in the presence of hexylamine and AIBN in DMF. Prior solution polymerization of linear MAIGal polymer yielded chains with an absolute number average molecular weight M_n = 94 700 g/mol, as determined by MALS-SEC. After grafting these chains onto the particle surface, a sugar-PDVB composition of 6.3 / 93.7 and corresponding weight increase of 6.7 percent could be determined by elemental analysis. The resulting grafting density of 0.20 chains per nm^2 is lower than the one achieved by Approach 1, in which during the early stage of the polymerization shorter chains link to the surface.

Deprotection of the sugar moieties via treatment with trifluoroacetic acid/water led to glycopolymer covered spheres that could easily be dispersed in water due to the hydrophilic side chains. Furthermore, deprotection led to sugar units along the chains´ backbone that should be able to interact with lectins. Therefore, the protein recognition activity of the deprotected galactose chains, which were formed in solution and separated from the microspheres, was investigated by turbidity measurements (Figure 10). For each run, linear glycopolymer chains were mixed with a protein solution, where emerging protein-saccharide interactions cause the formation of aggregates due to the multiple binding sides of proteins and therefore a decrease in transmission occurs. As a control experiment, Concanavalin A (Con A) and Bovine serum albumin (BSA) were mixed with the polymer solution and displayed no decrease in transmission. In contrast to BSA and Con A, *Ricinus communis* agglutinin (RCA_{120}) specifically binds to galactose residues and therefore should result in precipitating the polymer from the solution and lead to a turbidity increase. As can be seen from Figure 10, the aggregate formation occurred fast and the transmission further decreased to 40% within 30 minutes.

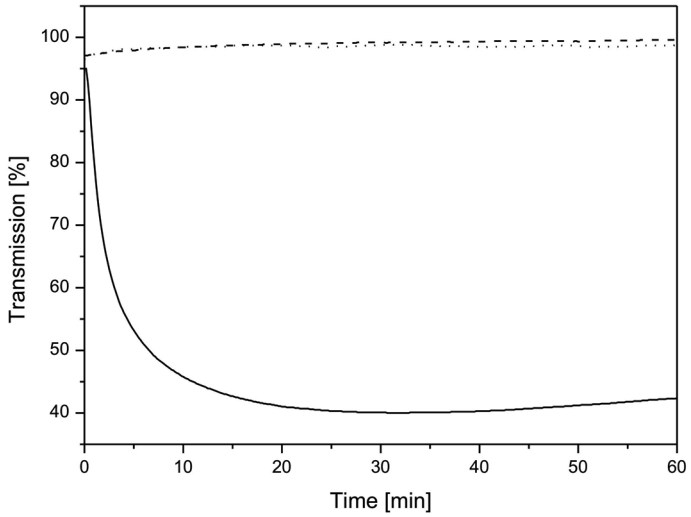

Figure 10. Interactions of poly-galactose chains with RCA_{120} (-), BSA (…) and Con A (---).

To determine the amount of protein that can be precipitated by galactose microspheres, UV/vis spectroscopy was performed. RCA_{120} (1.95 mg) in HEPES-buffer (2 mL) was mixed with microspheres (3.89 mg, prepared by Approach 2) and stirred over night. Subsequent separation of the spheres by ultracentrifugation gave a transparent solution which was analyzed by UV/vis spectroscopy (Figure 11). The solid line represents the lectin in solution before addition of the spheres. After treatment with sugar-coated spheres and separation of the microsphere-lectin aggregates, the decrease of peak height at λ = 280 nm corresponds to the adsorbed protein on galactose particles. The amount of protein left in solution could therefore be calculated to be 1.57 mg (Δm = 0.38 mg) which led to a weight increase of the sugar particles of 9.8 percent. Given a sugar-PDVB composition of 6.1 / 93.9, after deprotection of the glycopolymer-grafted microspheres obtained by Approach 2, and absolute number average molecular weights, M_n = 51 780 and 120 000 g/mol, of the sugar chains and lectin, one grafted glycopolymer chain is capable of binding to 0.7 molecules of RCA_{120}. Assuming that the grafted polymer chains are saturated with lectin after being exposed to the solution overnight, this result would support that multiple galactose moieties on both a single and neighboring grafted polymer chain are binding to a single RCA_{120} molecule. Diehl and Schlaad[29] reported the synthesis of microspheres covered with galactose unimers by thiol-ene reaction of thio-galactose to poly(2-[isopropyl/3-butenyl]-2-oxazoline) microspheres. 10 mg of these microspheres contained 2,8 μmol of galactose and

were able to precipitate 2 nmol of RCA. The high amount of grafted galactose can be explained by the high surface area due to the rough surface of the particles. Our glycopolymer-grafted microspheres contain 2.5 µmol of galactose and bind 8.1 nmol. The strong increase in binding affinity can be ascribed to the "glyco-cluster" effect. Even though galactose units next to the core are not accessible for binding, the overall amount of bound lectin is four times larger. SEM-images of the galactose- and the lectin-galatose-covered microspheres can be seen in Figure 12.

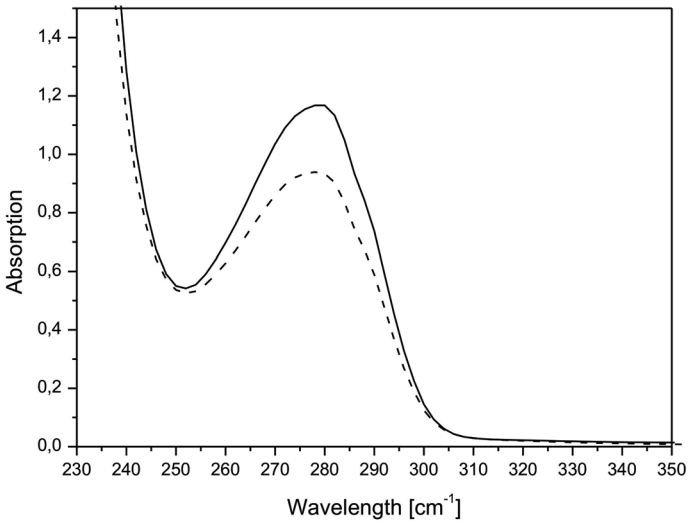

Figure 11. UV/vis spectra of RCA_{120} in solution before (-) and after treatment with galactose microspheres (---).

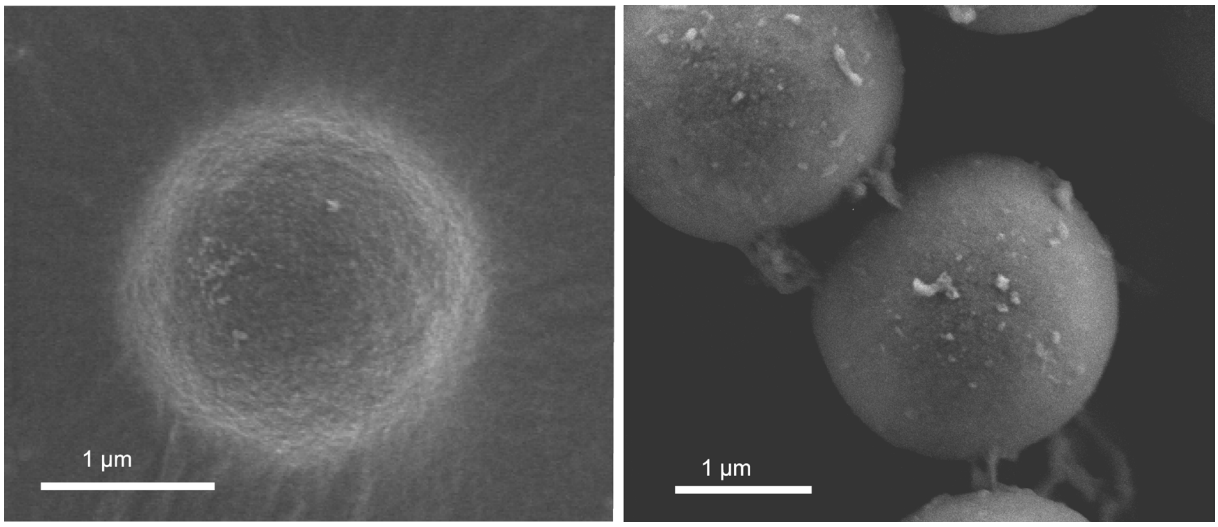

Figure 12. Scanning electron microscopy images of galactose-grafted microspheres (left) and protein-microsphere agglomerates (right).

4.4 Conclusion

The preparation and characterization of glycopolymer-grafted microspheres was successful. Using reversible addition fragmentation chain transfer polymerization, we synthesized both mannose and galactose covered PDVB-particles with high grafting densities (0.20 – 0.43 chains / nm^2) corresponding to 3.5 – 7.5 · 10^6 chains / sphere. Protein recognition activity of mannose-containing polymer towards different lectins was absent, apparently due to the loss of the free hydroxy group at the 6-carbon position of the sugar molecule after enzymatic linkage to the methacrylic unit, no sugar-protein complex can be formed. However, galactose-grafted microspheres revealed a strong binding of the glycopolymer towards the lectin RCA_{120}. On average, each glycopolymer chain binds 0.7 RCA_{120} molecules. In comparison to recently reported galactose covered microspheres, the use of glycopolymers instead of sugar unimers could increase the binding affinity towards RCA_{120} dramatically, due to the "glyco-cluster effect".

Acknowledgements

This work was supported by the European Science Foundation within the SONS 2 program (project BioSONS) and the Australian Research Council (ARC, Discovery Grant DP0877122). We thank Marietta Böhm, Thomas Ruhland and Susanne Edinger for GPC, SEM and MALDI-ToF MS measurements, respectively.

4.5 References

1. Sihorkar, V.; Vyas, S. P. *J. Pharm. Pharm. Sci.* **2001,** 4, 138.
2. Wadhwa, M. S.; Rice, K. G. *J. Drug Trageting* **1995,** 3, 111.
3. Chaikof, E. L.; Garnde, D.; Baskaran, S. *US US 0255021* **2002**.
4. Karamuk, E.; Mayer, J.; Wintermantel, E.; Akaike, T. *Artificial Organs* **1999,** 23, 881.
5. Gordon, E. J.; Strong, L. E.; Kiessling, L. L. *Bioorg. Med. Chem* **1998,** 6, 1293.
6. Kiessling, L. L.; Gestwicki, J. E.; Strong, L. E. *Curr. Opin. Chem. Biol.* **2000,** 4, 696.
7. Miyata, T.; Nakamae, K. *Trends Polym. Sci.* **1997,** 5, 198.
8. Wulff, G.; Zhu, L.; Schmidt, H. *Macromolecules* **1997,** 30, 4533.
9. Aoi, K.; Tsutsumichi, K.; Okada, M. *Macromolecules* **1994,** 27, 875.
10. Fraser, C.; Grubbs, R. H. *Macromolecules* **1995,** 28, 7248.

11. Wulff, G.; Schmid, H.; Venhoff, T. *Macromol. Chem. Phys.* **1996,** 197, 259.
12. Loykulnant, S.; Hayashi, M.; Hirao, A. *Macromolecules* **1998,** 31, 9121.
13. Yamada, K.; Yamaoka, K.; Minoda, M.; Miyamoto, T. *J. Polym. Sci. Part A: Polym. Chem.* **1997,** 35, 255.
14. Manning, D. D.; Hu, X.; Beck, P.; Kiessling, L. L. *J. Am. Chem. Soc.* **1997,** 119, 3161.
15. Ohno, K.; Tsujii, Y.; Miyamoto, T.; Fukuda, T.; Goto, M.; Kobayashi, K.; Akaike, T. *Macromolecules* **1998,** 28, 7248.
16. Lowe, A. B.; Sumerlin, B. S.; McCormick, C. L. *Polymer* **2003,** 44, 6761.
17. Ohno, K.; Tsujii, Y.; Fukuda, T. *J. Polym. Sci. Part A: Polym. Chem.* **1998,** 36, 2473.
18. Serizawa, T.; Yasunaga, S.; Akashi, M. *Biomacromolecules* **2001,** 2, (2), 469.
19. Maruyama, A.; Ishihara, T.; Adachi, N.; Akaike, T. *Biomaterials* **1994,** 15, (13), 1035.
20. Serizawa, T.; Uchida, T.; Akashi, M. *Journal of Biomaterials Science, Polymer Edition* **1999,** 10, 391.
21. Ting, S. R. S.; Min, E. H.; Zetterlund, P. B.; Stenzel, M. H. *Macromolecules* **2010,** 43, (12), 5211.
22. Bernard, J.; Save, M.; Arathoon, B.; Charleux, B. *J. Polym. Sci., Part A: Polym. Chem.* **2008,** 46, (8), 2845.
23. Bernard, J.; Schappacher, M.; Deffieux, A.; Viville, P.; Lazzaroni, R.; Charles, M.-H.; Charreyre, M.-H.; Delair, T. *Bioconjugate Chemistry* **2006,** 17, (1), 6.
24. Muthukrishnan, S.; Zhang, M.; Burkhardt, M.; Drechsler, M.; Mori, H.; Muller, A. H. E. *Macromolecules* **2005,** 38, (19), 7926.
25. Muthukrishnan, S.; Plamper, F.; Mori, H.; Müller, A. H. E. *Macromolecules* **2005,** 38, (26), 10631.
26. Downey, J. S.; Frank, R. S.; Li, W.-H.; Stöver, H. D. H. *Macromolecules* **1999,** 32, 2838.
27. Barner, L. *Advanced Materials* **2009,** 21, (29), NA.
28. Barner, L.; Li, C.; Hao, X.; Stenzel, M. H.; Barner-Kowollik, C.; Davis, T. P. *J. Polym. Sci., Part A: Polym. Chem.* **2004,** 42, (20), 5067.
29. Diehl, C.; Schlaad, H. *Chemistry - A European Journal* **2009,** 15, (43), 11469.
30. Goldmann, A. S.; Walther, A.; Nebhani, L.; Joso, R.; Ernst, D.; Loos, K.; Barner-Kowollik, C.; Barner, L.; Müller, A. H. E. *Macromolecules* **2009,** 42, (11), 3707.
31. Gu, W.; Chen, G.; Stenzel, M. H. *J. Polym. Sci., Part A: Polym. Chem.* **2009,** 47, (20), 5550.

32. Joso, R.; Reinicke, S.; Walther, A.; Schmalz, H.; Müller, A. H. E.; Barner, L. *Macromol. Rapid Commun.* **2009,** 30, (12), 1009.

33. Joso, R.; Stenzel, M. H.; Davis, T. P.; Barner-Kowollik, C.; Barner, L. *Australian Journal of Chemistry* **2005,** 58, 468.

34. Lee, Y. C.; Lee, R. T. *Acc. Chem. Res.* **2002,** 28, (8), 321.

35. Zheng, G.; Stover, H. D. H. *Macromolecules* **2002,** 35, (18), 6828.

36. Nebhani, L.; Sinnwell, S.; Inglis, A. J.; Stenzel, M. H.; Barner-Kowollik, C.; Barner, L. *Macromol. Rapid Commun.* **2008,** 29, (17), 1431;
Nebhani, L.; Schmiedl, D.; Barner, L.; Barner-Kowollik, C.; *Adv. Funct Mater.* **2010,** 20, 2010.

37. Bird, T. P.; Black, W. A. P.; Colquhoun, J. A.; Dewar, E. T.; Rutherford, D. *J. Chem. Soc. C* **1966**, 1913.

38. Granville, A. M.; Quémener, D.; Davis, T. P.; Barner-Kowollik, C.; Stenzel, M. H. *Macromol. Symp.* **2007,** 255, 81.

39. Le, T. P.; Moad, G.; Rizzardo, E.; Thang, S. H. *PCT Int. Appl.* WO 9801478.

40. Mitsukami, Y.; Donovan, M. S.; Lowe, A. B.; McCormick, C. L. *Macromolecules* **2001,** 34, (7), 2248.

41. Bai, F.; Yang, X.; Huang, W. *Macromolecules* **2004,** 37, (26), 9746.

42. Lowe, A. B.; Wang, R. *Polymer* **2007,** 48, (8), 2221.

43. Albertin, L.; Stenzel, M. H.; Barner-Kowollik, C.; Foster, L. J. R.; Davis, T. P. *Macromolecules* **2004**, (37), 7530.

44. Albertin, L.; Stenzel, M. H.; Barner-Kowollik, C.; Foster, L. J. R.; Davis, T. P. *Macromolecules* **2005**, (38), 9075.

45. Barsbay, M.; Gueven, O.; Stenzel, M. H.; Davis, T. P.; Barner-Kowollik, C.; Barner, L. *Macromolecules* **2007,** 40, (20), 7140.

46. Bartholome, C.; Beyou, E.; Bourgeat-Lami, E.; Chaumont, P.; Zydowicz, N. *Macromolecules* **2003,** 36, (21), 7946.

47. Perrier, S. b.; Takolpuckdee, P.; Mars, C. A. *Macromolecules* **2005,** 38, (16), 6770.

48. von Werne, T.; Patten, T. E. *J. Am. Chem. Soc.* **2001,** 123, (31), 7497.

49. Wang, W.; Cao, H.; Zhu, G.; Wang, P. *J. Polym. Sci., Part A: Polym. Chem.* **2010,** 48, (8), 1782.

50. Jiang, X.; Housni, A.; Gody, G.; Boullanger, P.; Charreyre, M.-T. r. s.; Delair, T.; Narain, R. *Bioconjugate Chemistry* **2010,** 21, (3), 521.

51. Ladmiral, V.; Mantovani, G.; Clarkson, G. J.; Cauet, S.; Irwin, J. L.; Haddleton, D. M. *J. Am. Chem. Soc.* **2006,** 128, (14), 4823.

52. Tagawa, K.; Sendai, N.; Ohno, K.; Kawaguchi, T.; Kitano, H.; Matsunaga, T. *Bioconjugate Chemistry* **1999,** 10, (3), 354.

53. Brewer, C. F.; Brown, R. D. *Biochemistry* **1979,** 18, (12), 2555.

54. Sekharudu, Y. C.; Biswas, M.; Rao, V. S. R. *International Journal of Biological Macromolecules* **1986,** 8, (1), 9.

55. Plummer, R.; Goh, Y.-K.; Whittaker, A. K.; Monteiro, M. J. *Macromolecules* **2005,** 38, (12), 5352.

56. Xu, J.; He, J.; Fan, D.; Wang, X.; Yang, Y. *Macromolecules* **2006,** 39, (25), 8616.

Chapter 5

Hyperbranched Glycopolymer Grafted Microspheres

André Pfaff and Axel H. E. Müller

Macromolecular Chemistry II, Universität Bayreuth, 95440 Bayreuth, Germany,

axel.mueller@uni-bayreuth.de

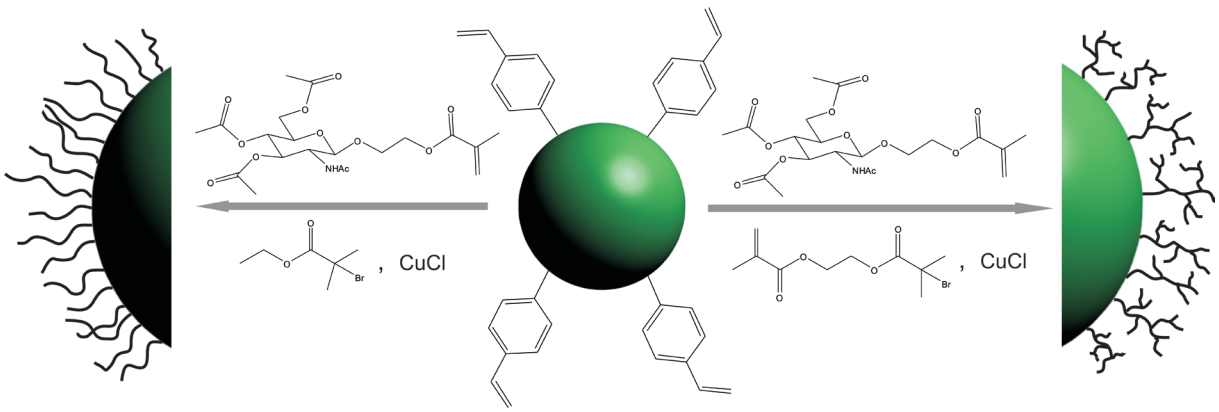

Abstract

The synthesis and characterization of acetylglucosamine-displaying microspheres consisting of poly(divinylbenzene) (PDVB) cores onto which chains of linear and branched glycopolymer chains were grafted via atom transfer radical polymerization (ATRP) and self-condensing vinyl copolymerization (SCVCP), respectively, are reported. PDVB particles with a diameter of 1.5 µm exhibit a layer of lightly cross-linked PDVB in the periphery of the particle and therefore enable a "grafting through" approach due to the residual vinyl groups on the surface. The incorporation of the hydrophobic initiator-monomer (inimer) 2-(2-bromoisobutyryloxy)ethyl methacrylate (BIEM) led to compact and branched structures in the shell of the core-shell particles, whereas the ratio of BIEM to 1-methacryloyloxyethyl 2-acetamido-2-deoxy-3,4,6-triacetylglucopyranoside (tetAcGlc) affected the surface coverage. Lectin-binding experiments indicated a strong affinity of wheat germ agglutinin (WGA), a glucosamine-specific lectin, toward the hyperbranched glycopolymer covered spheres, increasing with the degree of branching.

Keywords: Atom transfer radical polymerization (ATRP), glycopolymer, microspheres, hyperbranched, lectin.

5.1 Introduction

In the past decades enormous emphasis has been put on the synthesis and characterization of synthetic polymers displaying carbohydrate moieties, well-known as glycopolymers. Extensive reviews were published on synthetic strategies toward all kinds of architectures via conventional and controlled radical polymerization, ionic and ring-opening polymerization.[1-3] Complex three-dimensional structures could be achieved by "arm-first" or "core-first" approaches yielding glycostars,[4-8] glycopolymer-covered nanoparticles[9, 10] or glycodendrimers. The latter were synthesized by attaching mono- or oligosaccharide units to the dendritic surface in the final synthetic step.[11-14] In addition to the efforts to achieve perfectly branched glycodendrimers, more facile synthetic strategies were performed to have access to imperfect dendrimer analogues. The synthesis of highly branched glycopolymers was achieved by the one-pot reaction of an acrylic or methacrylic AB*

initiator-monomer (inimer) and glucose-containing monomers via self-condensing vinyl copolymerization (SCVCP) toward free and surface-grafted hyperbranched glycopolymers.[15-19] Additionally, self-condensing ring-opening copolymerizations (SCROCP) of anhydro- and dianhydro-sugars led to branched glycopolymers with controlled molecular weights and low polydispersity indices.[20] Furthermore, the copolymerization of a functional glycomonomer and a cross-linker such as divinylbenzene or ethylene glycol dimethacrylate in the presence of a chain transfer agent, the so-called "Strathclyde methodology", was performed successfully.[21]

In this paper, we report the synthesis and characterization of hyperbranched acetylglucosamine-containing polymers via SCVCP of an initiator monomer 2-(2-bromoisobutyryloxy)ethyl methacrylate (BIEM) and the protected methacrylic acetylglucosamine-displaying glycomonomer 1-methacryloyloxyethyl 2-acetamido-2-deoxy-3,4,6-triacetylglucopyranoside (tetAcGlc) (Scheme 1). As the inimer BIEM carries both a methacrylic unit and an initiator group for atom transfer radical polymerization (ATRP), it operates simultaneously as initiator and monomer. Deprotection of the sugar moieties leads to hyperbranched polymers with a high density of hydroxy groups. Furthermore, this approach was adapted to create core-shell particles consisting of poly(divinylbenzene) (PDVB) microspheres onto which hyperbranched polymers have been grafted (Scheme 2). One aim of this study was to investigate whether the composition of the hyperbranched glycopolymers affects the binding behavior toward the lectin wheat germ agglutinin (WGA) and whether the branched polymer might be superior in binding affinity compared to linear glycopolymers prepared via ATRP. Lectins, sugar binding proteins, bind reversibly and highly specifically to carbohydrates. These interactions are usually weak but can be markedly increased by displaying multiple saccharides in close proximity to each other, yielding multivalent binding sites, commonly known as the "glyco-cluster effect".[22] Introducing branch points toward a complex three-dimensional sugar-containing structure might therefore influence the multivalency effect.

Scheme 1. General Route toward branched glycopolymers via self-condensing vinyl copolymerization.

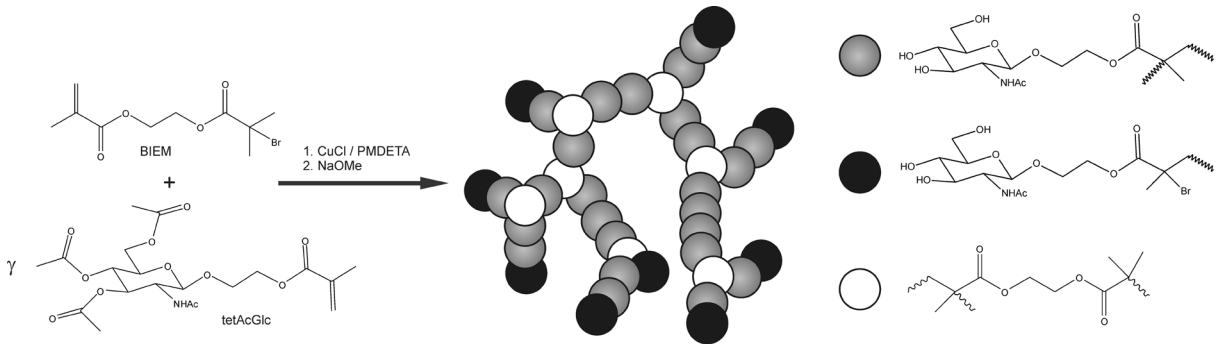

Scheme 2. Synthesis of linear (path a) and hyperbranched (path b) glycopolymer covered microspheres.

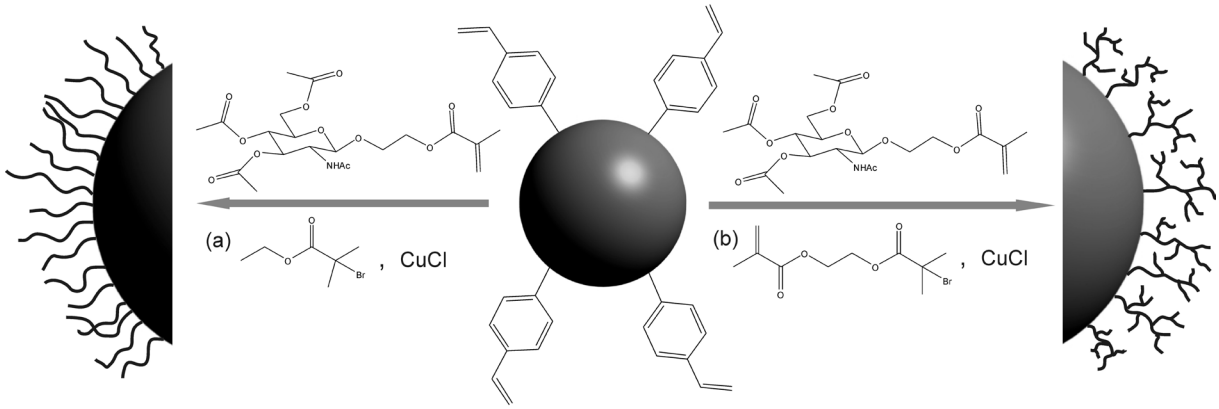

5.2 Experimental Section

Materials

Wheat germ agglutinin (WGA; 36 kDa, Aldrich), 4-(2-hydroxyethyl)piperazine-1-ethanesulfonic acid (HEPES, 99%, Aldrich), 2-acetamido-1,3,4,6-tetra-*O*-acetyl-2-deoxy-*D*-glucopyranose (99%, Glycon), trimethylsilyl trifluoromethanesulfonate (98%, Aldrich), CuCl (99%, Acros), 10-camphorsulfonic acid (98%, Aldrich) and hydroxyethyl methacrylate (98%, Acros) were used without further purification. 1,1,4,7,10,10-hexamethyltriethylene-tetramine (HMTETA; 97%, Aldrich), divinylbenzene (DVB, Aldrich) and ethyl 2-bromoisobutyrate (EBIB; 98%, Aldrich) were distilled prior to use. The two-step synthesis of the protected glycomonomer tetAcGlc was carried out according to the literature.[23, 24] The synthesis of methacrylic inimer 2-(2-bromoisobutyryloxy)ethyl methacrylate (BIEM) was performed according to the method described earlier.[25, 26] PDVB microspheres were prepared by distillation polymerization of divinylbenzene (Aldrich, 80% divinylbenzene

isomers and 20% ethylstyrene isomers) according to the literature.[27] The average particle size was determined by measuring the diameters in TEM images (1.5 ± 0.2 µm).

Characterization

Gel permeation chromatography (GPC) measurements were performed on a set of 30 cm SDV-gel columns of 5 µm particle size having a pore size of 10^2, 10^3, 10^4 and 10^5 Å with refractive index and UV (λ = 254 nm) detection. GPC was measured at an elution rate of 1 mL/min with THF as solvent. SEC with multiangle light scattering detector (MALS-GPC) was used to determine the absolute molecular weights. THF was used as eluent at a flow rate of 1.0 mL · min^{-1}; column set, 5 µm PSS SDV-gel 10^3, 10^5 and 10^6 Å, 30 cm each; detectors, Agilent Technologies 1200 Series refractive index detector and Wyatt HELEOS MALS detector equipped with a 632.8 nm He-Ne laser. The refractive index increments of the different polymers in THF at 25 °C were measured using a PSS DnDc-2010/620 differential refractometer.

NMR spectroscopy: ^{1}H NMR spectra were recorded on a Bruker 300 AC spectrometer using DMSO-d_6 as solvent.

Fourier-Transform Infrared Spectroscopy (FT-IR) was carried out on a Spectrum 100 FT-IR spectrometer from Perkin Elmer. The dried samples were directly placed on top of a U-ATR unit for measurements.

Elemental analysis was performed by Mikroanalytisches Labor Pascher, Remagen, Germany. The oxygen content of bare particles (1.1 wt.-%) was subtracted to yield the absolute values for the grafted particles.

Field-emission scanning electron microscopy (FESEM) was performed using a LEO Gemini microscope equipped with a field emission cathode. 0.1 g/L polymer solutions were dropped on the sample carrier and the solvent evaporated.

UV/vis spectroscopy was performed on a Lambda 25 spectrometer of Perkin Elmer.

Polymerizations

All polymerizations were carried out in round-bottom flasks sealed with a plastic cap. A representative example for the SCVCP of (γ = $[tetAcGlc]_0$ / $[BIEM]_0$ = 1) in solution is as follows: a mixture of tetAcGlc (249 mg, 0.54 mmol), BIEM (151 mg, 0.54 mmol), CuCl (1.0 mg, 0.01 mmol) and DMSO (4 mL) was deoxygenized for several minutes by purging with nitrogen. After addition of HMTETA (2.3 mg, 0.01 mmol), samples of the reaction were withdrawn at timed intervals to monitor the reaction kinetics. The conversion was detected by ^{1}H-NMR and the reaction was quenched at ~ 95 % conversion. The solution was passed through a silica column and the polymer finally precipitated from THF into diethyl ether. The setup was adopted for the preparation of copolymer-covered microspheres. In all experiments, the microspheres (50 wt.-% with respect to the total amount of comonomers) were added to tetAcGlc, BIEM, CuCl and DMSO and the mixture degassed. After addition of HMTETA the mixture was stirred for 10 days at room temperature, and the resulting grafted microspheres were isolated by filtration through a 0.45 µm membrane, washed extensively with THF and dried in a vacuum oven. For the synthesis of linear grafted glycopolymer microspheres ethyl 2-bromoisobutyrate (EBIB) was used to initiate the polymerization of tetAcGlc with a monomer to initiator to catalyst ratio of $[tetAcGlc]_0$ / $[EBIB]_0$ / $[catalyst]_0$ = 40:1:1.

Deprotection of free and surface grafted hyperbranched glycopolymers was performed according to the literature under basic conditions via NaOMe in a 1:1 mixture of $CHCl_3$ and MeOH.[28]

5.3 Results and Discussion

Synthesis of Hyperbranched Glycopolymers via SCVCP in Solution. To find a suitable catalyst system for the synthesis of linear and surface-grafted PtetAcGlc, we previously investigated the effect of the ATRP catalyst system on the homopolymerization of tetAcGlc.[29] CuCl as catalyst and HMTETA as ligand were found to be the system of choice for the preparation of well-defined glucosamine-displaying glycopolymers. On the basis of these results, self-condensing vinyl copolymerizations of tetAcGlc and BIEM in solution were performed using different ratios of glycomonomer to inimer,γ. From γ = 15, corresponding to

15 glycomonomers per inimer, the amount of inimer was steadily increased until an equal ratio of tetAcGlc and BIEM ($\gamma = 1$), yielding a library of branched to hyperbranched polymers. The copolymerizations were carried out at room temperature in DMSO while keeping the comonomer to catalyst ratio constant.

Figure 1 shows first-order kinetics of the prepared branched glycopolymers. Although the initial concentration of BIEM in solution decreases with increasing γ, the apparent rate of polymerization k_{app} increases. Although more initiator groups were introduced with decreasing γ, the lower k_{app} might indicate a fast formation of macroinimers but slow condensation of these macroinimers among each other. Furthermore, the increase of the $[initiator]_0$ / $[catalyst]_0$ ratio by decreasing γ might cause the lower k_{app}.

For comparison, the results of an earlier reported polymerization toward linear PtetAcNGlc via ATRP with a monomer to initiator ratio $[tetAcGlc]_0/[EBIB]_0$ = 100 were added.[29] The fast homopolymerization of tetAcGlc corroborates the assumption that a slow condensation of the macroinimers is responsible for the decrease of k_{app}. The experimental results are summarized in Table 1.

The molecular weights and molecular weight distributions of the copolymers were characterized by conventional GPC and GPC/viscosity and are shown in Table 1. All samples show relatively low polydispersities, whereby the elution curves (Figure 2) shift to higher molecular weights with decreasing amount of BIEM in the feed. Furthermore, the GPC traces show two populations indicating the presence of macroinimers and condensation products thereof.

Table 1. Self-condensing vinyl copolymerisation of BIEM and tetAcGlc at different comonomer ratios,γ.

γ [a]	$[Initiator]_0$ / $[catalyst]_0$	$[Initiator]_0$ / [mmol· L^{-1}]	Reaction time [h]	k_{app} [min^{-1}]	M_n (M_w/M_n) [b] [g mol^{-1}]	M_n (M_w/M_n) [c] [g mol^{-1}]	α [d]
1	50	135	20	0.003	5 000 (1.45)	9 900 (1.32)	0.22
2	33	84	12	0.005	5 500 (1.43)	10 600 (1.24)	0.25
5	17	39	4	0.016	7 000 (1.38)	12 400 (1.27)	0.26
15	6	14	2	0.044	11 000 (1.29)	19 500 (1.23)	0.31
Linear [e]	1	5	2.5	0.026	49 900 (1.09)	-	0.47 [f]

[a] $\gamma = [tetAcGlc]_0$ / $[BIEM]_0$. Copolymerisation at room temperature with CuCl and HMTETA at a constant comonomer to catalyst ratio: μ = ($[tetAcGlc]_0$ + $[BIEM]_0$)/$[catalyst]_0$ = 100. Reactions were stopped at ~ 95 % conversion. [b] Determined by GPC using THF as eluent with PtBMA standards. [c] Determined by GPC/viscosity measurements. [d] Mark-Houwink exponent as determined by GPC/viscosity measurement. [e] The synthesis of linear PtetAcGlc, $[tetAcGlc]_0/[EBIB]_0$ = 100, was reported earlier.[29] [f] Determined from a mixture of PtetAcGlc with different molecular weights.

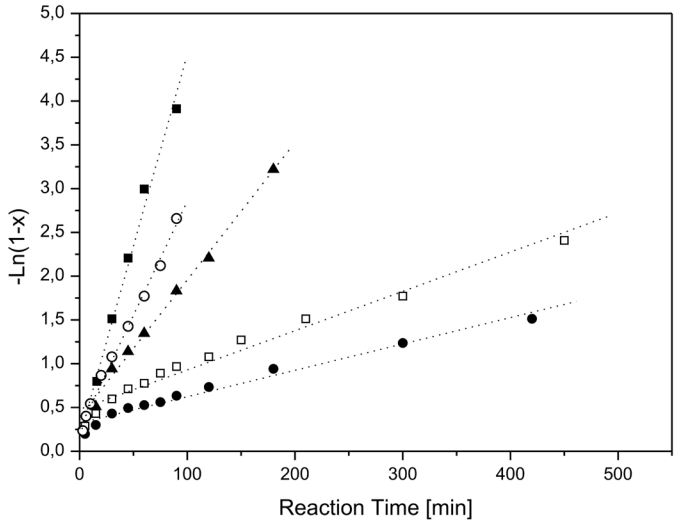

Figure 1. First-order kinetic plots for the SCVCP of BIEM and tetAcGlc at different comonomer ratios γ. Filled squares: γ = 15; filled triangles: γ = 5; open squares: γ = 2; and filled circles: γ = 1. The ATRP of linear PtetAcGlc with a monomer to initiator ratio $[tetAcGlc]_0/[EBIB]_0$ = 100 was reported earlier (open circles).[29]

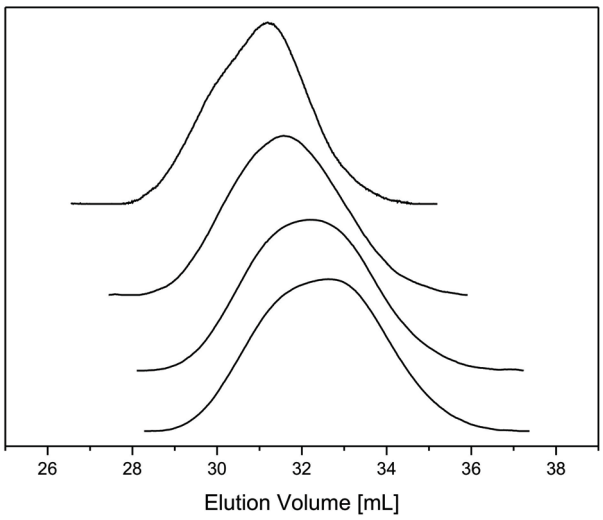

Figure 2. GPC traces of branched glycopolymers obtained at different comonomer ratios. Curves from top to bottom: γ = 15, γ = 5, γ = 2, and γ = 1.

Mark-Houwink plots and contraction factors $g' = [\mu]_{branched} / [\mu]_{linear}$ as a function of the molecular weight are shown in Figure 3. The decrease of g' with increasing molecular weight and the decrease of α with decreasing comonomer ratio γ indicate compact and branched structures. The dependence of the Mark-Houwink exponent α on the theoretical fraction of branch points is depicted in Figure 4. In contrast to the Mark-Houwink exponent of a mixture of linear PtetAcGlc, α = 0.47, indicating a random coil conformation, the exponents of the synthesized branched polymers are in the range of 0.22 – 0.31. The decrease of the Mark-Houwink exponent α from γ = 15 to γ = 1 confirms the increase of branch points within the polymer and therefore compact structures.

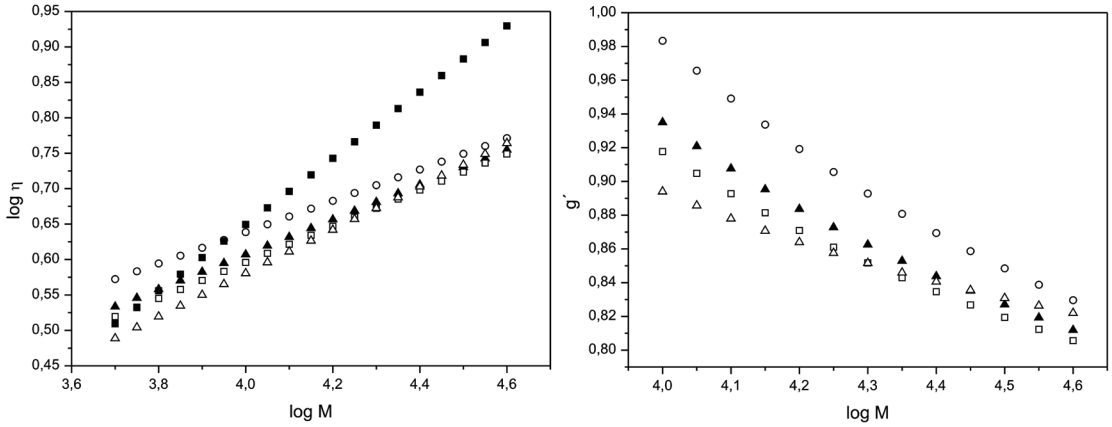

Figure 3. (left) Mark-Houwink plots and (right) contraction factors $g' = [\mu]_{branched} / [\mu]_{linear}$ for the obtained polymers. Filled squares: linear poly(tetAcGlc); open circles: $\gamma = 1$; filled triangles: $\gamma = 2$; open squares: $\gamma = 5$; open triangles: $\gamma = 15$.

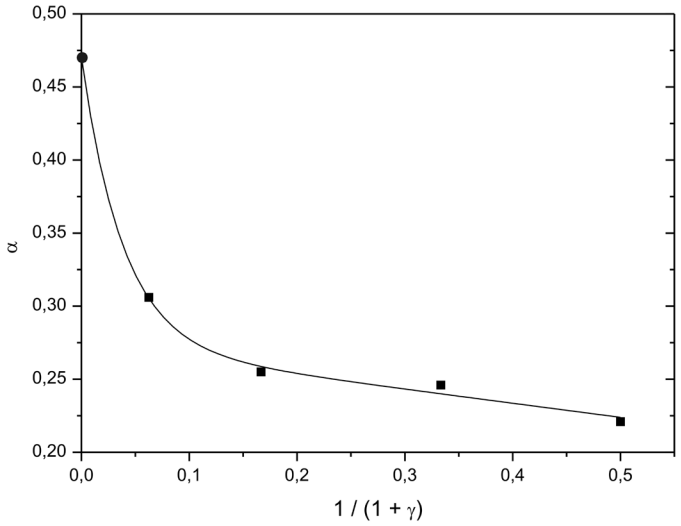

Figure 4. Dependence of the Mark-Houwink exponent α on the comonomer ratio γ. Filled square: mixture of linear PtetAcGlc with different molecular weights.

Deprotection of the sugar moieties was performed according to the literature[28] under basic conditions via NaOMe in a 1:1 mixture of $CHCl_3$ and MeOH and led to water-soluble polymers in the whole range of $\gamma = 1$ to $\gamma = 15$. FT-IR spectra of the linear and hyperbranched glycopolymers before and after deprotection are shown in Figure 5. In the case of poly(tetAcGlc) a characteristic peak at 1750 cm^{-1}, which can be attributed to –NH-CO-bonds, is observed whereas poly(BIEM) showed strong absorption bands in the fingerprint area at 1100 cm^{-1}. The branched glycopolymer, $\gamma = 1$, revealed the mentioned characteristic absorption bands of both tetAcGlc and BIEM, indicating the incorporation of both

monomers. Furthermore, after deprotection of the sugar moieties, higher absorption bands at 3400 cm^{-1}, due to stretching vibrations of the hydroxyl groups of the sugar, can be observed.

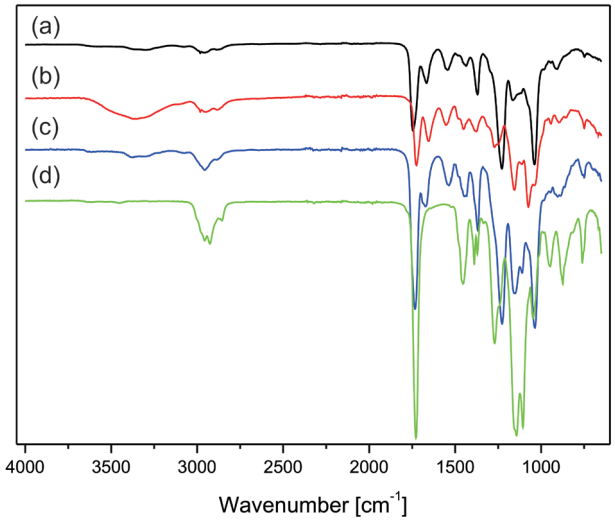

Figure 5. IR spectra of (a) linear poly(tetAcGlc), (b) deprotected copolymer $\gamma = 1$, (c) protected copolymer $\gamma = 1$ and (d) poly(BIEM).

Synthesis of Hyperbranched Glycopolymer-Covered Microspheres via Surface-Grafting SCVCP. PDVB core particles were prepared via distillation-precipitation polymerization of divinylbenzene in acetonitrile as reported by Bai et al.,[27] yielding microspheres with a diameter of 1.5 µm. PDVB spheres display residual vinyl groups on the surface due to a layer of lightly cross-linked PDVB in the outer periphery of the particle.[30] The remaining double bonds enable the attachment of polymer chains to the surface via various grafting techniques.[31-37] The "grafting through" approach in this study led to microspheres covered with linear or hyperbranched glycopolymers via ATRP and SCVCP, respectively. In this approach hyperbranched polymers first grow in solution, then add to the PDVB vinyl groups, and grow further in a grafting onto - grafting from fashion. Given that surface grafted and free polymers in solution have comparable molecular weights and polydispersity indices,[38-42] the characterization of the unbound glycopolymers is a facile way to determine the properties of the grafted polymers. The experimental results are summarized in Table 2. Because of the extended reaction time in comparison to the preparation of free hyperbranched glycopolymers reported above, almost full conversion could be achieved in all runs. Furthermore, the extended reaction time assures the maximal coverage of the

particles with linear or hyperbranched glycopolymers. Figure 6 shows ^{1}H NMR spectra of linear poly(tetAcGlc), hyperbranched glycopolymer (γ = 1) and poly(BIEM). The characteristic peaks at 4.0 – 4.5 ppm for poly(BIEM), obtained via a homo-SCVCP of BIEM, can be attributed to the four protons of the ethylene linkage of BIEM. Linear poly(tetAcGlc) displays three protons in the range of 4.5 – 5.3 ppm and eight protons at 3.5 – 4.5 ppm. The BIEM content in the copolymers obtained by SCVCP could be determined by comparing the peaks at 3.5 – 4.5 ppm attributed to the sum of eight protons of the poly(tetAcGlc) segment and four protons of the ethylene linkage of BIEM and the peaks at 4.5 – 5.3 ppm corresponding to three protons of poly(tetAcGlc) according to previous studies (Figure S1).[17] The contents of BIEM within the copolymers obtained by NMR are in good agreement with the theoretical ones calculated from the composition in feed.

Once the content of BIEM within the copolymer is known, the oxygen content of the formed polymers can be calculated. These oxygen contents range from 38.3 wt.-% for the linear poly(tetAcGlc) to 30.9 wt.-% for the hyperbranched copolymer with equal amounts of BIEM and tetAcGlc (γ = 1). After elemental analysis of the different polymer grafted spheres to determine the oxygen content, one can calculate the amount of grafted copolymer. In the case of the microspheres with γ = 1 an oxygen content of 0.74 wt.-% was found via elemental analysis, which corresponds to a copolymer / DVB composition of 2.4 / 97.6 and a weight increase of 2.5 percent. As the ratio of incorporated BIEM is 0.48, the amount of grafted tetAcGlc can be calculated to be 1.53 wt.-%. The results of the surface-grafting SCVCP experiments are summarized in Table 2. An increase in incorporated inimer, which results in more compact and branched structures, leads to an increase in particle coverage (1.6 – 2.4 wt.-%). This might be caused by the generation of a high number of possible anchor groups within the copolymer that can attack the double bonds on the particle surface. As expected, the corresponding amount of sugar that is grafted on the spheres is increasing with increasing ratio of sugar in the feed in case of the branched copolymers (1.5 – 1.9 wt.-%). The total absence of BIEM in the case of the linear PtetAcGlc grafted microspheres led to a weight increase of 1.64 percent.

Table 2. Synthesis of linear and hyperbranched covered microspheres.

Run	M_n (M_w/M_n) [c] [g mol^{-1}]	$BIEM_{NMR}$ [d]	$BIEM_{theo}$ [e]	Oxygen content [f] [wt.-%]	Grafted copolymer [f] [wt.-%]	Grafted tetAcGlc [f] [wt.-%]
γ = 1 [a]	5 500 (1.44)	0.48	0.50	0.74	2.39	1.53
γ = 2 [a]	5 700 (1.42)	0.34	0.33	0.71	2.15	1.65
γ = 5 [a]	7 400 (1.35)	0.18	0.17	0.74	2.08	1.86
Linear [b]	20 800 (1.13)	-	-	0.62	1.62	1.62

[a] γ = $[tetAcGlc]_0$ / $[BIEM]_0$. Comonomer to catalyst ratio: ($[tetAcGlc]_0$ + $[BIEM]_0$) / $[catalyst]_0$ = 100. [b] Monomer to initiator to catalyst ratio: $[tetAcGlc]_0$ / $[EBIB]_0$ / $[catalyst]_0$ = 40:1:1. [c] Determined by GPC using THF as eluent with PtBMA standards. [d] BIEM ratio in the polymer as determined by ^{1}H-NMR. [e] Theoretical BIEM content calculated from the composition in feed. [f] Determined from elemental analysis. The oxygen content of the bare particles is subtracted.

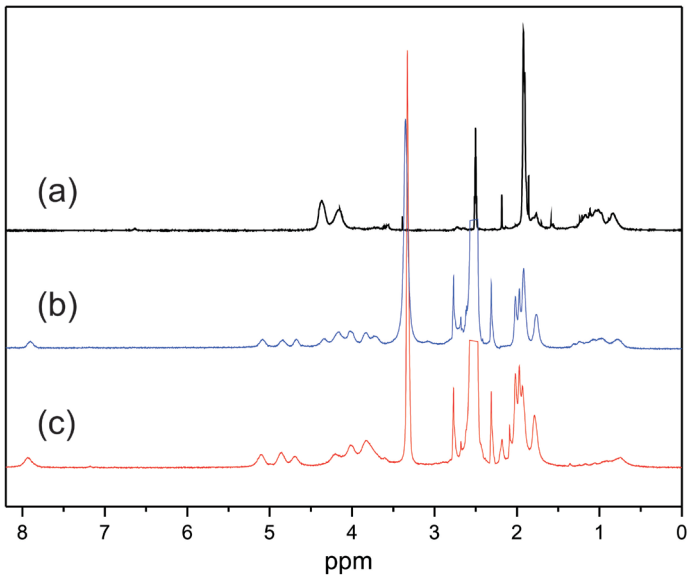

Figure 6. ^{1}H-NMR spectra of poly(BIEM) (a), hyperbranched poly(tetAcGlc) (γ = 1, b) and linear poly(tetAcGlc) (c) in DMSO-d_6.

Deprotection of the sugar moieties via treatment with NaOMe led to acetylglucosamine-displaying spheres that could be easily dispersed in water and therefore enabled the investigation of the binding behavior of these sugar-covered microspheres toward lectins. As the glycopolymer spheres display sugar units along the surface, it should be possible to detect a positive recognition activity toward wheat germ agglutinin (WGA), a lectin that binds specifically to glucosamine residues. To determine the amount of lectin that could be bound by the different glycopolymer grafted microspheres, UV/vis spectroscopy was

performed. Therefore, 2 mL of a stock solution of WGA in HEPES buffer (0.33 mg · mL^{-1}) was mixed with 2 mg of glycopolymer-covered microspheres and stirred for 5 hours. After centrifugation of the microsphere-lectin aggregates the supernatant was analyzed by UV/vis spectroscopy. By comparison of the spectra taken before and after treatment with the microspheres the amount of adsorbed lectin can be calculated. Representative UV/vis spectra for γ = 1 are shown in Figure 7. The decrease of peak height at λ = 276 nm corresponds to the adsorbed protein on the microspheres and was found to be $4.0 \cdot 10^{-2}$ mg per mg of microsphere. After deprotection of the sugar moieties, the amount of grafted glycopolymer is found to be $1.1 \cdot 10^{-2}$ mg which leads to 3.6 mg of adsorbed protein per mg of grafted acetylglucosamine on the sphere. The results of all UV/vis experiments are summarized in Table 3. With increasing content of BIEM in the copolymer the amount of adsorbed protein per mg of grafted acetylglucosamine on the sphere is increasing. It is remarkable that the incorporation of ~50% of the hydrophobic linker BIEM for γ = 1 led to an increase in adsorption of 26% compared to the branched glycopolymer with γ = 5. This indicates a further increase of the “glyco-cluster effect” with implementation of branch points. In comparison to this, the linear grafted microspheres showed a higher binding affinity than the branched glycopolymer with γ = 5 but a lower binding affinity than the branched glycopolymer with γ = 2. Two competing mechanisms could cause this phenomenon. On the one hand, the implementation of branch points creates a compact structure that hampers the diffusion of protein molecules inside the copolymers. On the other hand, they increase the interaction between saccharides and proteins by displaying multiple saccharides in close proximity to each other, yielding multivalent binding sites, and therefore increase the “glyco-cluster effect”.

Field emission scanning electron microscopy (FESEM) images of the ungrafted and grafted microspheres are shown in Figure 8. After grafting hyperbranched glycopolymer a coarser surface in comparison with the blank microspheres is observed. After adsorption of wheat germ agglutinin more organic materials that cover the spheres as well as a strong agglutination of the spheres can be recognized.

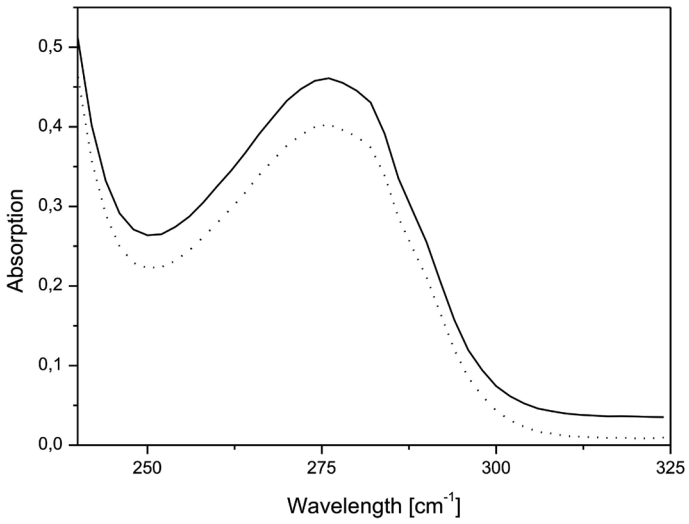

Figure 7. UV/vis spectra of WGA in solution before (solid curve, c = 0.33 mg mL^{-1}) and after treatment with hyperbranched glycopolymer-covered microspheres (γ = 1) (dotted curve).

Table 3. Protein adsorptions on linear and hyperbranched microspheres as determined by UV/vis measurements.

Run	Adsorbed Protein per mg Microsphere [10^{-2} mg]	Grafted NGlc per mg Microsphere [c)] [10^{-2} mg]	Adsorbed Protein per mg NGlc [mg]
γ = 1 [a)]	4.01	1.11	3.61
γ = 2 [a)]	4.19	1.20	3.50
γ = 5 [a)]	3.85	1.35	2.86
Linear [b)]	3.66	1.17	3.12

[a)] γ = $[tetAcGlc]_0$ / $[BIEM]_0$. Comonomer to catalyst ratio: ($[tetAcGlc]_0$ + $[BIEM]_0$) / $[catalyst]_0$ = 100. [b)] Monomer to initiator to catalyst ratio: $[tetAcGlc]_0$ / $[EBIB]_0$ / $[catalyst]_0$ = 40:1:1. [c)] After deprotection of sugar moieties.

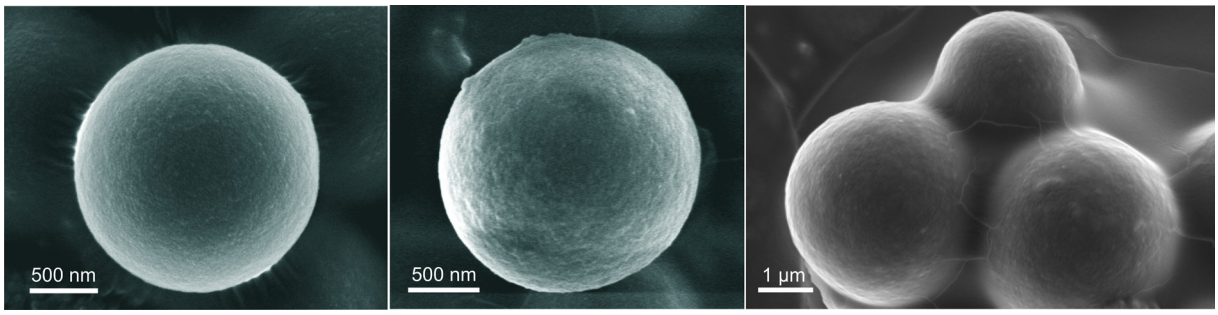

Figure 8. FESEM images of (left) ungrafted and glycopolymer grafted (γ = 1) microspheres (middle) before and (right) after addition of wheat germ agglutinin.

5.4 Conclusions

The preparation and characterization of linear and hyperbranched glycopolymer grafted microspheres were successful. The surface coverage of the poly(divinylbenzene) particles is directly related to the composition of the copolymers in the feed. An equal molar amount of the hydrophobic linker and methacrylic glycomonomer led to the most compact three-dimensional structure within the shell and the highest weight increase. Furthermore, this hyperbranched copolymer showed the highest capability to adsorb the lectin wheat germ agglutinin in relation of grafted glucosamine repeating units, whereby an increase of 16 percent to the linear grafted glycopolymer chains could be detected.

Acknowledgement. This work was supported by the European Science Foundation within the SONS 2 program (project BioSONS). The authors thank *Marietta Böhm* and *Martina Heider* for GPC and SEM measurements, respectively.

5.5 References

1. Ladmiral V, Melia E, Haddleton DM. European Polymer Journal 2004;40:431-449.
2. Narumi A, Kakuchi T. Polym. J 2008;40:383-397.
3. Okada M. Progress in Polymer Science 2001;26:67-104.
4. Bernard J, Favier A, Zhang L, Nilasaroya A, Davis TP, Barner-Kowollik C, Stenzel MH. Macromolecules 2005;38:5475-5484.

5. Bernard J, Hao X, Davis TP, Barner-Kowollik C, Stenzel MH. Biomacromolecules 2005;7:232-238.
6. Dai X-H, Dong C-M. Journal of Polymer Science Part A: Polymer Chemistry 2008;46:817-829.
7. Qiu S, Huang H, Dai X-H, Zhou W, Dong C-M. Journal of Polymer Science Part A: Polymer Chemistry 2009;47:2009-2023.
8. Zhang L, Stenzel MH. Australian Journal of Chemistry 2009;62:813-822.
9. Dai X-H, Zhang H-D, Dong C-M. Polymer 2009;50:4626-4634.
10. Muthukrishnan S, Plamper F, Mori H, Müller AHE. Macromolecules 2005;38:10631.
11. Baigude H, Katsuraya K, Okuyama K, Tokunaga S, Uryu T. Macromolecules 2003;36:7100-7106.
12. Bhadra D, Yadav AK, Bhadra S, Jain NK. International Journal of Pharmaceutics 2005;295:221-233.
13. Fernandez-Megia E, Correa J, Rodriguez-Meizoso I, Riguera R. Macromolecules 2006;39:2113-2120.
14. Klajnert B, Appelhans D, Komber D, Morgner N, Schwarz S, Richter S, Brutschy B, Ionov M, Tonkikh AK, Bryszewska M, Voit B. Chemistry - A European Journal 2008;14:7030-7041.
15. Muthukrishnan S, Erhard DP, Mori H, Müller AHE. Macromolecules 2006;39:2743-2750.
16. Muthukrishnan S, Jutz G, Andre X, Mori H, Muller AHE. Macromolecules 2004;38:9-18.
17. Muthukrishnan S, Jutz G, André X, Mori H, Müller AHE. Macromolecules 2005;38:9.
18. Muthukrishnan S, Mori H, Müller AHE. Macromolecules 2005;38:3108.
19. Muthukrishnan S, Nitschke M, Gramm S, Oezyuerek Z, Voit B, Werner C, Mueller AHE. Macromol. Biosci. 2006:658.
20. Muthukrishnan S, Zhang M, Burkhardt M, Drechsler M, Mori H, Muller AHE. Macromolecules 2005;38:7926-7934.
21. Satoh T, Kakuchi T. Macromolecular Bioscience 2007;7:999-1009.
22. Besenius P, Slavin S, Vilela F, Sherrington DC. Reactive and Functional Polymers 2008;68:1524-1533.
23. Lee YC, Lee RT. Accounts of Chemical Research 1995;28:321-327.

24. Akinori T, Terumi N, Hisashi I, Yoshihito I, Tadamichi H. Macromolecular Rapid Communications 2000;21:764-769.
25. Nishimura S-I, Furuike T, Matsuoka K, Maruyama K, Nagata K, Kurita K, Nishi N, Tokura S. Macromolecules 1994;27:4876-4880.
26. Matyjaszewski K, Gaynor GS, Kulfan A, Podwika M. Macromolecules 1997;30:5192.
27. Mori H, Boeker A, Krausch G, Mueller AHE. Macromolecules 2001:6871.
28. Bai F, Yang X, Huang W. Macromolecules 2004;37:9746-9752.
29. Vazquez-Dorbatt V, Maynard HD. Biomacromolecules 2006;7:2297-2302.
30. Pfaff A, Shinde VS, Lu Y, Wittemann A, Ballauff M, Müller AHE. Macromolecular Bioscience 2010:10.1002/mabi.201000324.
31. Downey JS, Frank RS, Li W-H, Stöver HDH. Macromolecules 1999;32:2838.
32. Barner L. Advanced Materials 2009;21:1-7.
33. Barner L, Li C, Hao X, Stenzel MH, Barner-Kowollik C, Davis TP. Journal of Polymer Science Part A: Polymer Chemistry 2004;42:5067.
34. Diehl C, Schlaad H. Chemistry - A European Journal 2009;15:11469.
35. Goldmann AS, Walther A, Nebhani L, Joso R, Ernst D, Loos K, Barner-Kowollik C, Barner L, Müller AHE. Macromolecules 2009;42:3707-3714.
36. Gu W, Chen G, Stenzel MH. Journal of Polymer Science Part A: Polymer Chemistry 2009;47:5550.
37. Joso R, Reinicke S, Walther A, Schmalz H, Müller AHE, Barner L. Macromolecular Rapid Communications 2009;30:1009.
38. Pfaff A, Barner L, Müller AHE, Granville AM. European Polymer Journal 2010;doi:10.1016/j.eurpolymj.2010.09.020.
39. Barsbay M, Gueven O, Stenzel MH, Davis TP, Barner-Kowollik C, Barner L. Macromolecules 2007;40:7140-7147.
40. Bartholome C, Beyou E, Bourgeat-Lami E, Chaumont P, Zydowicz N. Macromolecules 2003;36:7946-7952.
41. Perrier Sb, Takolpuckdee P, Mars CA. Macromolecules 2005;38:6770-6774.
42. von Werne T, Patten TE. Journal of the American Chemical Society 2001;123:7497-7505.
43. Wang W, Cao H, Zhu G, Wang P. Journal of Polymer Science Part A: Polymer Chemistry 2010;48:1782-1790.

5.6 Supporting Information

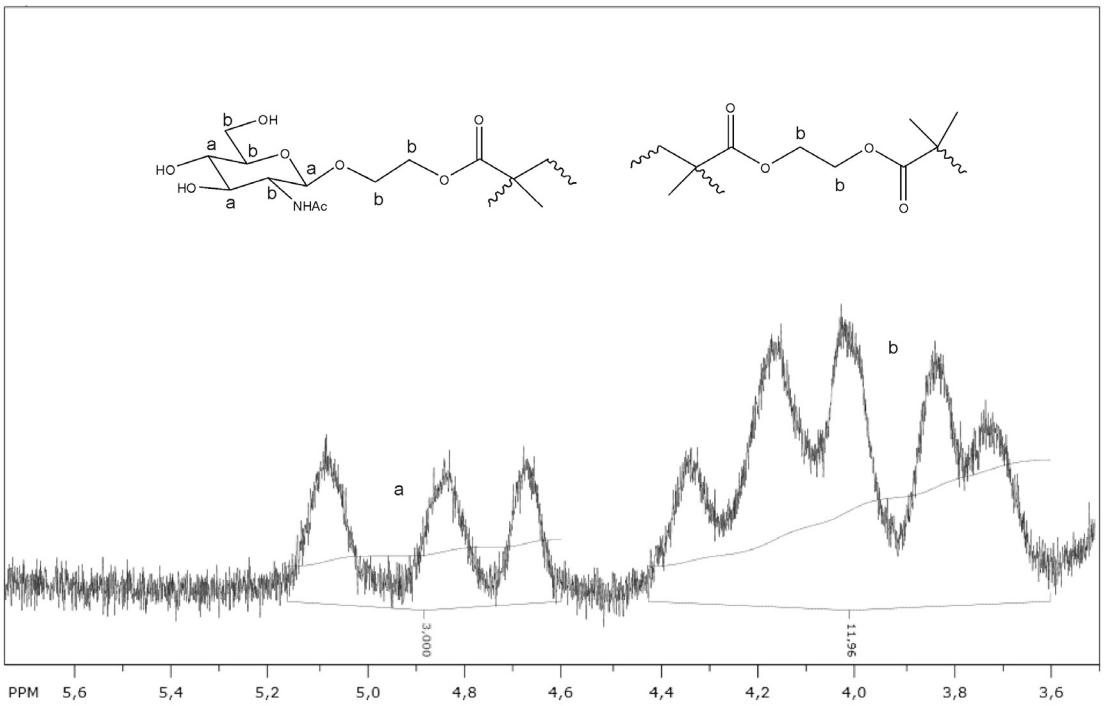

Figure S1. ^{1}H-NMR spectrum of hyperbranched glycopolymer with γ = 1.

Chapter 6

Magnetic, Fluorescent Glycopolymer Hybrid Nanoparticles for Intranuclear Optical Imaging

André Pfaff[1], Anja Schallon[2], Thomas M. Ruhland[1], Alexander P. Majewski[1], Holger Schmalz[1], Ruth Freitag[2] and Axel H. E. Müller[1]

[1]Makromolekulare Chemie II and [2] Bioprozesstechnik, Universität Bayreuth, 95440 Bayreuth, Germany

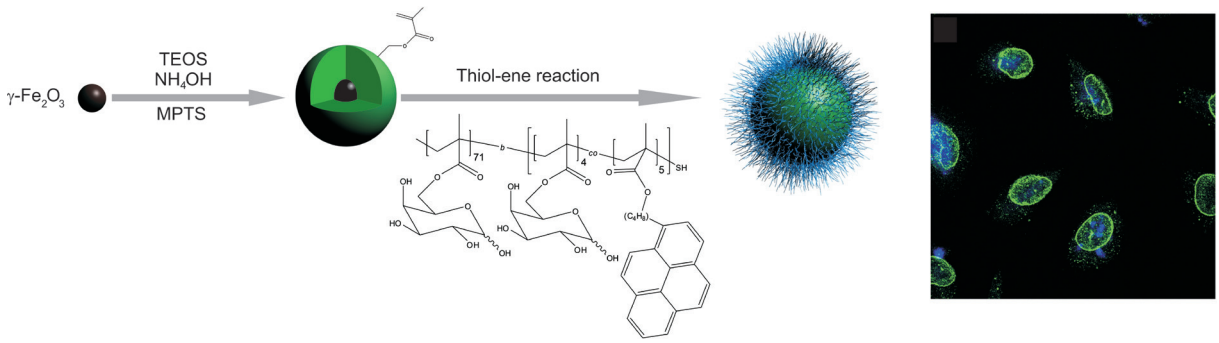

6.1 Introduction

The development of superparamagnetic nanoparticles for potential applications in cell targeting, bioseparation, drug delivery and magnetic resonance imaging (MRI) is of considerable current interest.[1-5] In general, iron oxide particles depict higher biocompatibility and chemical stability compared to other metal oxides and can be easily encapsulated by nontoxic materials such as silicon oxide. For this the well-known Stöber method as well as reverse microemulsion have been performed to provide access to silica-encapsulated iron oxide particles.[6, 7] In addition to superparamagnetic nanoparticles, fluorescent materials show likewise enormous potential in biotechnological applications and find application in sensor technology or biological imaging.[8-11] However, the therapeutic use of these particles is often hampered by unfavorable solubility, stability and toxicity of the compounds. The latter applies especially for quantum dots, which are of special interest for biological imaging but limited in use due to the leakage of heavy metals.[12-14] To overcome these disadvantages and to broaden the applications of composite particles in biosensors and diagnostic medical devices, emphasis has been put on the synthesis of both magnetic and fluorescent silica particles.[15-18] The combination of these two functionalities leads to fluorescent nanoparticles that can be physically manipulated by an external magnetic field or provide contrast enhancement in magnetic resonance imaging (MRI). By functionalizing these nanoparticles with targeting ligands, e. g. carbohydrates, it should be possible to target specific structures and tissues in vivo.

Carbohydrate-protein interactions are involved in a multitude of cellular recognition processes such as cell growth regulations, adhesion, cancer cell metastasis, inflammation by bacteria and viruses and immune response.[19, 20] Furthermore, the uptake of saccharides by specific receptors is essential for the cell. The lock-and-key interactions between saccharides and proteins are generally weak but can be increased dramatically by displaying multiple saccharides in close proximity to each other, commonly known as the “glyco-cluster effect”.[21] Therefore, the surface modification of functional particles with carbohydrates should not only improve the biocompatibility and solubility, but have an influence on the cellular uptake of the particles. As the cellular uptake of unmodified silica particles is usually confined to endosomes or phagosomes, surface modification should overcome the limits of using silica particles as cytoplasmic and nuclear imaging agents.[22, 23]

We report the synthesis of fluorescent, magnetic galactose-displaying core-shell nanospheres by grafting a glycocopolymer consisting of 6-O-methacryloyl-galactopyranose (MAGal) and 4-(pyrenyl)butyl methacrylate (PyMA) onto silica encapsulated iron oxide particles (Scheme 1). In the first step, highly crystalline iron oxide (maghemite, γ-Fe_2O_3) nanoparticles were prepared by thermal decomposition of iron pentacarbonyl in the presence of oleic acid. The second step contained the encapsulation of the maghemite particles with silicon oxide via a reverse microemulsion method. The protective silica shell does not only serve to protect the magnetic particles against degradation, but can also be used for further functionalization. Here, the surface modification of the nanospheres via 3-(trimethoxysilyl)propyl *methacrylate* (MPTS) led to methacrylate-carrying particles onto which glycopolymer chains could be grafted via the thiol-ene reaction. In general, the incorporation of a hydrophilic shell allows the good solubility of the particles in aqueous medium and can prevent the early detection by the reticuloendothelial system in vivo and therefore elongating the blood circulation time of the particles.

Scheme 1. Synthesis of glycopolymer-grafted magnetic and fluorescent nanoparticles.

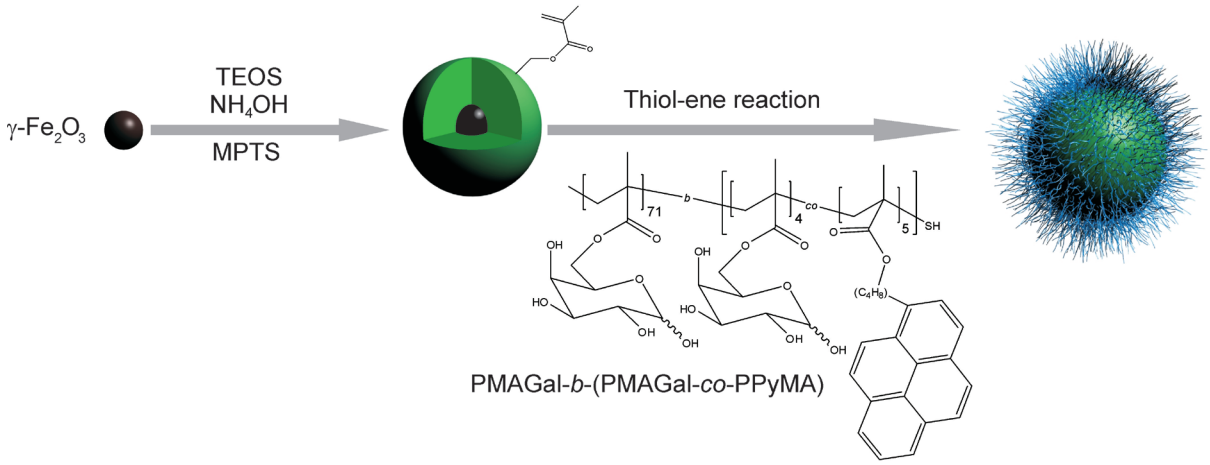

6.2 Experimental Section

Materials

Polyoxyethylene nonylphenylether (Igepal® CO 520), 3-(trimethoxysilyl) propylmethacrylate (MPTS; 98%), ammonium hydroxide (NH_4OH, 28% in H_2O), tetraethoxysilane (TEOS; 98%), hexylamine (99%), dimethylphenylphosphine (99%) and hydroquinone (99%) were obtained from Aldrich and used without further purification. 2,2'-Azobis(isobutyronitrile) (AIBN, Aldrich, 98%) was recrystallized twice from methanol prior to use. Glycomonomer 6-O-

methacryloyl-1,2:3,4-Di-O-isopropylidene-galactopyranose (MAIGal),[24] magnetic iron oxide particles,[25] 4-(pyrenyl)butyl methacrylate (PyMA)[26] and chain transfer agent 2-cyanoprop-2-yl dithiobenzoate (CPDB)[27] were prepared according to the literature.

Synthesis

Synthesis of a galactose- and pyrene-containing glycocopolymer via RAFT polymerization. 30.4 mg (0.13 mmol) CPDB and 5.6 mg (0.03 mmol) AIBN were added to 2.7 g (8.22 mmol) of MAIGal in 35 mL DMF and the mixture degassed by bubbling with nitrogen. After placing the reaction vessel in a 70 °C oil bath, the reaction was monitored by near-infrared spectroscopy. After 22 h (86% conversion) a sample was drawn to analyze the glycopolymer by GPC and ^{1}H-NMR spectroscopy. Subsequent addition of degassed 469 mg (1.37 mmol) PyMA in 1 mL DMF enabled the incorporation of the fluorescent dye in the glycocopolymer. The reaction was quenched after 6 h, analyzed by ^{1}H-NMR spectroscopy and GPC and the glycocopolymer purified by dialysis against THF for 3 days. The solvent was evaporated and the polymer finally freeze-dried from dioxane. The purified copolymer was analyzed by ^{1}H-NMR spectroscopy and GPC-MALS to determine the composition and the absolute molecular weight of the copolymer. Deprotection of the sugar moieties towards water soluble PMAGal-*b*-(PMAGal-*co*-PPyMA) chains was performed according to literature.[28]

Synthesis of silica encapsulated iron oxide nanospheres. 2.3 g (5.44 mmol) Igepal CO-520 in 45 mL cyclohexane in a 100 mL vial was placed in an ultrasonic bath for 10 min. After addition of 4 mL of iron oxide particles in toluene, the mixture was vortexed for 30 min, followed by the addition of 0.4 mL ammonia hydroxide (30 % in water) to form a reverse microemulsion. Encapsulation of the maghemite particles took place after the addition of 0.3 mL TEOS after which the mixture was vortexed for 48 h. The resulting particles were repeatedly centrifuged and redispersed in EtOH (3x) and toluene (3x). To 80 mg of the particles in 10 mL toluene, 1 mL MPTS and a catalytic amount of triethylamine and hydroquinone was added and the mixture stirred for 48 h at 90° C to create double bonds on the particle surface. Repeated centrifugation and redispersion of the particles in DMSO yielded methacrylate-carrying magnetic particles that were kept in solution.

Michael addition towards magnetic and fluorescent glycopolymer-displaying silica particles. To 100 mg of the deprotected glycocopolymer PMAGal-*b*-(PMAGal-*co*-PPyMA) in 3

mL DMSO, 30 µL hexylamine, 10 µL DMPP and 30 mg of silica-encapsulated magnetic particles (dispersed in 2 mL DMSO) were added and the mixture stirred for 24 h at room temperature. In presence of hexylamine the CTA undergoes aminolysis to form a thiol-group that is able to react with the double bond carrying particles via the Michael addition. Isolation of the magnetic glycopolymer particles was performed by extensive magnetically collecting and redispersion cycles.

Characterization

Gel permeation chromatography (GPC) measurements were performed on a set of four 30 cm SDV-gel columns of 5 µm particle size having pore sizes of 10^2, 10^3, 10^4 and 10^5 Å with refractive index and UV (λ = 254 nm) detection. GPC was measured at an elution rate of 1 mL/min with THF as solvent. SEC with multi-angle light scattering detector (MALS-GPC) was used to determine the absolute molecular weights. THF was used as an eluent at a flow rate of 1.0 mL · min^{-1}: column set, 5µm PSS SDV-gel 10^3, 10^5 and 10^6 Å, 30 cm each; detectors, Agilent Technologies 1200 Series refractive index detector and Wyatt HELEOS MALS detector equipped with a 632.8 nm He-Ne laser. The refractive index increments of the different polymers in THF at 25 °C were measured using a PSS DnDc-2010/620 differential refractometer.

NMR-spectroscopy: ^1H and ^{13}C NMR spectra were recorded on a Bruker 300 AC spectrometer using $CDCl_3$ or DMSO-d_6 as solvent and internal solvent signal.

Field-emission scanning electron microscopy (FESEM) was performed using a LEO Gemini microscope equipped with a field emission cathode.

UV/vis spectroscopy measurements were performed on a Shimadzu RF-5301 PC fluorescence spectrometer and a Hitachi U-300 spectrophotometer.

Online FT-NIR spectroscopy measurements were recorded with a Zeiss MCS 611 NIR 2,0 HR. Online monitoring was accomplished using a all-quartz probe (Hellma, 661.060) with an optical path length of 10 mm that is connected to the spectrometer via 2 m fibre-optical cables. Data processing was performed with processXplorer software, whereby the change in peak height at 1628 cm^{-1} was recorded.

Vibrating Sample Magnetometry (VSM) monitors the magnetization curves at room temperature with an ADE Magnetics Vibrating Sample Magnetometer EV7 up to a maximum field strength of 2.2 T. A typical experiment consisted of a virgin curve, followed by a full hysteresis loop. Samples were measured in sealed Teflon vessels, placed on a glass sample holder between two poles of an electromagnet and vibrated at a frequency of 70 Hz.

Transmission electron microscopy (TEM) images were taken with a Zeiss CEM902 EFTEM electron microscope operated at 80 kV or a Zeiss EM922 OMEGA EFTEM electron microscope operated at 200 kV. Both machines are equipped with an in-column energy filter. Samples were prepared through deposition of a drop of the solution (concentration 0.1 g· L^{-1}) onto carbon-coated TEM grids. Afterwards the remaining solvent was removed with a filter paper.

Cell Culture. A549 (CCL-185) lung epithelial cells were purchased from LGC Standards ATCC (Wesel, Germany) and were cultured in DMEM (high glucose, PAA, Cölbe, Germany) supplemented with 10% FCS (PAA, Cölbe, Germany), 100 μg/mL streptomycin (PAA, Cölbe, Germany) ,100 IU/mL penicillin (PAA, Cölbe, Germany), and 2 mM L-Glutamine (PAA, Cölbe, Germany). Cells were cultivated at 37 °C in a humidified 5% CO_2 atmosphere.

Delivery Assay. A549 cells were inoculated at a density of 2×10^5 cells/well in six-well plates 24 h before experiment. The culture media was replaced by OptiMEM (Invitrogen, Carlsbad, California) 1 h before 20 µg of the polymers were added to the cells for 24 h.

Cell staining and microscopy. After 24 h of incubation, the cells were washed with PBS, fixed with 4% *para*-formaldehyde and permeabilized with methanol at -20 °C for 10 min. Samples were blocked with 5% bovine serum albumin plus 0.3% TritonX-100 in phosphate-buffered saline (PBS, blocking solution) for 60 min. Primary antibody (mouse anti-NUP98, NEB, Ipswich, Massachusetts) was diluted 1:50 in block solution and cells were incubated for 2 h at 37 °C and washed four times with PBS. Fluorescent secondary antibody (goat anti-mouse FITC, Sigma Aldrich, St. Louis, Missouri) diluted 1:160 in block solution was applied for 30 min and cells were washed as described above. Coverslips were mounted in Prolong Gold mounting medium (Invitrogen, Carlsbad, California) according to the manufacturer's instructions. The cells were observed with an epifluorescence microscope (Olympus BX51TF, Hamburg, Germany). In addition, images were obtained using a laser

scanning confocal microscope (Leica TCS-SP5, Leica, Wetzlar, Germany) equipped with argon, neon, and UV lasers. Fluorescence images were captured and processed with a digital imaging processing system (Leica TCS software, Leica, Wetzlar, Germany). The different excitation/emission conditions for pyrene and FITC were used in separate channels with the X63 oil immersion objective.

6.3 Results and Discussion

Synthesis of fluorescent galactose-displaying glycopolymer. To create a fluorescent glycopolymer that can be attached to silica spheres, we performed the sequential RAFT polymerization of the glycomonomer MAIGal and PyMA in the presence of the chain transfer agent CPDB in DMF. The synthesis of the first block, consisting of the homoglycopolymer PMAIGal containing protected galactose moieties, was performed with an initial molar ratio of monomer to CTA of 60, $[MAIGal]_0/[CPDB]_0/[AIBN]_0$ = 60:1:0.25, and monitored via near-infrared spectroscopy (Figure 1). The mixture was stirred for 22 hours at 70 °C, yielding a monomer conversion of 86%. After the addition of PyMA ($[MAIGal]_0/[PyMA]_0$ = 6:1), the reaction was continued for additional 6 hours to yield the fluorescent glycocopolymer PMAIGal-*b*-(PMAIGal-*co*-PPyMA). Figure 2 shows first-order kinetics even to high monomer conversion indicating the absence of undesired side reactions. This is confirmed by monomodal GPC traces and the absence of high molecular weight shoulders, which would indicate a bi-molecular reaction (Figure 3). The number-average molecular weight of the homoglycopolymer before addition of PyMA was found to be M_n = 13 700 g· mol $^{-1}$ with a corresponding polydispersity index of 1.22, determined by conventional GPC. The further incorporation of glycomonomer as well as PyMA increased the molecular weight to M_n = 14 800 g · mol $^{-1}$ whereas the molecular weight distribution was lowered to 1.18. To determine the absolute composition and molecular weight of the diblock, ^{1}H-NMR spectroscopy and GPC measurements with MALS detection were performed. Given an absolute molecular weight M_n = 26 100 g mol $^{-1}$, the first block was found to contain 71 units of galactose-containing repeating units, whereas the second block was built up by a statistical copolymer of 4 sugar and 5 pyrene units. Deprotection of the sugar moieties via treatment with trifluoroacetic acid and water led to a fluorescent diblockcopolymer as shown in Figure 4.

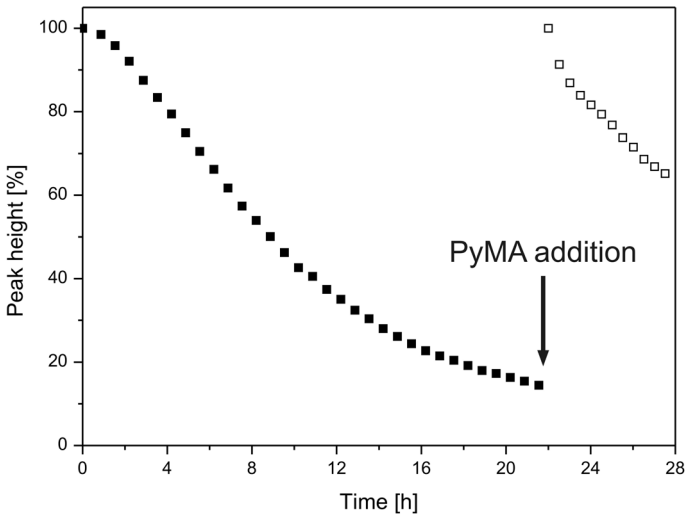

Figure 1. RAFT polymerization of MAIGal (filled squares) with CPDB as chain transfer agent. Addition of PyMA led to the formation of the second block containing a statistical sequence of MAIGal and PyMA (open squares).

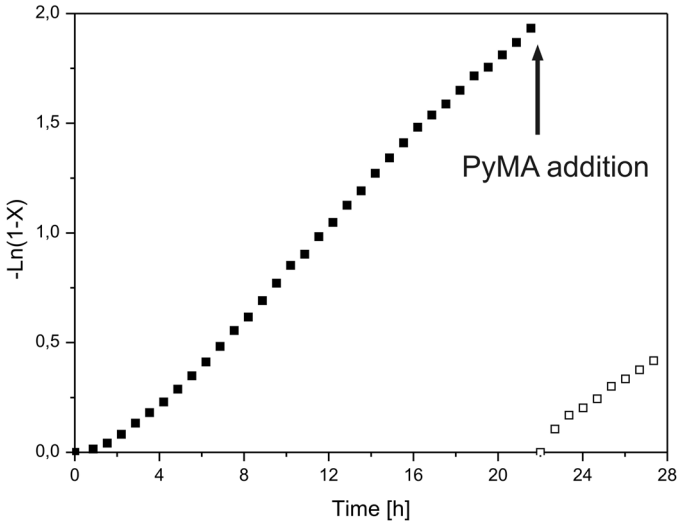

Figure 2. First-order kinetic plot for the polymerization of MAIGal (filled squares) and after addition of PyMA (open squares).

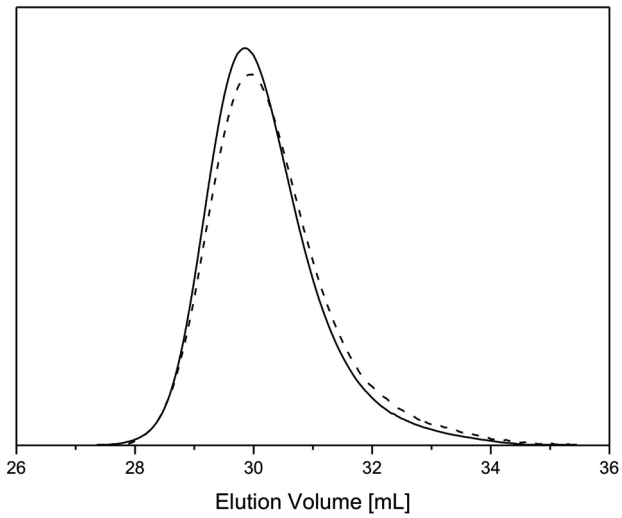

Figure 3. Gel permeation chromatographs of PMAIGal homopolymer (dashed line) and fluorescent copolymer (solid line).

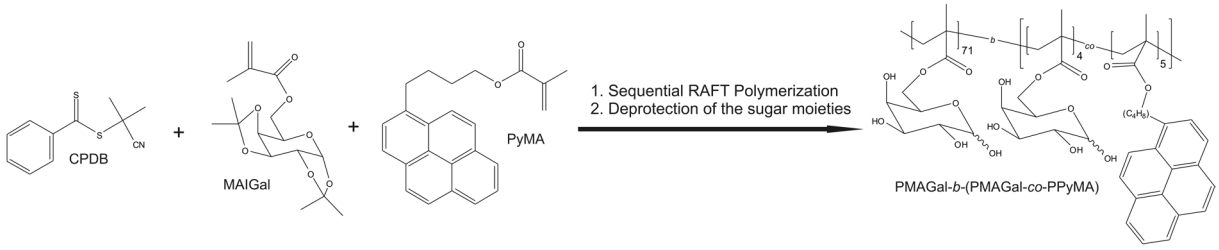

Figure 4. Composition of the fluorescent diblockcopolymer after RAFT polymerization and deprotection of the sugar moieties via treatment with trifluoro acetic acid and water.

Synthesis of magnetic and fluorescent glycopolymer-displaying nanospheres. Highly crystalline and monodispers maghemite nanoparticles with a diameter of 14 nm were prepared by controlled oxidation of iron nanoparticles that were generated from the thermal decomposition of an iron complex as described by Hyeon et al.[25] In the next step, the oleic acid covered γ-Fe_2O_3 particles were coated with a silica shell by adopting a method described by Yi et al.[29] for the preparation of silica encapsulated nanocomposites of magnetic particles and quantum dots. Therefore the black solution of iron oxide particles in toluene was introduced to a solution of the surfactant Igepal CO-520 in cyclohexane and vortexed. The addition of ammonium hydroxide formed a reverse microemulsion whereas subsequent addition of tetraethyl orthosilicate started the growth of the silica shell. The nanocomposite particles were aged for 48 hours and purified by several cycles of centrifugation and redispersion in ethanol and toluene. By this, highly monodisperse silica

particles containing exclusively one maghemite core could be obtained. TEM measurements led to a particle size of 65.2 nm and corresponding shell thickness of 25.6 nm that encapsulated the 14 nm sized iron oxide particles.

The hydrophilic silica particles were transformed into double-bond bearing spheres that are suitable for grafting approaches by condensation of MPTS onto the surface of the particles. Optical evidence of the successful reaction is the easy dispersion of the formed hydrophobic particles in the aprotic solvent toluene.

Various approaches can be performed to attach polymer chains to solid substrates, among them RAFT-hetero Diels-Alder cycloaddition (RAFT-HDA)[30] or copper-catalyzed Huisgen 1,3-dipolar cycloaddition of azides and alkynes (CuAAC).[31] These methods are widely investigated but still exhibit some disadvantages. In CuAAC traces of heavy metals might not be excluded whereas in RAFT-HDA only specific chain transfer agents can be used that may include elaborate synthesis steps. In contrast to this, thiol-ene chemistry is a more facile strategy to attach polymers on surfaces. In the presence of primary or secondary amines, RAFT agents undergo aminolysis to form a thiol end group, which is able to react with double-bond bearing substrates in a thiol-ene reaction via radical or anionic mechanism.[32, 33]

Here, the surface modification of the silica particles towards methacrylic-displaying spheres enabled the Micheal addition of the thiol group to the methacrylic units. In presence of the electron withdrawing carboxy group, no radical source is needed to initiate the reaction. To the mixture of deprotected fluorescent glycocopolymers and the double-bond-functionalized particles in DMSO, hexylamine and DMPP were added to start the aminolysis and anionic chain reaction, whereby the loss of the characteristic color of the chain transfer agent indicated the formation of the thiol group. TEM- and SEM images of the different particles can be seen in Figure 5.

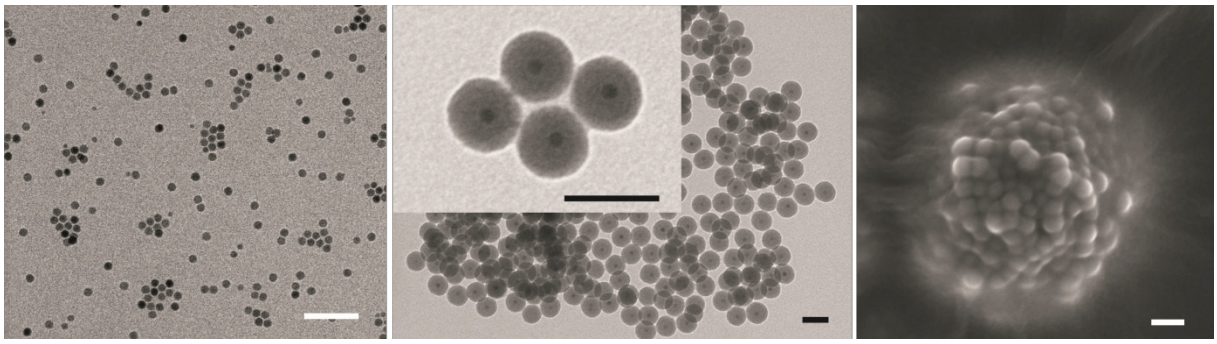

Figure 5. (left) TEM-image of oleic acid stabilized maghemite particles. (middle) TEM-images of ungrafted MPS-functionalized magnetic silica particles. (right) SEM-image of the protected glycopolymer covered spheres. The scale bars represent 100 nm.

Optical and magnetic properties. After isolation of the glycopolymer-covered particles via repeated magnetically collecting and redispersing cycles, the successful attachment of the fluorescent glycocopolymer chains to the magnetic silica spheres was confirmed by UV/vis spectroscopy measurements (Figure 6). The absorption curve demonstrates that the particles absorb light at wavelengths < 400 nm and emit light with a fluorescence maximum at 475 nm, measured at an excitation wavelength of 317 nm.

To quantify the magnetic properties of the iron oxide particles vibrating sample magnetometer (VSM) measurements were performed. The resulting magnetization curve confirms the superparamagnetic properties of the glycocopolymer grafted silica nanoparticles. The magnetization curve does not show a hysteresis. The saturation magnetization-normalized curves of the different particles match well, indicating that neither the encapsulation of the maghemite particles with silica nor the grafting of glycocopolymer chains had a significant influence on the superparamagnetic properties (Figure 7 left). Figure 7 (right) shows, that the glycopolymer hybrid particles can easily be magnetically collected.

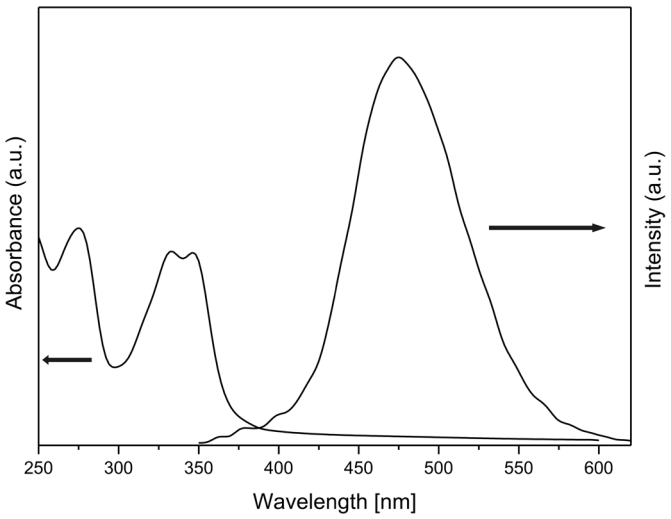

Figure 6. UV/vis absorption and fluorescence spectra of glycocoplymer grafted nanospheres.

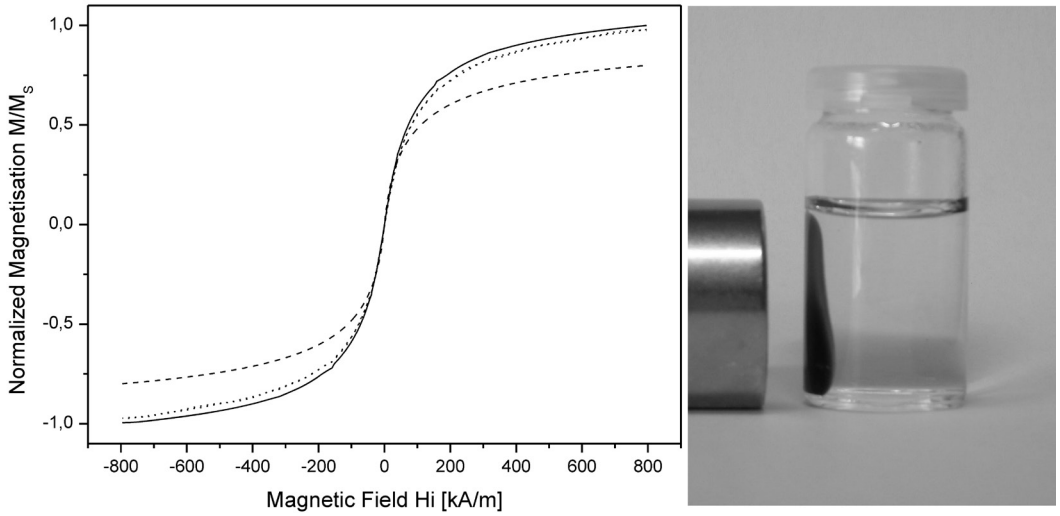

Figure 7. (Left) Magnetic hysteresis curves of γ-Fe_2O_3 nanoparticles (solid line), silica encapsulated γ-Fe_2O_3 particles (dotted line) and glycocoplymer grafted nanospheres (dashed line). (Right) image of the magnetically collected particles.

Cellular localization of the glycopolymer grafted magnetic particles. The incorporation of fluorescent pyrene in the core-shell particles allows an easy localization of the particles within cells by microscopy experiments as pyrene is a highly fluorescent dye with a long lifetime despite laser irradiation. The localization of the particles in the cells was investigated with both epifluorescence and confocal microscopes. As far as the cells showed no significant signal after few hours in the cells, the incubation time was increased to 24 h,

whereby most of the cells internalised the particles. Epifluorescence microscopy images (Figure 8, A-D) showed a significant presence of the nanospheres next to and within the cell nucleus, the membrane of which was stained with anti-NUP98-FITC (Figure 8 C and F). Confocal microscopy experiments confirmed the presence of glycocopolymer grafted magnetic particles within the cell nucleus (Figure 8, E-G); confocal z-stacks proved that the particles were indeed located inside the cells and not stacked to the cell surface.

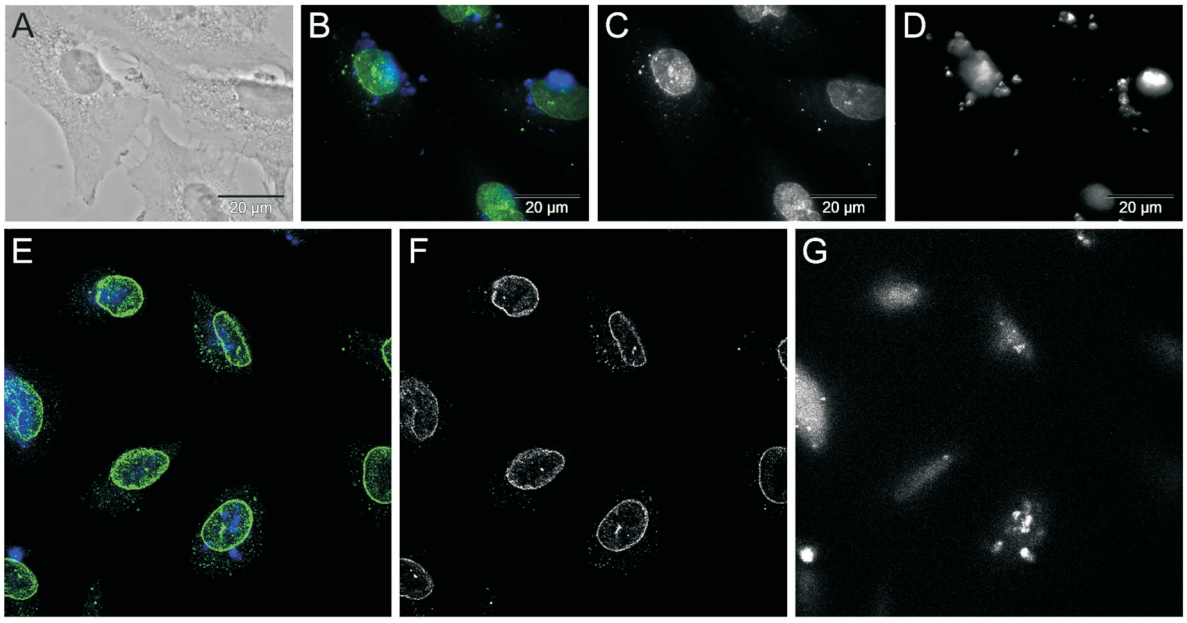

Figure 8. Microscope images of A549 cells exposed to glycopolymer-grafted nanoparticles: (A-D) epifluorescence microscope, (E-G) confocal microscope. (A) transmission image of cells, (B, E) merged fluorescence images, (C, F) fluorescence image that exclusively shows the green light emitting parts (nuclear membrane) and (D, G) blue (pyrene) emitting part (glycocopolymer covered nanospheres).

As both glycoconjugates and carbohydrate-binding proteins are omnipresent in the cytoplasm and the nucleus,[34] the galactose moieties in the outer sphere of the nanoparticle could cause the nuclear uptake. Due to the binding affinity towards β-galactosides a member of the galectin family might be the responsible lectin for the cellular uptake of the fluorescent particles. Galectin-1, for instance, is present in adult mammalian tissues, including muscle, liver, lung, heart, and skin and is expressed both i n the cytoplasm and cell nucleus. Next to galectin-1 also galectin-3, -7 and others have been found in the nucleus.[34] The uptake of the galactose-displaying particles in the used adenocarcinomic human alveolar basal epithelial cells (A549) indicates the participation of a member of the galectin family in this process. As the overexpression of Galectin-1 in tumour tissues must be considered as a

sign of the malignant tumor growth, Galectin-1 is a promising molecular target for the development of therapeutic tools.[35, 36]

The designed glycopolymer-covered particles show potential as delivery agents into the nucleus without being toxic or inhibitive for the cells. The cellular localisation of nanoparticles were also observed in CHO-K1 (hamster ovary cells) and HEK (human kidney cells), who both express galectin-1.[34] Therefore, the internalisation of nanoparticles is not an A549 cell specific phenomenon but might be another hint that galectin is responsible for the cellular uptake.

6.4 Conclusions

The thiol-ene reaction towards magnetic and fluorescent glycopolymer covered silica spheres was successful, whereby neither the prior encapsulation of the iron oxide particles with silica nor the grafting of glycocopolymer chains had a significant influence on the superparamagnetic properties. The incorporation of a galactose-displaying shell seems to enable the internalisation of the fluorescent particles within the cell cytoplasm and nucleus. As both glycoconjugates and lectins are omnipresent in the cytoplasm and the nucleus, carbohydrate-lectin recognition effects might be responsible for the uptake of the glycopolymer-covered particles.

Acknowledgement. We thank Prof. Dr. Stemmann, Martina Heider, Marietta Böhm, Melanie Förtsch and Thomas Friedrich for confocal microscopy, SEM, GPC, TEM and VSM-measurements, respectively. This work was supported by the European Science Foundation within the SONS 2 program (project BioSONS).

6.5 References

1. Deng, Y.; Qi, D.; Deng, C.; Zhang, X.; Zhao, D. *J. Am. Chem. Soc.* **2007,** 130, (1), 28-29.
2. Guo, J.; Yang, W.; Deng, Y.; Wang, C.; Fu, S. *Small* **2005,** 1, (7), 737-743.
3. Gupta, A. K.; Gupta, M. *Biomaterials* **2005,** 26, (18), 3995-4021.
4. Selvan, S.; Patra, P.; Ang, C.; Ying, J. *Angew. Chem. Int. Ed.* **2007,** 46, (14), 2448-2452.
5. Wuang, S. C.; Neoh, K. G.; Kang, E.-T.; Pack, D. W.; Leckband, D. E. *Biomaterials* **2008,**

29, (14), 2270-2279.

6. Lu, Y.; Yin, Y.; Mayers, B. T.; Xia, Y. *Nano Letters* **2002,** 2, (3), 183-186.
7. Vestal, C. R.; Zhang, Z. J. *Nano Letters* **2003,** 3, (12), 1739-1743.
8. Jaiswal, J. K.; Mattoussi, H.; Mauro, J. M.; Simon, S. M. *Nat Biotech* **2003,** 21, (1), 47-51.
9. Li, G.; Shi, L.; An, Y.; Zhang, W.; Ma, R. *Polymer* **2006,** 47, (13), 4581-4587.
10. Terai, T.; Nagano, T. *Curr. Opin. Chem. Biol.* **2008,** 12, (5), 515-521.
11. Müllner, M.; Schallon, A.; Walther, A.; Freitag, R.; Müller, A. H. E. *Biomacromolecules* **2009,** 11, (2), 390-396.
12. Smith, A. M.; Dave, S.; Nie, S.; True, L.; Gao, X. . *Expert Rev. Mol. Diagn.* **2006,** 6, (2), 231-244.
13. Smith, A. M.; Duan, H.; Mohs, A. M.; Nie, S. *Adv. Drug Deliv. Rev.* **2008,** 60, (11), 1226-1240.
14. Smith, A. M.; Nie, S. *Analyst* **2004,** 129, (8), 672-677.
15. Li, G.; Zeng, D. L.; Wang, L.; Baoyu; Zong; Neoh, K. G.; Kang, E. T. *Macromolecules* **2009,** 42, (21), 8561-8565.
16. Nagao, D.; Yokoyama, M.; Yamauchi, N.; Matsumoto, H.; Kobayashi, Y.; Konno, M. *Langmuir* **2008,** 24, (17), 9804-9808.
17. Salgueiriño-Maceira, V.; Correa-Duarte, M.; Spasova, M.; Liz-Marzán, L.; Farle, M. *Adv. Funct. Mat.* **2006,** 16, (4), 509-514.
18. Yoon, T. J.; Kim, J. S.; Kim, B. G.; Yu, K. N.; Cho, M. H.; Lee, J. K. *Angew. Chem. Int. Ed.* **2005,** 44, (7), 1068-1071.
19. Goldstein, I. J.; Iyer, R. N.; Smith, E. E.; So, L. L. *Biochemistry* **1967,** 6, (8), 2373-2377.
20. Hong, C. H. *Carbohydrate-Based Drug Discovery* **2003,** Wiley-VCH, Weinheim, Germany.
21. Lee, Y. C.; Lee, R. T. *Accounts of Chemical Research* **1995,** 28, (8), 321-327.
22. Burns, A.; Sengupta, P.; Zedayko, T.; Baird, B.; Wiesner, U. *Small* **2006,** 2, (6), 723-726.
23. Xing, X.; He, X.; Peng, J.; Wang, K.; Tan, W. *Journal of Nanoscience and Nanotechnology* **2005,** 5, 1688-1693.
24. Bird, T. P.; Black, W. A. P.; Colquhoun, J. A.; Dewar, E. T.; Rutherford, D. *J. Chem. Soc. C* **1966**, 1913.

25. Hyeon, T.; Lee, S. S.; Park, J.; Chung, Y.; Na, H. B *J. Am. Chem. Soc.* **2001,** 123, (51), 12798-12801.

26. Yoo, M.; Heise, A.; Hedrick, J. L.; Miller, R. D.; Frank, C. W. *Macromolecules* **2002,** 36, (1), 268-271.

27. Mellon, V.; Rinaldi, D.; Bourgeat-Lami, E.; D'Agosto, F. *Macromolecules* **2005,** 38, (5), 1591-1598.

28. Lowe, A. B.; Wang, R. *Polymer* **2007,** 48, (8), 2221-2230.

29. Yi, D. K.; Selvan, S. T.; Lee, S. S.; Papaefthymiou, G. C.; Kundaliya, D.; Ying, J. Y. *J. Am. Chem. Soc.* **2005,** 127, (14), 4990-4991.

30. Nebhani, L.; Sinnwell, S.; Inglis, A. J.; Stenzel, M. H.; Barner-Kowollik, C.; Barner, L. *Macromolecular Rapid Communications* **2008,** 29, (17), 1431-1437.

31. Goldmann, A. S.; Walther, A.; Nebhani, L.; Joso, R.; Ernst, D.; Loos, K.; Barner-Kowollik, C.; Barner, L.; Müller, A. H. E. *Macromolecules* **2009,** 42, (11), 3707-3714.

32. Xu, J.; He, J.; Fan, D.; Wang, X.; Yang, Y. *Macromolecules* **2006,** 39, (25), 8616-8624.

33. Hoyle, C.; Bowman, C. *Angew. Chem. Int. Ed.* **2010,** 49, (9), 1540-1573.

34. Wang, J. L.; Gray, R. M.; Haudek, K. C.; Patterson, R. J. *Biochimica et Biophysica Acta (BBA) - General Subjects* **2004,** 1673, (1-2), 75-93.

35. Dings, R. P. M.; Van Laar, E. S.; Loren, M.; Webber, J.; Zhang, Y.; Waters, S. J.; MacDonald, J. R.; Mayo, K. H. *Bioconjugate Chemistry* **2009,** 21, (1), 20-27.

36. Thijssen, V. L. J. L.; Postel, R.; Brandwijk, R. J. M. G. E.; Dings, R. P. M.; Nesmelova, I.; Satijn, S.; Verhofstad, N.; Nakabeppu, Y.; Baum, L. G.; Bakkers, J.; Mayo, K. H.; Poirier, F. o.; Griffioen, A. W. *Proceedings of the National Academy of Sciences* **2006,** 103, (43), 15975-15980.

Chapter 7

Summary

Glycopolymers containing different kinds of carbohydrates were grafted from various spherical templates, whereby the glycopolymer chains were prepared via controlled radical polymerization techniques, namely ATRP and RAFT. A library of carbohydrate-displaying spheres and their interaction with lectins is presented.

Glucose- or acetylglucosamine-displaying nanospheres were prepared via the combination of emulsion polymerization and photo-induced conventional polymerization or ATRP, respectively. The particles were able to stabilize gold nanoparticles to form catalytically active hybrid particles that were capable of reducing *p*-nitrophenol in the presence of $NaBH_4$. Investigation of the interactions between acetylglucosamine-displaying polymers and a series of lectins revealed a selective binding towards the lectin wheat germ agglutinin (WGA) whereby the binding affinity of the protein to the polymer brushes was found to be magnitudes higher than to acetylglucosamine unimers. Lectin precipitation experiments revealed that 1 mg of glycopolymer brush was able to precipitate 0.5 mg of WGA.

Surface modification of poly(divinylbenzene) microspheres was performed using two different glycomonomers and various types of grafting techniques. “Grafting through” of a mannose-displaying glycomonomer yielded core-shell particles with densely grafted glycopolymer arms that were found to show no binding affinity towards a series of lectins. The nexus of the carbohydrate moiety to the polymer backbone seemed to hamper the key-lock interaction of the sugar and protein. Grafting experiments of a galactose-displaying glycomonomer yielded particles with grafting densities ranging from 0.20 to 0.35 chains per nm^2 depending on the utilized grafting approach. These particles showed a selective binding towards the lectin *Ricinus communis* agglutinin (RCA_{120}), whereby each grafted glycopolymer chain was capable of binding to 0.7 molecules of RCA_{120}. Furthermore, the particles were

found to have a superior binding affinity towards RCA_{120} in comparison to microspheres covered with galactose unimers.

The preparation of core-shell particles consisting of a poly(divinylbenzene) microsphere core and a shell of highly branched glycopolymers was achieved via self-condensing vinyl copolymerization of an initiator-monomer and acetylglucosamine-displaying glycomonomer. It was found that an increase in incorporated inimer, which results in more compact and branched structures, directly led to an increase in particle coverage (1.6 – 2.4 wt.-%). Carbohydrate-lectin binding studies revealed that the incorporation of approximately 50% of the hydrophobic inimer led to an increase in adsorption of 26% compared to a less branched glycopolymer and 16% compared to linear glycopolymer grafted particles. These results indicated that the three-dimensional glycopolymer architecture directly affects the strength of the key-lock interaction of sugar and sugar-binding protein.

Studies on the interactions between glycopolymers and lectins were extended towards the cellular uptake of fluorescent, magnetic galactose-displaying core-shell nanospheres. These particles were prepared by grafting a galactose-displaying glycocopolymer onto silica-encapsulated iron oxide particles via thiol-ene chemistry. Due to the carbohydrate-containing shell, these particles could be localized not only in the cytoplasm but also in the nucleus of human lung cancer cells. This cell line expresses a galactose-binding protein which indicates that carbohydrate-lectin interactions are responsible for the uptake of the functionalized particles.

In general, these studies show the capability of utilizing carbohydrate-lectin interactions for potential applications like lectin precipitation and cellular imaging.

Zusammenfassung

Glykopolymere unterschiedlicher Zuckerarten wurden auf verschieden sphärische Template aufgepfropft, wobei der Aufbau der Glykopolymerketten mittels kontrolliert radikalischen Polymerisationstechniken bewerkstelligt wurde, namentlich ATRP und RAFT. Eine Reihe von zucker-modifizierten Nano- und Mikrokugeln und deren Wechselwirkungen mit Lektinen wird hier vorgestellt.

Glucose- oder Acetylglucosamin-modifizierte Nanokugeln wurden durch die Kombination von Emulsionspolymerisation und photoinduzierter konventioneller Polymerisation oder ATRP hergestellt. Diese Partikel waren in der Lage Goldnanopartikel in Lösung zu stabilisieren, was zu katalytisch aktiven Hybridpartikeln führte, welche im Stande waren *p*-Nitrophenol in Gegenwart von $NaBH_4$ zu reduzieren. Untersuchungen zur Wechselwirkung zwischen Polymeren mit Acetylglucosaminresten und einer Reihe von Lektinen offenbarten eine selektive Anbindung an das Lektin Weizenkeim-Agglutinin (WGA), wobei sich herausstellte, dass die Bindungsaffinität des Proteins zu den Polymerbürsten weit höher ist als zu einzelnen Acetylglucosamin-Molekülen. Lektin-Fällungsexperimente offenbarten, dass 1 mg Glykopolymerbürsten in der Lage sind 0,5 mg des Lektins WGA zu fällen.

Die Oberfläche von Poly(divinylbenzol)-Mikrokugeln (PDVB) konnte mit zwei unterschiedlichen Glykomonomeren mittels verschiedener Pfropftechniken modifiziert werden. Die “Grafting through” Methode wurde angewandt um ein Mannose-beinhaltendes Glykomonomer aufzupropfen um Kern-Schale Partikel mit hoher Pfropfdichte zu erhalten. Hierbei zeigten die aufgepfropften Glykopolymerketten keine Bindungsaffinität zu einer Reihe von Lektinen auf. Die Verknüpfung der Zuckergruppe an das Polymerrückgrat verhindert in diesem Fall die Schlüssel-Schloss Wechselwirkung zwischen Zucker und Protein. Pfropfexperimente eines Galaktose-beinhaltenden Glykomonomeren führten zu Partikeln mit Pfropfdichten von 0.20 bis 0.35 Ketten pro nm^2 in Abhängigkeit der verwendeten Pfropfmethode. Diese Partikel zeigen eine selektive Anbindung an das Lektin *Ricinus communis* Agglutinin (RCA_{120}), wobei jede Glykopolymerkette 0.7 RCA_{120} Moleküle binden konnte. Im Vergleich zu Partikeln welche mit einzelnen Galaktosemolekülen versehen sind, zeigten Glykopolymer-gepfropfte Partikel eine überlegene Bindungsaffinität zu RCA_{120}.

Die Herstellung von Kern-Schale Partikeln bestehend aus PDVB-mikrosphärischen Kernen und einer Schale aus hochverzweigten Glykopolymeren konnte mittels selbst-kondensierender Vinyl-Copolymerisation einens Initiator-Monomers und Acetylglucosamin-enthaltenden Glykomonomers erzielt werden. Eine Erhöhung des Anteils des eingebauten Inimers führt zu kompakteren und stärker verzweigten Strukturen, was eine höhere Bedeckung der Partikel begünstigt (1.6 – 2.4 wt.-%). Zucker-Lektin-Bindungsstudien offenbarten, dass ein Einbau von ungefähr 50% des hydrophoben Inimers zu einer Erhöhung der Proteinadsorption von 26% im Vergleich zu einem schwächer verzweigten Glykopolymer und 16% zu Partikeln welche mit linearen Glykopolymeren gepfropft wurden führt. Diese Ergebnisse deuten an, dass die dreidimensionale Glykopolymer-Architektur direkte Auswirkung auf die Schlüssel-Schloss-Wechselwirkung von Zucker und Zucker-bindendem Protein hat.

Die Untersuchungen zur Wechselwirkung zwischen Glykopolymeren und Lektinen wurden auf die Aufnahme von fluoreszierenden, magnetischen Galaktose-beinhaltenden Kern-Schale-Nanokugeln in Zellen ausgeweitet. Diese Partikel wurden durch die Aufpfropfung von Galaktose-beinhaltenden Glykopolymeren auf mit Silica verkapselten Eisenoxid-Partikeln mittels Thiol-En-Chemie erhalten. Aufgrund der zuckerhaltigen Schale konnten diese Partikel nicht nur im Zytoplasma sondern auch im Zellkern von menschlichen Lungenkrebs-Zellen lokalisiert werden. Da diese Zelllinie ein Galakose-bindendes Protein exprimiert, kann darauf geschlossen werden, dass Zucker-Lektin Wechselwirkungen für die Aufnahme der funktionalisierten Partikel verantwortlich sind.

Diese Studien deuten das hohe Potential an Zucker-Lektin Wechselwirkungen für mögliche Anwendung wie die Lektinfällung oder die Darstellung von Zellen zu nutzen.

Chapter 8

List of Publications

During the course of this thesis the following papers have been published (or to be submitted):

1. **Pfaff, A.**; Schallon, A.; Ruhland, T. M.; Majewski, A. P.; Schmalz, H.; Freitag, R.; Müller, A. H. E., *Magnetic, Fluorescent Glycopolymer Hybrid Nanoparticles for Intranuclear Optical Imaging*. 2011, submitted to **Biomacromolecules**.

2. **Pfaff, A.**; Müller, A. H. E., *Hyperbranched Glycopolymer-Grafted Microspheres*, **Macromolecules**, 2011, 44, 1266,1272.

3. **Pfaff, A.**; Shinde, V. S.; Lu, Y.; Wittemann, A.; Ballauff, M.; Müller, A. H. E., *Glycopolymer-Grafted Polystyrene Nanospheres*, **Macromol. Biosci.**, 2011, 11, 199-210.

4. **Pfaff, A.**; Barner, L.; Müller, A. H. E.; Granville, A. M., *Surface Modification of Polymeric Microspheres using Glycopolymers for Biorecognition*, **Eur. Polym. J.**, 2011, 47, 805-815.

5. **Pfaff, A.**; Walther, A.; Lu, Y.; Wittemann, A.; Ballauff, M.; Müller, A. H .E., *Spherical Glycopolymer Brushes*, ***Polym. Prepr.*** *(Am. Chem. Soc., Div. Polym. Chem.)*., 2008, **49**, (2), 604.

6. **Pfaff, A.**; Schallon, A.; Freitag, R.; Müller, A. H. E., *Fluorescent Glycopolymer Capsules for Cellular Optical Imaging*, 2011, to be submitted.

7. Müller, A. H. E.; **Pfaff, A.**, *Bioactive Particles by Grafting Glycopolymers to Micro- and Nanospheres,* **Polym. Prepr.** (Am. Chem. Soc., Div. Polym. Chem.) 52 (2), 2011.

8. Aissou, K.; **Pfaff, A.**; Giacomelli, C.; Travelet, C.; Müller, A. H. E.; Borsali, R., *Fluorescent Vesicles Consisting of Galactose-Based Amphiphilic Copolymers with a π-Conjugated Sequence Self-assembled in Water*, 2011, accepted for publication in **Macromol. Rapid Comm**.

9. Hardy, J.; **Pfaff, A**.; Leal-Egana, A.; Müller, A. H. E.; Scheibel, T., *Biocompatible coatings of spider silk modified with glycopolymers for improved cell adhesion*, 2011, to be submitted.

10. Arslan, H.; **Pfaff, A.**; Müller, A. H. E., *pH- and Temperature-Responsive Block Copolymers and Spherical Brushes Based on D-Galactopyranose and 2-(Dimethylamino)ethyl Methacrylate*, 2011, to be submitted.

Acknowledgements

Firstly, I would like to thank my supervisor Prof. Axel H. E. Müller for giving me the chance to become a member of the MC^2 family. I appreciate his constructive suggestions and patience while proof-reading manuscripts and for all the help he provided me during my stay in his group. I am grateful for all the opportunities I have been offered especially for being sent to several conferences all around the world to present my work. I am also very grateful for giving me the chance to spend three months as an exchange student at the Centre of Advanced Macromolecular Design at the University of New South Wales in Sydney.

I also thank the MC^2 group for being a helpful and kind accumulation of funny people. A big thank you goes to Pierre Millard who introduced me to the world of ATRP and RAFT and never became tired of answering my questions. Furthermore to our technical assistants Marietta Böhm, Melanie Förtsch, Susanne Edinger, Annette Krökel, Annika Pfaffenberger, Sabine Wunder, Kerstin Küspert and Martina Heider (MC1) for doing all the measurements regarding GPC, TEM, SEM, MALDI and for keeping the system running. To my MC^2 PhD colleagues for giving me support in every thinkable way inside and outside the university. Without these desired distraction and "group meetings" I would have never found the strength to finish this thesis. So I would like to make use of the occasion to thank: Eva Betthausen, Markus Drechsler, André Gröschel, Anja Goldmann, Andreas Hanisch, Raymond Joso, Jie Kong, Marina Krekhova, Alex Majewski, Markus Müllner aka µ, Ramon Novoa-Carballal, Sergey Nosov, Stefan Reinicke, Thomas Ruhland, Felix Schacher, Holger Schmalz, Alex Schmalz, Joe Schmelz, Maunela Schumacher, Vaishhali Shinde, Christopher Synatschke, Hansi Voigtländer, Andreas Walther, Stephan Weiß, Michael Witt, Andrea Wolf, Youyong Xu, Jiayin Yuan, Weian Zhang and Zhicheng Zheng. I am particularly grateful to Gaby Oliver for her help with all the little things that had to be done.

Furthermore, I would like to thank the CAMD group that provided me a very nice stay in Sydney and in particular Tony Granville and Istvan Jacenyik for organizing this trip.

Thanks to Prof. Matthias Ballauff, Yan Lu, Alexander Wittemann, Prof. Ruth Freitag, Anja Schallon, Karim Aissou and John Hardy for collaborating closely on joint research projects.

Thanks a lot to my friends and colleagues. In my 8.5 years here in Bayreuth I got to know a bunch of people that one can always rely on. Thanks for your support in all this years, especially in not chemistry related topics.

Most importantly I want to thank my family for their continuous support during my life and helping me to get where I am now. And a special thank to Sandrine for cheering me up and steering me through this quite exhausting trip called thesis.

Erklärung

Die vorliegende Arbeit wurde von mir selbstständig verfasst und ich habe dabei keine anderen als die angegeben Hilfsmittel und Quellen benutzt.

Ferner habe ich nicht versucht, anderweitig mit oder ohne Erfolg eine Dissertation einzureichen oder mich der Doktorprüfung zu unterziehen.

Bayreuth, den 22.05.2011

(André Pfaff)